FINAL REPORT

Feasibility and Guidelines for the Development of Microgrids in Campus-Type Facilities

SERDP Project EW-1710

APRIL 2012

Professor Saifur Rahman
Advanced Research Institute, Virginia Tech

SERDP
DOD ▪ EPA ▪ DOE

REPORT DOCUMENTATION PAGE

Form Approved
OMB No. 0704-0188

Public reporting burden for this collection of information is estimated to average 1 hour per response, including the time for reviewing instructions, searching existing data sources, gathering and maintaining the data needed, and completing and reviewing this collection of information. Send comments regarding this burden estimate or any other aspect of this collection of information, including suggestions for reducing this burden to Department of Defense, Washington Headquarters Services, Directorate for Information Operations and Reports (0704-0188), 1215 Jefferson Davis Highway, Suite 1204, Arlington, VA 22202-4302. Respondents should be aware that notwithstanding any other provision of law, no person shall be subject to any penalty for failing to comply with a collection of information if it does not display a currently valid OMB control number. **PLEASE DO NOT RETURN YOUR FORM TO THE ABOVE ADDRESS.**

1. REPORT DATE *(DD-MM-YYYY)* 05-04-2012	2. REPORT TYPE Final Report	3. DATES COVERED *(From - To)* 2010 – 2012
4. TITLE AND SUBTITLE Feasibility and Guidelines for the Development of Microgrids on Campus-Type Facilities		5a. CONTRACT NUMBER 09-C-0058
		5b. GRANT NUMBER
		5c. PROGRAM ELEMENT NUMBER
6. AUTHOR(S) Dr. Saifur Rahman, Dr. Manisa Pipattanasomporn		5d. PROJECT NUMBER EW-1710
		5e. TASK NUMBER
		5f. WORK UNIT NUMBER
7. PERFORMING ORGANIZATION NAME(S) AND ADDRESS(ES) Virginia Tech – Advanced Research Institute 900 N. Glebe Road Arlington, VA 22203		8. PERFORMING ORGANIZATION REPORT NUMBER
9. SPONSORING / MONITORING AGENCY NAME(S) AND ADDRESS(ES) Strategic Environmental Research & Development Program 901 N. Stuart Street, Suite 303 Arlington, VA 22203		10. SPONSOR/MONITOR'S ACRONYM(S) SERDP
		11. SPONSOR/MONITOR'S REPORT NUMBER(S)

12. DISTRIBUTION / AVAILABILITY STATEMENT
Unlimited

13. SUPPLEMENTARY NOTES

14. ABSTRACT

This report describes the work conducted under the project EW 1710 "Feasibility and Guidelines for the Development of Microgrids in Campus-Type Facilities", sponsored by the Department of Defense (DoD)'s Strategic Environmental Research and Development Program (SERDP). The objective of this work was to explore the feasibility of and provide guidelines for the development of microgrids in campus-type facilities. This work was carried out through the development of a methodology including technology assessment, as well as modeling and simulation.

15. SUBJECT TERMS

Microgrid, Energy, Security, Islanding, Energy Modeling, Guidelines, Renewable Energy, Distributed Generation

16. SECURITY CLASSIFICATION OF: Unclassified			17. LIMITATION OF ABSTRACT	18. NUMBER OF PAGES	19a. NAME OF RESPONSIBLE PERSON
a. REPORT U	b. ABSTRACT U	c. THIS PAGE U	UU	116	19b. TELEPHONE NUMBER *(include area code)*

Standard Form 298 (Rev. 8-98)
Prescribed by ANSI Std. Z39.18

Table of Contents

List of Tables

List of Figures

List of Acronyms

AMR	:	Automated meter reading
CAIDI	:	Customer Average Interruption Duration Index
CERTS	:	Consortium for Electric Reliability Technology Solutions
DER	:	Distributed energy resource
DEW	:	Distribution Engineering Workstation
DG	:	Distributed generation
DoD	:	Department of Defense
EDD	:	Electrical Distribution Design, Inc.
ESM	:	Sandia's Energy Surety Microgrid
FSEC	:	Florida Solar Energy Center
HVAC	:	Heating, ventilation, and air conditioning
IC	:	Internal combustion engine
PMSG	:	Permanent magnet synchronous generator
PV	:	Solar photovoltaics
RDSI	:	Renewable and Distributed Systems Integration
SAM	:	Sandia Advisor Model
STC	:	Standard test condition
SERDP	:	Strategic Environmental Research and Development Program
SAIDI	:	System Average Interruption Duration Index
SPIDERS	:	Smart Power Infrastructure Demonstration for Energy Reliability and Security
TED	:	The Energy Detective

Keywords

Acknowledgements

1.0 Abstract

This report describes the work conducted under the project EW 1710 "Feasibility and Guidelines for the Development of Microgrids in Campus-Type Facilities", sponsored by the Department of Defense (DoD)'s Strategic Environmental Research and Development Program (SERDP). The objective of this work was to explore the feasibility of and provide guidelines for the development of microgrids in campus-type facilities. This work was carried out through the development of a methodology including technology assessment, as well as modeling and simulation. The work was divided into two phases:

Phase I: Develop a microgrid simulation tool; and

Phase II: Develop a real-world case study for microgrid feasibility analysis and guideline development based on the information from Ft. Bragg.

The objective of the first phase was to develop a microgrid simulation test bench at Virginia Tech. The developed simulation tool included both distributed energy resource (DER) and load models as well as demand response algorithms. The simulation tool can be used for planning and evaluation of microgrid deployment and is capable of estimating benefits of deploying a microgrid in campus-type facilities. The objective of the second phase was to identify a set of technical and operational criteria for developing a microgrid on a military base like Ft. Bragg, including the introduction of renewable energy sources. These criteria were applied to quantify reliability benefits of a microgrid hosting energy efficient equipment along with renewable energy sources.

The technical approach consisted of: (1) development of the microgrid simulation test bench including various distributed generation and storage options; (2) expansion of the test bench to include load models; (3) development of microgrid management strategies to perform demand response; (4) development of case studies to analyze benefits of microgrid operations; (5) submission of the interim report; (6) gathering necessary information from Ft. Bragg; (7) identification of microgrid development criteria, including its boundary parameters; (8) development of a microgrid case study using a part of an electric power distribution system at the base; (9) analysis of operational (reliability) benefits of the microgrid; and lastly (10) preparation of the final technical report and general guidelines for microgrid deployment in a campus-type facility.

The set of design procedures and guidelines developed as a part of this report were based on experience gained during the course of this project including extensive discussions with engineers from the Public Works Department at the base, and Sandhills Utility Services – the power distribution company that serves Ft. Bragg. These guidelines include (1) A microgrid definition and its boundary selection criteria; (2) Recommended microgrid design criteria to achieve three microgrid properties - robustness, resilience and security; (3) Recommended microgrid design criteria for selecting type and size of distributed energy resources (DER) for microgrid deployment; (4) Recommended microgrid design criteria for load classification and prioritization; (5) Recommended microgrid operation strategies; (6) Recommended system studies and necessary standards; (7) Potential risks in microgrid deployment and operation; and (8) Guideline to estimate microgrid benefits.

With this set of guidelines and the experience of evaluating the benefits of a microgrid in one facility, DoD will be able to plan, analyze and evaluate the operational benefits and risks of deploying such microgrids on many of their bases.

2.0 Objective

The overall objective of this project was to explore the feasibility of and provide guidelines for the development of microgrids in a campus-type facility. This was carried out through the development of a methodology that encompasses technology assessment, modeling, and simulation.

Specific tasks pertaining to the proposed research were divided in two phases. The first phase of the project involved the development of a microgrid simulation tool that includes various distributed generation and storage options, together with campus-type facility load models, as well as demand response algorithms. The simulation tool can be used for planning and evaluation of microgrid deployment and is capable of estimating benefits of deploying a microgrid in campus-type facilities. These include, for example, peak shaving and energy reduction potentials with more energy efficient light fixtures; electricity saving potentials with HVAC control in commercial buildings by adjusting temperature set points; peak shifting and energy saving potentials with the use of solar photovoltaic (PV) panels; and benefits of demand response implemented at the end-user level.

The second phase of the project involved a real-world case study for analyzing the applicability of a microgrid at Ft. Bragg. A set of technical, operational, and economic criteria for developing a microgrid at the base, including the introduction of renewable energy sources, was identified. An operational analysis on the selected microgrid was performed and general guidelines were developed for microgrid deployment at Ft. Bragg.

The outcome of this work is a set of design procedures and guidelines that can be used for planning and evaluating microgrid deployment in a campus-type facility. Such a case study can also be used by other DoD facilities to design and evaluate the potential benefits of their own microgrids.

3.0 Background

The Department of Defense (DoD) is the largest single energy consumer in the United States. The department manages close to 2 billion sq ft of facility space and spends roughly $4 billion on energy usage annually. The Department has three key energy goals: (1) improve energy security, (2) reduce energy usage and intensity, and (3) increase renewable energy generation. The relevant design and case-specific operation of a microgrid can go a long way in achieving these three energy goals. A microgrid is defined as [1, 2] an integrated energy system consisting of interconnected distributed generation (DG) sources along with energy storage devices and controllable loads located at or near the end-use customers at the distribution level. The portfolio of these small-scale generation and storage technologies, which are generally known as distributed energy resources (DER), includes renewable energy technologies, internal combustion engines, microturbines, fuel cells, battery storage, flywheel energy storage, and alike. Such systems can operate in parallel with the grid during normal conditions or in a controlled islanded mode during emergency conditions. The deployment of a microgrid is expected to increase system robustness, resilience and security, deliver higher power security to critical loads, allow renewable integration and enable inclusion of emerging technologies.

In the past few years, several federal government entities and others have initiated programs to address the issue of microgrid development. These include the Renewable and Distributed Systems Integration (RDSI) program [3], the Consortium for Electric Reliability Technology Solutions (CERTS) microgrid project [4], the Sandia's Energy Surety Microgrid (ESM) [5] and the Smart Power Infrastructure Demonstration for Energy Reliability and Security (SPIDERS) program [6].

The RDSI program focuses on demonstrating the reduction in peak electricity demand at distribution feeders by means of integrating renewable energy, distributed generation, energy storage, thermally activated technologies, and demand response. The CERTS microgrid project showcases a full-scale test bed demonstration with American Electric Power with the following foci: 1) a method for effecting automatic and seamless transitions between grid-connected and islanded modes of operation; 2) an approach to electrical protection within the microgrid; and 3) a method for microgrid control that achieves voltage and frequency stability under islanded conditions. Sandia's ESM is one of the very few reported work that focuses on microgrid development at military bases with the objective of creating analytical tools and a methodology to evaluate the impact of infrastructure disruption on base missions. The SPIDERS program is a follow-on work of the Sandia's ESM, which aims at demonstrating that the microgrids developed using Sandia's ESM methodology have the ability to maintain operational surety to mission critical loads. As of October 2011, proposals are being sought under the SPIDERS program [7] to design and build an electrical microgrid at Joint Base Pearl Harbor Hickam (JBPHH), Oahu, HI and Fort Carson, Colorado.

While on many military bases, there are local back-up generation, solar photovoltaics, some automated meter reading (AMR) applications, and load monitoring networks, these devices are not integrated to take advantage of their synergy. Therefore, most of the military bases have no functioning microgrids on their campuses. As far as the electricity consumption is concerned, Fort Bragg had a peak electricity demand of 136 MW in 2011, and consumed close to 700 million kWh of electricity. As the electricity price can go as high as 80 cents/kWh during a hot summer day, there are significant potential savings opportunities through implementing load controls in a microgrid environment. Given the above situation, several challenges are faced by military bases with regard to microgrid development. First, there is the lack of design criteria and appropriate guidelines for microgrid development that take into account security, reliability, resiliency and economics. Secondly, there is the lack of algorithms that allow qualification of microgrid benefits.

In this project, we proposed to explore the feasibility of and provide guidelines for the development of microgrids in a campus-type facility. This was carried out through the development of a methodology including technology assessment, as well as modeling and simulation. In this report, methodology and methods are presented in Section 4.0; and results and discussions are presented in Section 5.0.

Section 4.0 has four subsections.

- Section 4.1 presents approaches to develop simulation models for distributed energy resources (DER), which include the models of solar photovoltaics (PV), wind turbines, internal combustion (IC) engines, microturbines and flywheel energy storage. All models developed include validation with manufacturers' or experimental data.

- Section 4.2 presents approaches to develop load models for both residential houses, e.g. military housing, and commercial buildings, e.g. office buildings. The load models developed include space cooling and space heating, water heating, clothes dryer and other loads. The developed models are validated against the measurement data.

- Section 4.3 presents approaches to perform microgrid management strategies, which include both load and generation controls. The control algorithms are divided into two categories: (1) the strategy to keep the electricity demand/consumption low to avoid high peak prices; and (2) the strategy to manage a microgrid during a utility outage.

- Section 4.4 presents approaches to analyze system reliability with and without distributed generators (DGs). Three models are described to account for the impact of both standard mode (parallel and emergency backup) and potential islanding mode (microgrid/smart grid) DG operation on the Fort Bragg circuit.

Section 5.0 presents results and discussions, including the set of guidelines for microgrid deployment and estimation of benefits from microgrid deployment. The models developed as described in Section 4.0 are used to analyze benefits of implementing a microgrid in a real-world environment. Guidelines for a microgrid deployment are developed based on experience gained during the course of the project. This section comprises three key parts:

Part I   -   General Guidelines for Microgrid Deployment

Part II   -   Impact of DGs on System Reliability and Load Shape

Part III   -   Analysis of Peak and Energy Saving Potentials with Energy Efficient
                    Technologies and Demand Response

In Section 5.0 - Part I, the team has gathered necessary system information from Ft. Bragg to evaluate a set of technical and operational criteria to implement a microgrid at the base and summarized the information as a set of guidelines. This includes the following:

Section 5.1 – A microgrid definition and its boundary selection criteria;

Section 5.2 – Recommended microgrid design criteria to achieve three microgrid properties - robustness, resilience and security;

Section 5.3 – Recommended microgrid design criteria for selecting type and size of DERs for microgrid deployment;

Section 5.4 – Recommended microgrid design criteria for load classification and prioritization;

Section 5.5 – Recommended microgrid operation strategies;

Section 5.6 – Recommended system studies and necessary standards;

Section 5.7 – Potential risks on microgrid deployment and operation; and

Section 5.8 – Guideline to estimate microgrid benefits.

In Section 5.0 - Part II, a microgrid test case is developed (based on real-world information) to analyze the impact of distributed generation (DG) on system reliability, voltage and load shape changes. Discussions in Section 5.9 present a base-case scenario with no DG. As a DG can be connected to the system in three ways (one – a current source operated in parallel at the secondary side of building transformer connections; two – a voltage source connected radially to the system on the primary side of building transformers; and three – when a DG is operated as a part of fixed islands with one DG in each island modeled as a voltage source and other DG in each island modeled as current sources), Sections 5.10, 5.11 and 5.12 present the impact of DGs on system reliability and voltage when DGs are connected as current sources, voltage sources and in an islanded mode, respectively. Sections 5.13 and 5.14 present the impact of solar PV on system reliability, voltage and load shape.

Section 5.9 presents a base case analysis with no DG;

Section 5.10 presents the impact of DGs as current sources on system reliability and voltage;

Section 5.11 presents the impact of DGs as voltage sources on system reliability and voltage;

Section 5.12 presents the impact of DGs in an islanded mode on system reliability and voltage;

Section 5.13 presents the impact of solar PV on system reliability and voltage; and

Section 5.14 presents the impact of solar PV on system load shapes.

In addition to its ability to provide an improvement in the robustness, resilience and security of a local power system, a microgrid will also allow peak shaving and energy reduction for day-to-day operations. This can be achieved by deploying energy efficient technologies, HVAC control and demand response. This is a topic of focus in *Section 5.0 - Part III*.

Discussions in Sections 5.15 and 5.16 focus on commercial buildings whose typical loads include lighting, HVAC and plug loads, while discussions in Section 5.17 focus on implementing demand response in military housing units to limit a household consumption below a certain level.

Section 5.15 looks at how much peak demand and energy can be saved by replacing existing linear fluorescent lamps (T12) with more energy efficient lighting technologies, including T8 and LED lamps;

Section 5.16 describes energy saving can be achieved by increasing the building's HVAC temperature set point; and

Section 5.17 presents examples of demand response implemented at a household level.

4.0 Materials and Methods

4.1 DER Models and Validation

This study focuses on developing distributed energy resource (DER) models for specific technologies. The DER models of interest include solar photovoltaics (PV) wind turbines, internal combustion engines, microturbines, fuel cells, and flywheel energy storage. This deliverable contains methodology to develop DER models, as well as the simulation results and validation, organized by DER type.

4.1.1 Solar Photovoltaics

A) Model Development

Solar photovoltaic (PV) is a technology that converts sunlight into electricity. This section presents a generic and scalable model for a PV generator in Matlab/Simulink environment. Previous work that developed PV generator models includes [8, 9, 10, 11, 12, 13, 14, 15]. Sandia National Laboratory also develops a simulation model for PV generator called Sandia Advisor Model (SAM) [16]. This study developed the PV generator model based on the simplified methodology presented in [8]. Good agreements are observed when comparing the model outputs with the measured data from Florida Solar Energy Center (FSEC) [17].

The block diagram of a PV generator developed in MATLAB/Simulink is presented in Fig. 4-1.

Model inputs	Solar PV generator model	Model outputs
External inputs: Ambient Temperature (°C) Solar Irradiation (W/m2) PV characteristic inputs: No of modules in series No of modules in parallel No of cells in series No of cells in parallel Temp coeff of Vmp (V/°C) Temp coeff of Imp (A/°C) Vmp, Imp at STC Vmp, Imp at two other temperatures and irradiations		DC voltage and current outputs at the maximum power point (Vmp, Imp)

Fig. 4-1. Schematic of the developed PV model

The model requires time-series ambient temperature and solar irradiation as inputs. Other inputs needed, which are already integrated into the model library for selected commercially available PV modules, include: number of modules in series and parallel, number of cells in series and parallel, temperature coefficient of voltage at the maximum power point (V/°C), the temperature coefficient of current at the maximum power point (A/°C), the voltage and current at the maximum power point (Vmp and Imp) at the standard test condition (STC) (1000 W/m2 and 25°C), as well as the voltage and current at the maximum power point (Vmp and Imp) at two other test conditions. The model outputs are DC voltage and current at the maximum power point.

Characteristics of two commercially available PV modules are integrated into the model library. These are a 165W Polycrystalline Schott unit (Schott SAPC165), and a 125W Polycrystalline Kyocera unit (Kyocera KC125G). A user can select a "user-defined" type to create a new PV module by entering the required input parameters.

Fig. 4-2 illustrates how the PV model is developed. The model comprises five main subsystems: (1) effective irradiation calculation; (2) cell temperature calculation; (3) coefficient calculation; (4) current at maximum power point (Imp) calculation; and (5) voltage at maximum power point (Vmp) calculation.
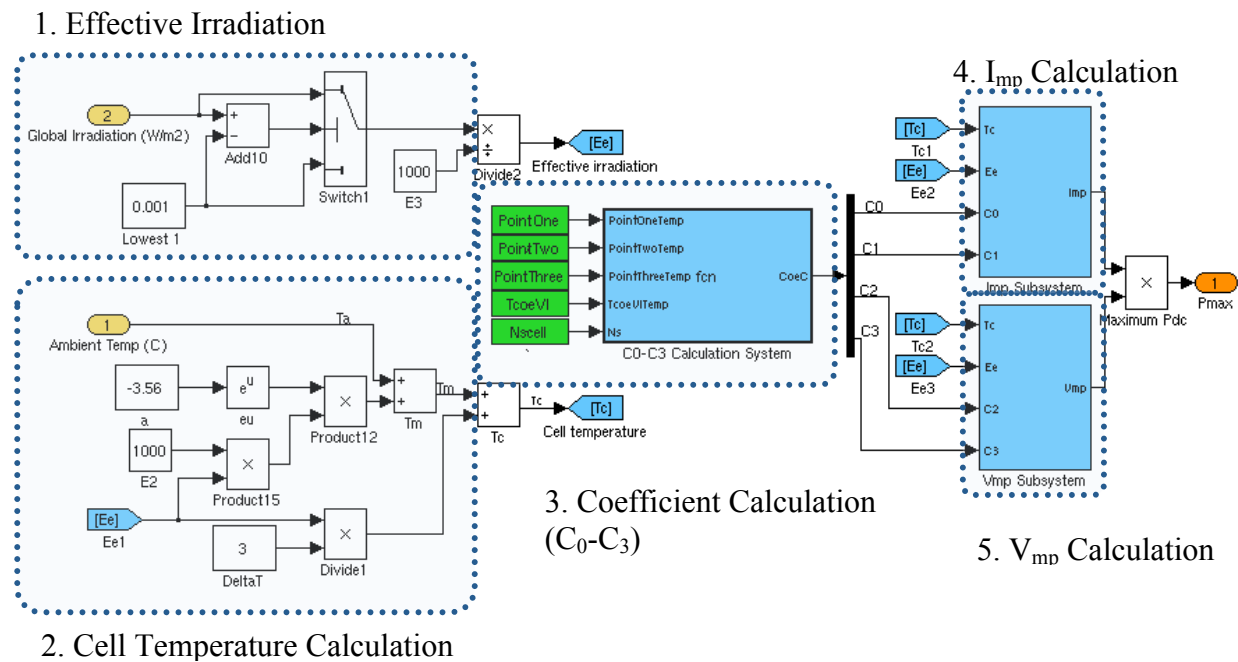
Fig. 4-2. PV model subsystems

In the developed model, the ambient temperature and the global irradiation (the sum of direct normal irradiation and diffuse horizontal irradiation) are used as the inputs. Subsystem 1 calculates effective irradiation (Ee) based on the global irradiation input. Subsystem 2 calculates cell temperature (Tc) based on the ambient temperature inputs. Subsystem 3 calculates some coefficients that take into account sensitivity of Vmp and Imp at different irradiation and temperature. Then the outputs from subsystems 1-3 are used calculate Imp and Vmp in subsystems 4-5.

B) PV Mathematical Model

The following section describes mathematical formula used in development of the PV model.

Subsystem 1: Effective Irradiation (Ee) Calculation

This subsystem calculates effective irradiation based on the global irradiation data. According to [18, 19], the effective irradiation (Ee) equation is calculated as:

$$E_e = f_1(AM_a) * (E_{dni} * \cos(AOI) * f_2(AOI) + f_d * E_{diff}) * \frac{SF}{E_0} \qquad \text{(Eq. 1)}$$

Where

$f_1(AM_a)$	:	Empirical polynomial relating solar spectral influences on short circuit current (Isc) to air mass variation over the day
E_{dni}	:	Direct normal irradiation (W/m2)
AOI	:	Solar angle of incidence (degree)
$f_2(AOI)$	:	Empirical polynomial relating optical influences on Isc to solar angle of incidence
f_d	:	Relative response of the module to diffuse versus beam irradiation, generally fd=1
E_{diff}	:	Diffuse horizontal irradiation (W/m2)
E_0	:	Reference solar irradiation on module (1000W/m2)
SF	:	Soiling factor, accounting for the unavoidable soiling loss present when array performance measurements are made, SF=1 when the array is clean

The developed model is based on the simplified version of this approach, neglecting the solar spectral and the influence of the solar angle-of-incidence.

Subsystem 2: Cell Temperature (Tc) Calculation

This subsystem calculates cell temperature based on the ambient temperature and irradiation data. The relationship between the cell temperature, the ambient temperature, and wind speed is presented in the following equation:

$$T_c = E * e^{a+b*WS} + \frac{E}{E_0} * \Delta T \qquad \text{(Eq. 2)}$$

Where,

Tc	:	Cell temperature (°C)
E	:	Global irradiation measured at the module (W/m^2)
a, b	:	Empirical coefficients relating wind speed to module temperature
WS	:	Wind speed (m/s)
Ta	:	Ambient Temperature (°C)
E0	:	Reference solar irradiation (1000W/m^2)
ΔT	:	Temperature difference between cell and module back surface at an irradiation level of 1000W/m^2, typically $\Delta T = 3°C$.

By neglecting the wind speed, the equation becomes:

$$T_c = E * e^{a} + \frac{E}{E_0} * \Delta T \qquad \text{(Eq. 3)}$$

The empirical coefficient "a", and the temperature difference "*ΔT*", can be obtained using experimental data. The following table summarizes values of the coefficient "a" and the temperature difference "*ΔT*" for different types of PV modules. For convenience, this study used "a" of -3.56, and "*ΔT*" of 3.

Module Type	a	ΔT
Glass/cell/glass	-3.47	3
Glass/cell/polymer sheet	-3.56	3
Polymer/thin-film/steel	-3.58	3

Subsystem 3: Coefficient (C$_0$-C$_3$) Calculation

This subsystem calculates coefficients that take into account sensitivity of V_{mp} and I_{mp} at different irradiation and temperature. The equations of I_{mp} and V_{mp} are shown below:

$$I_{mp} = I_{mp0} * (C_0 * E_e + C_1 * E_e^2) * (1 + \alpha_{I_{mp}} * (T_c - T_0)) \qquad \text{(Eq. 4)}$$

$$V_{mp} = V_{mp0} + C_2 * N_s * \delta(T_c) + C_3 * N_s * [\delta(T_c) * \ln(E_e)]^2 + \beta_{V_{mp}} * (T_c - T_0) \quad \text{(Eq. 5)}$$

Where,

$$C_0 + C_1 = 1 \qquad \text{(Eq. 6)}$$

and

I_{mp}	:	Current at maximum power point (A)
I_{mp0}	:	Current at maximum power point at STC (A)
V_{mp}	:	Voltage at maximum power point (V)
V_{mp0}	:	Voltage at maximum power point at STC (V)
T_c	:	Cell Temperature (°C)
T_0	:	Reference cell temperature (25°C)
E_e	:	Effective irradiation (W/m2)
α_{Imp}	:	Temperature coefficient of Imp (A/°C)
β_{Vmp}	:	Temperature coefficient of V_{mp} (V/°C)
N_s	:	No of cells in series
C_0, C_1	:	Empirical coefficients relating I_{mp} to E_e,
C_2, C_3	:	Empirical coefficients relating V_{mp} to E_e
$\delta(T_c)$	:	Thermal voltage per cell at T_c, $\delta(T_c) = n*k*(Tc+273)/q$
n	:	Diode factor
k	:	Boltzmann's constant, 1.38066e-23 (J/K)
q	:	Elementary charge, 1.60218e-19(coulomb)

Eqs (4) and (6) have two unknowns, which are C0 and C1. By using the data from I-V curve at the STC, C0 and C1 can be determined. To determine C2 and C3, Eq (5) can be solved using the data form two I-V curves at the temperature or irradiation at the conditions other than the STC.

Subsystem 4: Current at the Maximum Power Point (Imp) Calculation

The current at the maximum power point (Imp) can be calculated using Eq (4). In practice, the PV array comprises several modules in series and/or parallel. Therefore, the module current at the maximum power point of a given PV generator is:

$$I_{mp,array} = I_{mp} * N_{parallel,module} \qquad \text{(Eq. 7)}$$

Subsystem 5: Voltage at the Maximum Power Point (Vmp) Calculation

The voltage at the maximum power point (Imp) can be calculated using Eq (5). In practice, the PV array comprises several modules in series and/or parallel. Therefore, the module voltage at the maximum power point of a given PV generator is:

$$V_{mp,array} = V_{mp} * N_{series,module} \qquad \text{(Eq. 8)}$$

C) Model Validation

To validate the developed PV model, a measured PV output data is compared with the model output. The measured PV output is from Florida Solar Energy Center (FSEC). The information of the PV generator is shown below:

Table 4-1. PV System in Tallahassee, FL

Location	Florida State University, Tallahassee, FL
Capacity	5,940W (2 arrays)
Latitude, longitude	30.42 deg, -84.32 deg
PV module	Schott SAPC-165

The PV generator has two arrays, each of which the capacity is 2,970W. Configuration of the PV array is as follow: 9 modules in series to form one string; 2 strings in parallel to form an array. Technical specifications of the PV module used (Schott SAPC-165) is summarized below:

Table 4-2. Information of Schott SAPC-165 PV

PV type	Polycrystalline Silicon
Maximum power at standard condition ($1000W/m^2$,25°C)	165W
Voltage and current at maximum power ($1000W/m^2$,25°C)	34.6V, 4.77A
Number of cells in series and parallel	72, 1
Temperature coefficient of Pmax	-0.8446W/°C
Temperature coefficient of Vmp	-0.1796V/°C
Temperature coefficient of Imp	0.0003513A/°C

The figure below shows the DC power comparison between actual data from Tallahassee, FL and the output from the developed PV model.
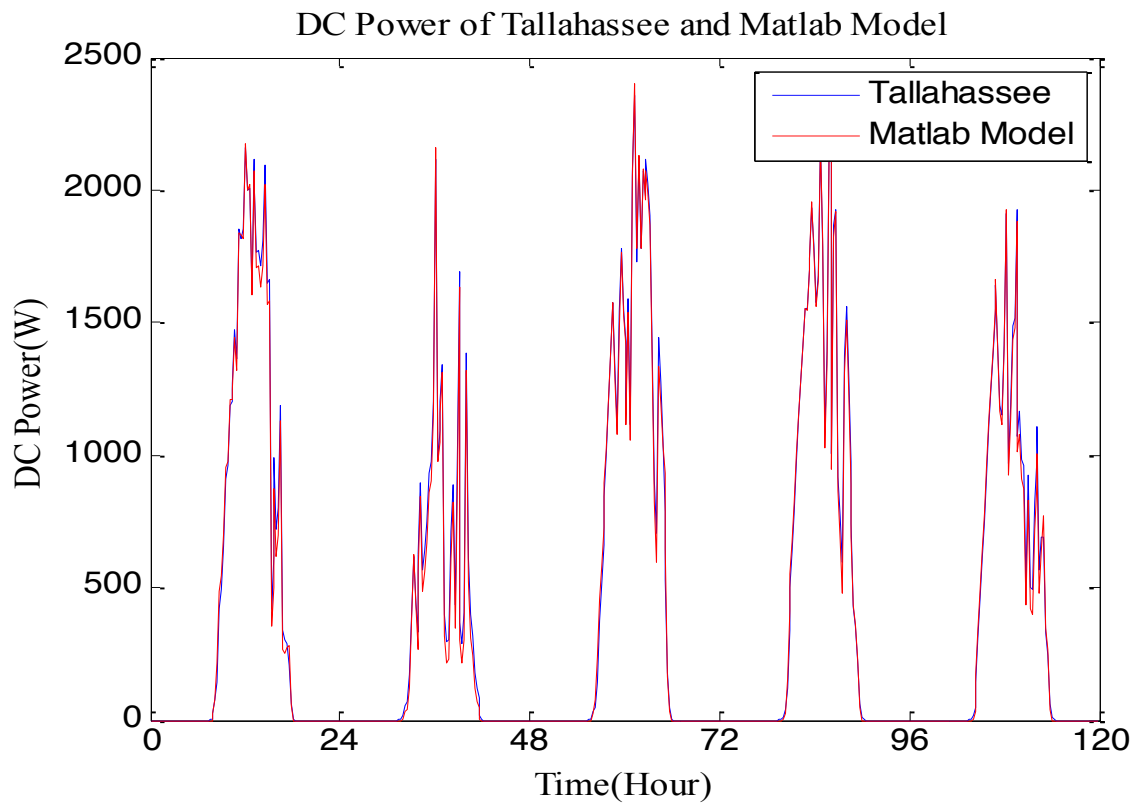
Fig. 4-3. Comparison between the measured PV output from Tallahassee, FL and the output from the developed PV model

The measure PV output data from Tallahassee is shown in blue, and the DC power output from the developed PV model is shown in red. The average power difference is less than <1.5% of the total system capacity. This discrepancy is considered very small and indicates that the developed PV model can be used to represent the actual PV generator.

4.1.2 Wind Turbines

A) Model Development

A wind turbine is an electromechanical energy conversion device that turns the kinetic energy from the wind into electricity. Previous work that developed wind turbine models includes [20, 21, 22, 23]. This section presents a generic model for a wind generator developed in Matlab/Simulink environment.

Three types of wind turbine models are presented: fixed speed, variable speed and double-fed induction generator. In this work, the fixed speed wind turbine model is developed based on the relationship presented in [24]. The pitch control algorithm is developed and integrated into the fixed speed model to obtain the variable speed wind turbine model. Good agreements are observed when comparing the model outputs with the manufacturer data. The double-fed wind turbine model is readily available in Matlab, and therefore it will not be further discussed here. All wind turbine models developed here is of 1.5MW as it is the most common wind turbine size currently deployed in the market.

The block diagram that shows the model's inputs and outputs is shown in Fig. 4-4. The model requires the wind speed (m/s) as an input. Other inputs needed, which are already integrated into the model library for a 1.5-MW turbine, include: wind rotor radius (m), rotor power coefficient (Cp), damping coefficient (D), stiffness coefficient (K) and moment of inertia (J). The model outputs are AC voltage and current.

Model inputs	Wind turbine model	Model outputs

External inputs:
Wind speed (m/s)

Wind turbine characteristic inputs (built-in):
Wind rotor radius (m)
Rotor power coefficient (Cp)
Damping coefficient (D)
Stiffness coefficient (K)
Moment of inertia (J)

AC voltage and current outputs
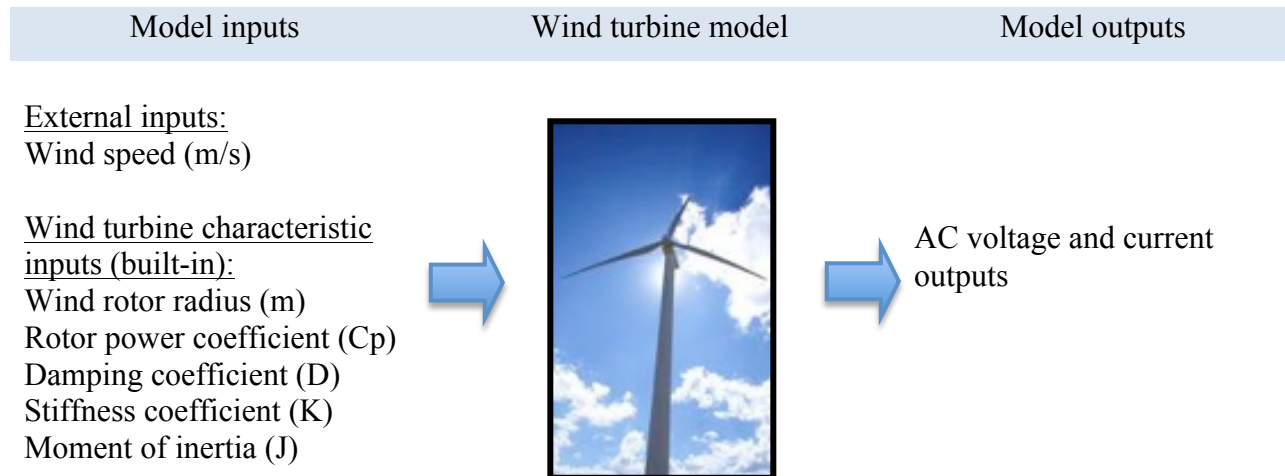
Fig. 4-4. Schematic of the developed wind turbine model

Fig. 4-5 illustrates how the fixed- and variable-speed wind turbine models are developed. The fixed-speed model comprises three subsystems: (1) aerodynamic model; (2) shaft model; and (3) generator model. The variable-speed model also has the pitch control model, which is neglected for the fixed-speed wind turbine model.
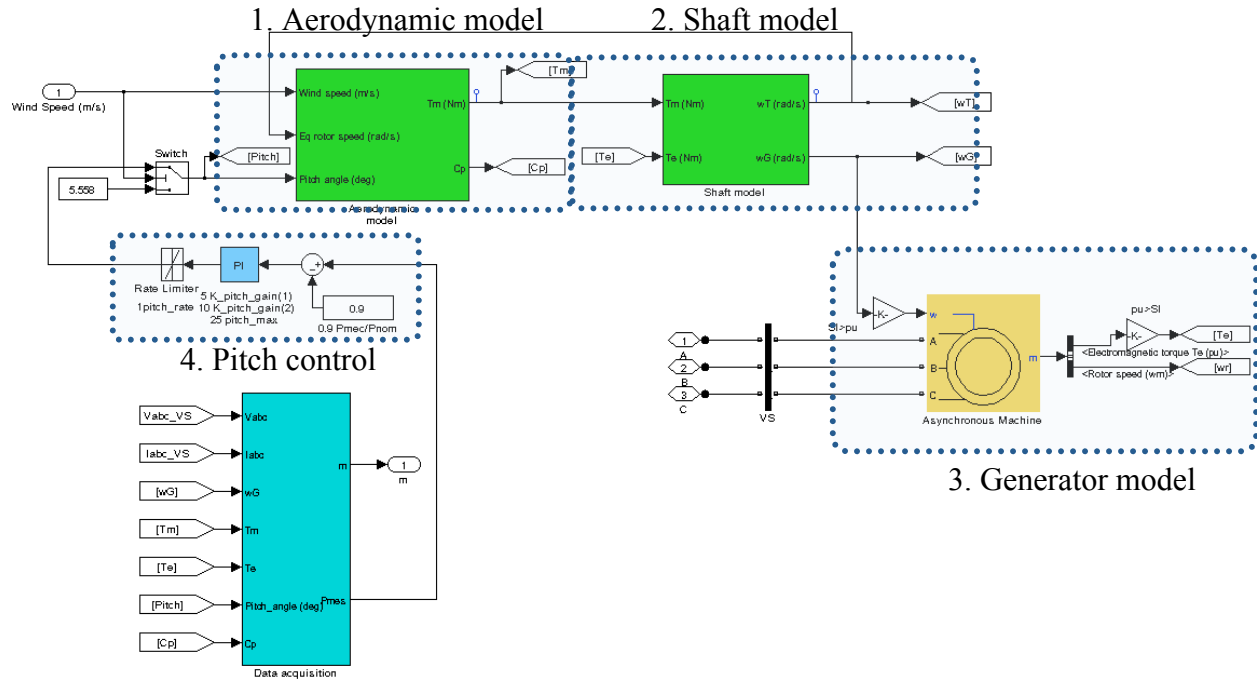
Fig. 4-5. Subsystems of the fixed- and variable-speed wind turbine model

In the developed model, the wind speed (m/s) is used as the only external input required. Subsystem 1 calculates mechanical torque or mechanical energy extracted from the wind. Subsystem 2 calculates generator speed based on the characteristics of wind turbine rotational systems with shaft. Subsystem 3 is the generator model that converts the machine rotational speed to electrical power output. Subsystem 4 is the pitch control that regulates the rotational speed of the turbine based on the wind speed input.

B) Wind Turbine Mathematical Model

The following section describes mathematical formula used in development of the fixed-speed and variable-speed wind turbine models.

Subsystem 1: Aerodynamic model

This subsystem calculates the aerodynamic torque based on the wind speed and the size of the rotor blade based on the following set of equations:

$$P_{rotor} = \frac{1}{2}C_p \rho v_{wind}^3 \pi R_{rotor}^2 \qquad \text{and} \qquad T_T = \frac{\frac{1}{2}C_p \rho v_{wind}^3 \pi R_{rotor}^2}{\varpi_T} \qquad \text{(Eq. 9)}$$

where,

Protor	:	Power extracted from the wind (W)
Cp	:	Rotor power coefficient – the Cp data is obtained from a manufacturer
ρ	:	Standard air density of 1.225 kg/m3
Vwind	:	Wind speed (m/s)
Rrotor	:	Wind turbine blade rotor radius
TT	:	Aerodynamic torque
ωT	:	Generator rotational speed (rad/s)

Subsystem 2: Shaft model

Torque equations describing the mechanical behavior of the wind turbine system can be written based on the two-mass model, as follows:

$$J_T \theta_T'' + D(\omega_T - \omega_G) + K(\theta_T - \theta_G) = T_T$$
$$J_G \theta_G'' + D(\omega_G - \omega_T) + K(\theta_G - \theta_T) = -T_G \qquad \text{(Eq. 10)}$$

Where,

J_T, J_G	:	Moments of inertia of wind rotor and generator rotor [kg*m2]
T_T, T_G	:	Aerodynamic torque and generator electromagnetic torque [Nm]
ω_T, ω_G	:	Wind rotor speed and generator speed [rad/s]
θ_T, θ_G	:	Angular position of wind rotor and generator rotor [rad]
D, K	:	Equivalent damping and stiffness [Nms/rad], [Nm/rad]
T_T	:	Aerodynamic torque
ωT	:	Generator rotational speed (rad/s)

By solving the above two equations using a state-space approach, speeds and torques of the turbine rotor and the generator can be determined for each simulation time step, using the following equations:

$$\frac{d}{dt}(\theta_T - \theta_G) = \omega_T - \omega_G$$

$$\omega_T' = (1/J_T)\left[T_T - D(\omega_T - \omega_G) - K(\theta_T - \theta_G)\right] \qquad (\text{Eq. 11})$$

$$\omega_G' = (1/J_G)\left[D(\omega_T - \omega_G) + K(\theta_T - \theta_G) + T_G\right]$$

The parameters, JT, D and K, can be derived for a 1.5MW wind turbine based on the turbine system data obtained from the manufacturer, as shown below.

Parameters	Definition	Value	Unit
J_T	Rotor moment of inertia	4,915,797.5	Kg*m2
R_{rotor}	Rotor radius	35	m
G_R	Gear ratio	70	-
J_G	Generator moment of intertia	81.2	Kg*
P_{gen}	Generator rated power	1500	kW
V_{rated}	Generator rated voltage	690	V
I_{rated}	Generator rated current	1397	A

In this case, the generator mechanical angular speed and rated torque are also calculated as follows:

$$J_T = \frac{J_{rot}}{GR^2} = \frac{4915797.5}{70^2} = 995.8 \; kgmm$$

$$D = D_{q2g} + D_{rq1}(1/GR)^2 = 30.3 \; Nm \cdot s / rad$$

$$K = K_{rq1}(1/GR)^2 = 19720 \; Nm / rad$$

$$\omega_n = \omega_{mech} = \frac{2\pi \cdot 60}{p} = 125.6637 \; rad / s$$

$$T_{gen\_rated} = \frac{P_{mech}}{\omega_n} = \frac{1.5 \times 10^6}{125.6637} = 11937 \; Nm$$

Note that the electromagnetic torque is positive when the induction generator speed is less than the synchronous speed (i.e. in motor mode) and is negative when the generator speed is greater than the synchronous speed (i.e. in generator mode).

Subsystem 3: Generator model

The induction generator is used to represent the wind turbine generator. This is the built-in induction generator model in Matlab.

Subsystem 4: Pitch control

The pitch control subsystem is modeled as a PI controller with the proportional gain of 5 and integral gain of 10. The proposed model applies pitch controller only when the wind speed input is greater than 15 m/s. This pitch control subsection is only applicable with the variable-speed wind turbine model.

C) Model Validation

The developed 1.5-MW fixed- and variable-speed wind turbine models are run with the wind speed input varies from 0 to 25 m/s in order to generate the power curves. The power curves as a result of the model are then compared with the power curve obtained from the manufacturer. This comparison is shown in Fig. 4-6. The results indicate that the fixed- and variable-speed wind turbine model behaves satisfactorily.
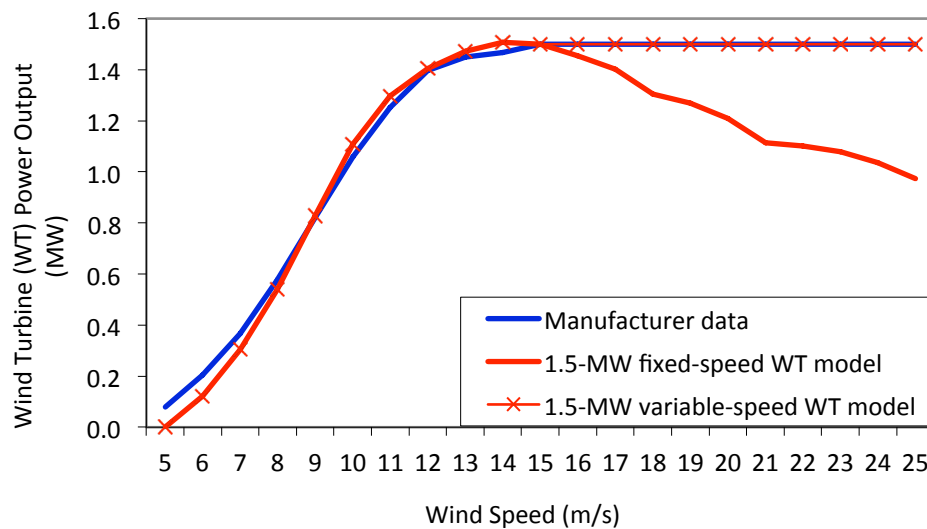
Fig. 4-6. Comparison of power curves (model outputs vs manufacturer data)

As shown, the power outputs of both fixed- and variable-speed wind turbine models are very close to the output pattern of the real-world wind turbine, up to the rated wind speed (<15 m/s). Both wind turbine models produce 1.5 MW at the rated wind speed of 15 m/s. For the wind speed above 15 m/s, the fixed-speed wind turbine model behaves differently from the power curve of the 1.5-MW (variable-speed) wind turbine obtained from the manufacturer. This is to be expected since the pitch angle of the wind turbine blades is fixed and the turbine produces less power when its rotor enters an aerodynamic-stall region. For the variable-speed wind turbine model, the output follows the power curve from the manufacturer. Small discrepancy between the power curves exists, which are deemed due to difference in CP calculation.

4.1.3 Internal Combustion (IC) Engines

Matlab/Simulink provides a comprehensive machine library that comprises synchronous machines, asynchronous machines and DC machines, together with the excitation and governor control units. Parameters of various machines' type and size are also available in the library. See Fig. 4-7 for the available pre-set models of synchronous machine units (left) and see the available pre-set models of asynchronous machine units (right).
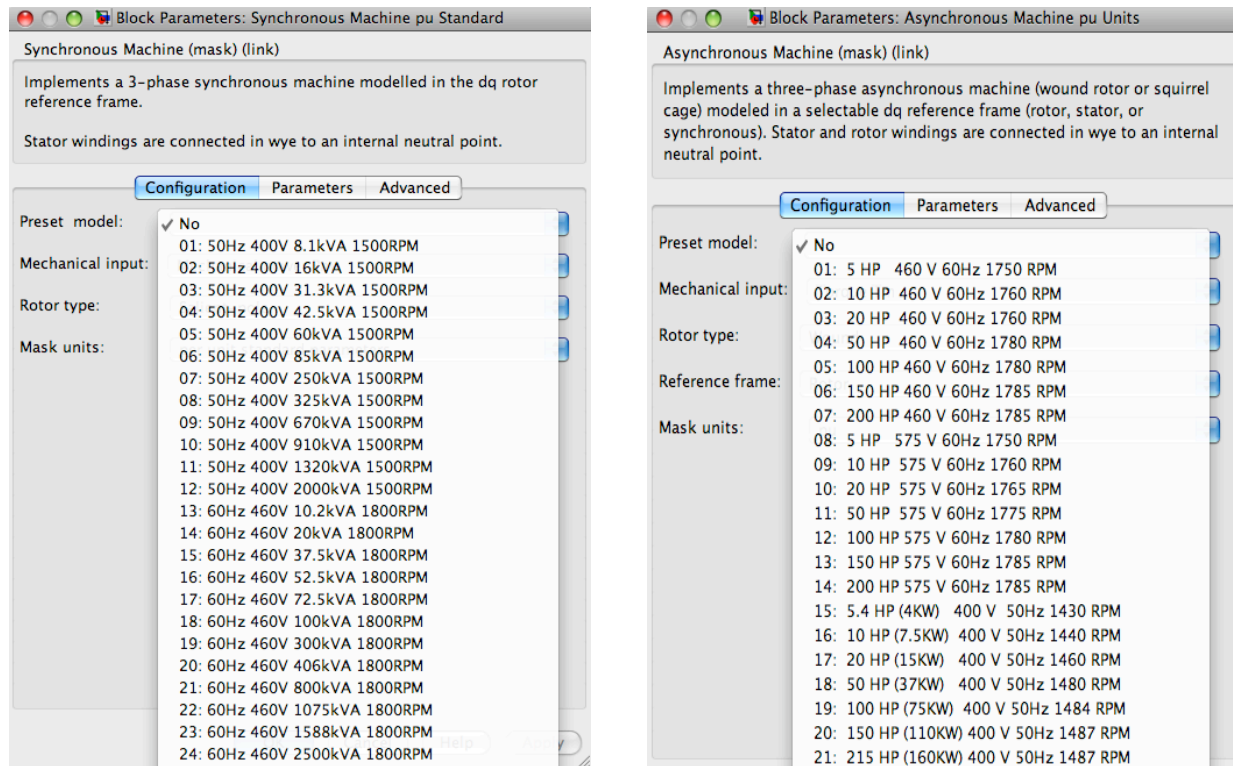
Fig. 4-7. Available pre-set models of synchronous machine units (left) and Available pre-set models of asynchronous machine units (right)

The detailed mathematical formula for these models is available in Matlab/Simulink reference, and will not be repeated here.

4.1.4 Fuel Cells

Matlab/Simulink provides a comprehensive fuel cell library that comprises four fuel cell units of various size and type. See Fig. 4-8 for the available pre-set models of fuel cell units.
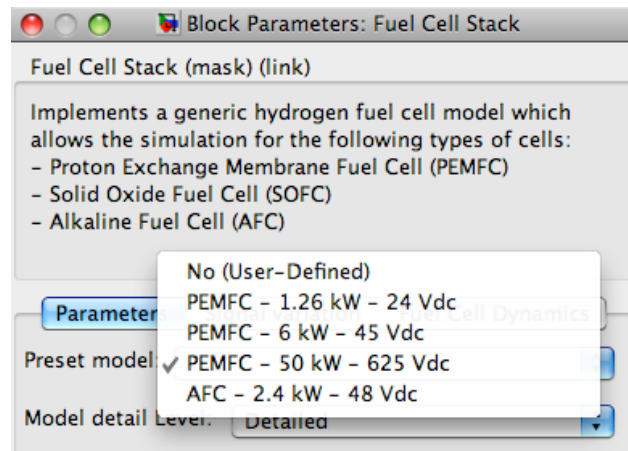
Fig. 4-8. Available pre-set models of fuel cell units

The detailed mathematical formula for these models is available in Matlab/Simulink reference, and will not be repeated here.

4.1.5 Microturbines

A) Model Development

Microturbines are small-combustion turbines that produce between 25kW and 500kW of power. They have a common shaft on which is mounted a compressor, a turbine and a generator. These components are mounted on an air bearing to eliminate friction and maintenance costs. Most microturbines operate at high rotating speeds of 90,000 to 120,000 rpm. As a result, the output frequency of a microturbine may vary from 1300 to 1600 Hz. Microturbines can be unrecuperated (simple cycle with no heat recovery unit) or recuperated (with recuperator to recover the heat from the exhaust gas to boost the temperature of combustion and increase the efficiency). Previous work that developed microturbine models includes [25, 26, 27, 28, 29]. The microturbine model developed for this work follows the work done in [30].

The microturbine model is developed in Matlab/Simulink. The block diagram that shows the model's inputs and outputs is shown in Fig. 4-9. The model only requires power control signal (kW) as an input. Other inputs needed, which are already integrated into the model library, include: temperature, torque and fuel system control parameters.

Model inputs	Microturbine model	Model outputs

External inputs:
Control signal (kW)

Microturbine   characteristic
inputs (built-in):
Speed control parameters
Fuel control parameters
Compressor-turbine
parameters
Temp control parameters

AC voltage and current
outputs
Fuel consumption
(gallon/hr)
Exhaust temperature (°C)
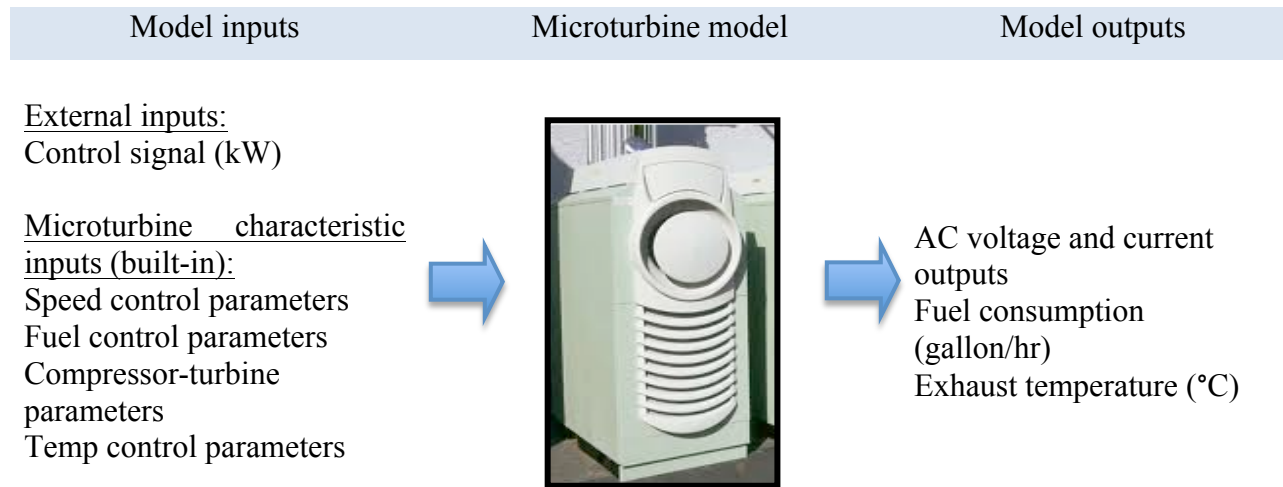
Fig. 4-9. Schematic of the developed microturbine model

Fig. 4-10 illustrates how the microturbine model is developed. The model comprises four subsystems: (1) speed control section; (2) fuel control section; (3) compressor-turbine section; and (4) temperature control section. The turbine torque output form section 4 is used as an input for the permanent magnet synchronous generator (PMSG). The PMSG model in Matlab library is used for the model development.
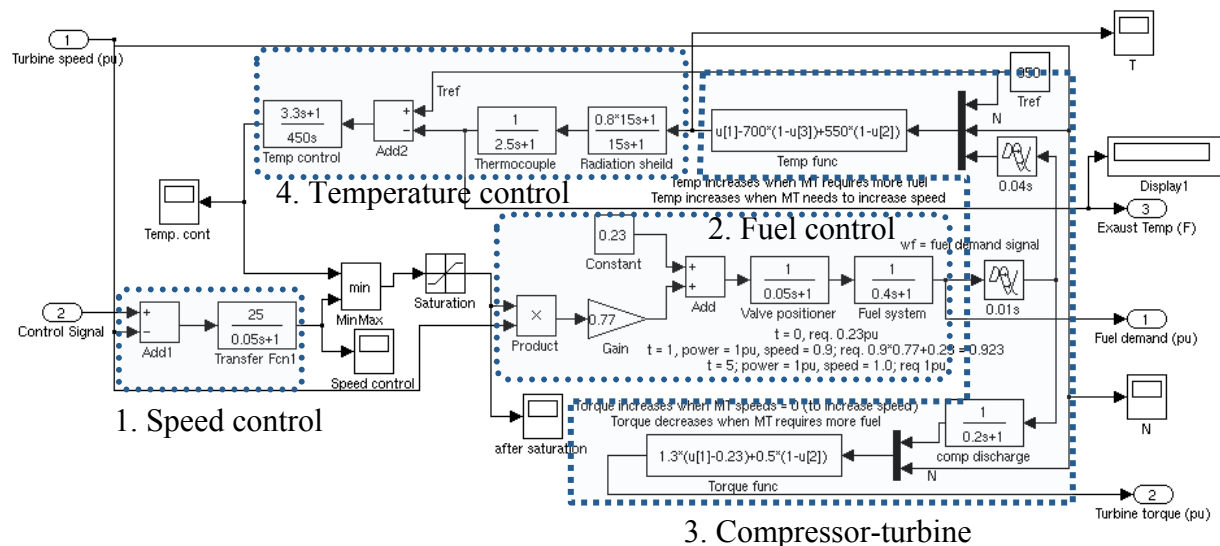
Fig. 4-10. Microturbine subsystems

B) Microturbine Mathematical Model

The following section describes mathematical formula used in development of the microturbine model.

Subsystem 1: Speed control section

The speed control section compares the current rotor speed (from PMSG) with the reference speed in per unit quantities. The dynamic response of the speed control section can be modified by adjusting parameters in the transfer function. The output of the speed control section is one of two inputs to the least value gate (LVG). The other input is from the temperature control section. The lowest value of the two inputs will be sent to the saturation block (for a typical gas the minimum and maximum limits are -0.1 and 1.5, respectively) and forwarded to the fuel control system.

Subsystem 2: Fuel control section

The output from LVG represents the least amount of per unit fuel needed for a particular operating point that corresponds directly to the per unit mechanical power on turbine base in steady state. For example, if mechanical power is 0.7 pu then the steady state value for fuel demand signal is also 0.7 pu. To obtain the final fuel demand signal, the per unit fuel demand from the LVG is multiplied by the per unit turbine speed. The output is then scaled with gain K = 0.77, then offset by the constant 0.23, which represents the minimum amount of fuel flow at no load rated speed. The fuel control system section of the diagram above can be interpreted as follows:

When no more fuel is required (fuel control = 0), fuel demand signal = 0.23.

When fuel control = 1, turbine speed = 0.5, fuel demand signal = 0.23+0.5*0.77 = 0.615.

When fuel control = 1, turbine speed = 1.0, fuel demand signal = 0.23+1.0*0.77 = 1.0.

The fuel control section also consists of the fuel valve positioner and fuel actuator. The transfer functions associated with valve positioner and fuel actuator generate some time delays, which in this case is modeled at 0.05 and 0.04 seconds, respectively.

Subsystem 3: Compressor-turbine section

The fuel combustion in the combustor results in turbine torque and in exhaust temperature. Inputs of the compressor-turbine section are the per unit turbine speed (N) and per unit fuel flow required (Wf). Outputs of the compressor-turbine section are per unit torque and exhaust temperature (in F), given as inputs. Torque and exhaust temperature relate to fuel flow (Wf) and turbine speed (N) linearly according to the following relationships.

$$\text{Torque} = \text{KHHV} (Wf - 0.23) + 0.5 (1 - N) \text{ (Nm)} \qquad \text{(Eq. 12)}$$

$$\text{Exhaust Temp (TX)} = \text{Tref} - 700 (1 - Wf) + 550 (1 - N) \text{ (F)} \qquad \text{(Eq. 13)}$$

Where:

Wf   :   per unit fuel flow

N   :   per unit rotor speed

| KHHV | : | coefficient that depends on the higher heating value of the gas stream in the combustion chamber (KHHV = 1.2 for a typical gas) |
| Tref | : | Reference temperature (950°F) |

In the compressor-turbine sections, time delay associated with the combustion reaction, time delay associated with the compressor discharge volume, and a transport delay associated with the transportation of gas from the combustion system through the turbine are modeled at 0.01 second, 0.2 second and 0.04 second, respectively.

Subsystem 4: Temperature control section

The temperature control section is designed to limit output power of the gas turbine if the exhaust temperature of the turbine is higher than a pre-determined reference temperature. In practice, the exhaust temperature is measured using a series of thermocouples incorporating radiation shields, both of which can be modeled by using transfer functions that result in very high time delays. The output of the thermocouple is compared with a reference temperature (950°F in this case). If the reference temperature is higher than the thermocouple temperature, which is usually the case, this will permit the dominance of speed control through the LVG. When the thermocouple output exceeds the reference temperature, the difference becomes negative and the temperature control output will be lower than the speed control output. This will allow the temperature control signal passing through the LVG and limits the turbine's output.

4.1.6 Flywheel Energy Storage

A) Model Development

Flywheel is one the oldest technologies in the human hands. Nowadays, many flywheel designs are developed for use as Flywheel Electricity Storage Systems (FESS). The FESS consists of a flywheel (a rotating disk) and a machine that acts as both a motor and a generator. During normal operation, the flywheel system converts electrical energy from the grid to kinetic energy using the motor. The kinetic energy is stored in the spinning flywheel. During outages or emergencies, the stored kinetic energy is converted back to electrical energy by the generator. This energy is then transferred to the connected electrical loads. The modeling and analysis of flywheel application in energy storage systems is available in the literatures [31, 32, 33, 34, 35, 36, 37]. This section presents the methodology to develop a generic flywheel model of various sizes. Model outputs are validated against manufacturer data, and good agreements are observed.

The model of a flywheel system is developed in Matlab/Simulink, of which the block diagram is shown in Fig. 4-11. The model inputs include flywheel control signal (power level), flywheel rating (kW), flywheel energy capacity (kW*sec), allowable discharge time at maximum power (sec) and allowable discharge time at half of maximum power (sec). The model outputs are AC voltage and current.

Model inputs	Flywheel model	Model outputs

External inputs:
Flywheel control signal (kW)

Flywheel characteristic inputs:
Flywheel rating (kW)
Flywheel energy capacity (kW*sec)
Allowable discharge time at maximum power (sec)
Allowable discharge time at half of maximum power (sec)

Flywheel Model

AC voltage and current outputs
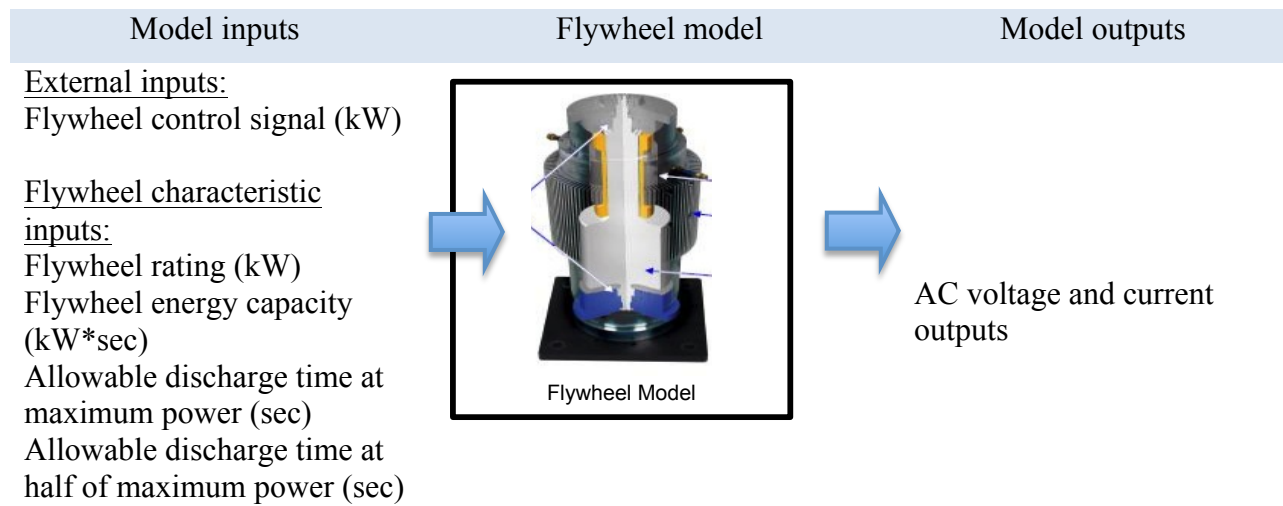
Fig. 4-11. Schematic of the developed flywheel model

Characteristics of three commercially available flywheel units are integrated into the model library. These are a 120kW flywheel unit from AFS Trinity Power Corp., a 160kW flywheel unit from Pentadyne Energy Corp., and a 150kW flywheel unit from Libert Corp. A user can select a "user-defined" flywheel type to create a new flywheel model by entering the required input parameters.

Fig. 12 illustrates how the flywheel model is developed. The model comprises five main subsystems: (1) discharging power calculation; (2) charging power calculation; (3) energy and power constraints; (4) charging and discharging clock; and (5) power and energy calculation, as well as a motor/generator subsystem that is connected to the charge/discharge subsystem but is not shown.
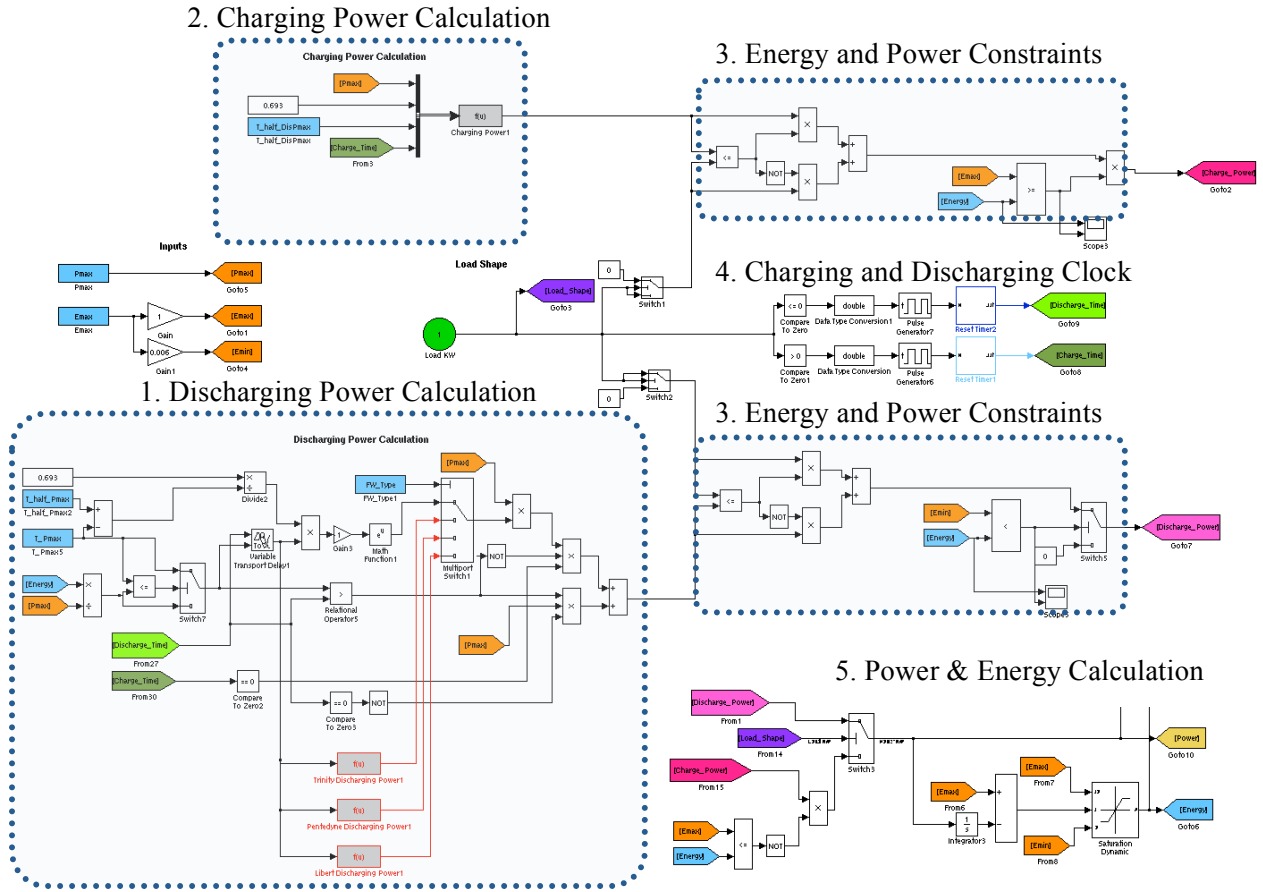
Fig. 4-12. Flywheel model subsystems

The following section describes mathematical formula used in development of the flywheel model. It starts with general mathematical relationships and goes into details of the five subsystems described above.

B) Flywheel Mathematical Model

General mathematical relationship

Nomenclatures:

E	:	Kinetic energy ($kg*m^2/s^2$)
E_{stored}	:	Stored kinetic energy in flywheel
J	:	Moment of inertia ($kg*m$)
k	:	The ratio of maximum speed to minimum speed
K_1	:	Torque conversion factor from mechanical to electrical energy

K_2	:	Coefficient related to system efficiency and mechanical characteristics (1/2J)
m	:	Mass (kg)
η	:	Flywheel discharge efficiency
ρ	:	Mass density (kg/m3)
P_c	:	Load power (watts)
r	:	Distance of rotating arm
t_{fw}	:	Allowable discharge duration (sec)
v	:	Velocity (m/s)
ω	:	Rotational speed (rad/s)

In this study, the flywheel model is developed based on the mathematical relationships in references [38, 39, 40]. Two components affect flywheel performance: polar moment of inertia and rotational speed. These factors appear in Eq. 14, which is the kinetic energy equation. The equation is used to calculate the stored energy in a body of mass (m) moving in a straight line with velocity (v):

$$E = \frac{1}{2} \cdot m \cdot v^2$$

(Eq. 14)

Eq. 14 implies that a body of mass (m) can store more energy with higher rotating speeds. Flywheel is a rotating mass; therefore kinetic energy equation is rewritten based on angular speed (ω) as shown in Eq. 15.

$$E = \frac{1}{2} \cdot m \cdot (r\omega)^2$$

(Eq. 15)

Fig. 4-13 represents the kinetic energy geometry in flywheel.
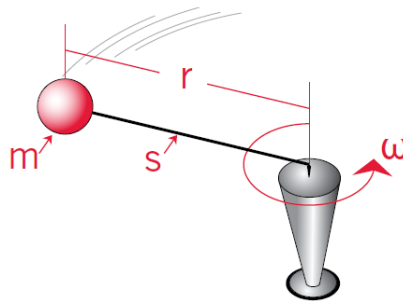
Fig. 4-13. Kinetic energy geometry in flywheel [31]

The other important factor to model a flywheel energy storage system is polar moment of inertia (J). It has the unit of mass time squared radius. For the straight solid cylinder flywheel with outer radius r_o, the polar moment of inertia is:

$$J = \frac{1}{2} \cdot m \cdot r_0^2$$

(Eq. 16)

The flywheel mass with density, ρ, can represent as:

$$m = \pi \cdot \rho \cdot l \cdot r^2$$

(Eq. 17)

Replacing m in Eq. 16 by m in Eq. 17:

$$J = \frac{1}{2} \cdot \pi \cdot \rho \cdot l \cdot r^4$$

(Eq. 18)

The stored kinetic energy in a flywheel can represent as:

$$E_{stored} = \frac{1}{2} \cdot J \cdot \omega_{max}^2$$

(Eq. 19)

Where J is polar moment of inertia (Kg.m) and ω_{max} is angular rotational speed (rad/s). In the flywheel energy system, mechanical aspects, such as motor-generator design and generator capacity, determine the limitation on the minimum and maximum speeds and the amount of the energy that can be stored in a flywheel. In Eq. 20 and 21, the ratio of maximum speed to minimum speed is defined as 'k' factor. Moreover, flywheel discharge efficiency, η, sets additional limitation on the energy that can be delivered to the loads. The extracted energy from the flywheel to the motor/generator is the difference of energy level at maximum and minimum rotating speed:

$$E_{extracted} = \frac{1}{2} \cdot J \cdot (\omega_{max}^2 - \omega_{min}^2) = \frac{1}{2} \cdot J \cdot \omega_{max}^2 \cdot [1 - \left(\frac{1}{k}\right)^2]$$

(Eq. 20)

The delivered energy to load is:

$$E_{load} = \eta \cdot \frac{1}{4} \cdot \pi \cdot \rho \cdot l \cdot r^4 \cdot \omega_{max}^2 \cdot [1 - \left(\frac{1}{k}\right)^2]$$

(Eq. 21)

When the rotor spins up to the regular speed, it can be discharged to produce power in generator. Flywheel discharge characteristic is explained in [41] with differential equation of torque in rotating motion.

$$\frac{d}{dt} J\omega = -K_1 \omega$$

(Eq. 22)

K1 is the torque conversion factor from mechanical to electrical energy. The angular speed during discharge period is a function of time, which can be solved as an exponential function:

$$\omega(t) = \omega_0 \cdot e^{-\frac{K_1}{J}t}$$

(Eq. 23)

Replacing ω_{max} in Eq. 19 by $\omega(t)$ in Eq. 23:

$$E = \frac{1}{2}J\omega_0^2 \cdot e^{-\frac{2K_1}{J}t}$$

(Eq. 24)

The power extracted from flywheel to the generator is:

$$P = K_2\omega_0^2 \cdot e^{-\frac{2K_1}{J}t}$$

(Eq. 25)

Where K1 is the torque conversion factor from mechanical to electrical and K2 is a coefficient related to the system efficiency and mechanical characteristics. Eqs. 23-25 are basis for the flywheel model in the MATLAB/Simulink.

Subsystem 1: Discharging power calculation

The flywheel discharging power is determined based on the manufacturer's suggested flywheel discharge curve. Fig. 4-14 illustrates characteristics of flywheel output power (kW) versus discharge time (sec) of three different flywheel units from three leading flywheel manufacturers.
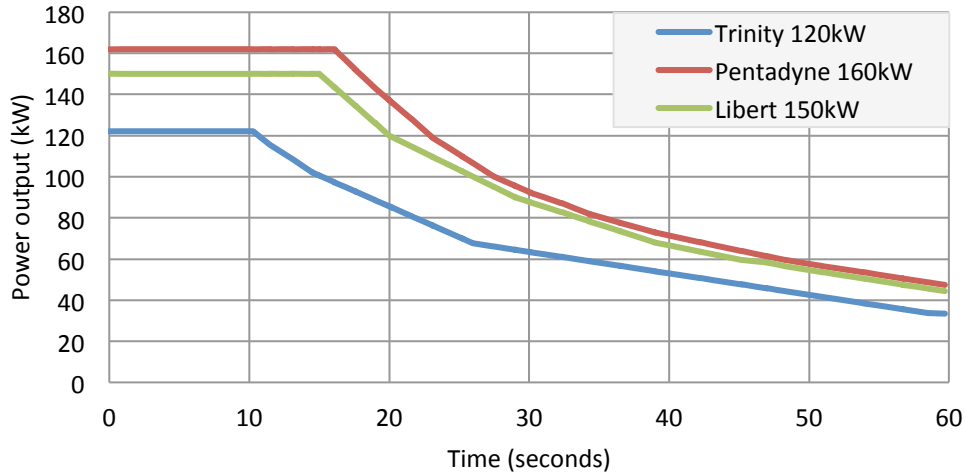
Fig. 4-14. Flywheel output power (kW) versus discharge time (sec)

The curve-fitting program "FZYFit" in MATLAB is used to perform curve fitting of the flywheel discharging characteristics. This module is available free of charge at (http://www.fast.u-psud.fr/ezyfit/). The flywheel discharging behavior can be represented by the exponential function as shown in Eq. 25.

Subsystem 2: Charging power calculation

Typically, flywheels can be charged very quickly, e.g. less than 10 seconds. Table 4-3 shows charging times of flywheels of different capacity and types from the literature.

Table 4-3. Flywheel Charging time in different literatures

Literature	[42]	[43]	[44]	[45]	[46]	[47]	[48]
Charging Time Sec	0.2	1.5	2	5	6	7	7.5
Machine Power	4.5 kW	-	-	11 kW	-	2 MW	2 kW
Rotating Speed rpm	1,775	4,000	58,000	8,000	20,000	15,000	-
Pole	4	-	-	-	-	-	2
Type	-	-	DC Brushless	IPMSM	PM	PM	DC

The flywheel charging time can be represented by an exponential function as follow:

$$P_{ch} = K_1 \omega^2 \left(1 - e^{-\frac{K_2}{J}t} \right) \qquad \text{(Eq. 26)}$$

Where;

K_1: FW charging power amplitude coefficient

K_2: FW charging power exponential time coefficient

K_1 is determined based on the maximum FW power level in kW divided by square nominal rotating speed:

$$K_1 = \frac{P_{ch\_max}}{\omega_{nom}^2} \qquad \text{(Eq. 27)}$$

K_2 represents the charging power rising time which depends on the electric machine type and capacity can be varied from some milliseconds to some seconds. The τ is time constant.

$$K_2 = \frac{J}{\tau} \qquad \text{(Eq. 28)}$$

For commercial flywheels, K_1 and K_2 depend on the electrical machine structure. In design case, user can determine the FW power and rising time.

Subsystem 3: Energy and Power Constraints

The energy constrains ensure that, during the discharge, the extracted energy from the flywheel does not exceed the stored energy; and that, during the charge, the total amount of energy charged does not exceed the allowable stored energy.

$\Sigma E_{dis} <= E_{stored}$

$\Sigma E_{charge} <= E_{capacity}$

The power constrains ensure that, during the discharge, the extracted power does not exceed the power requirement; and that, during the charge, the charged power does not exceed that from the system.

P_{dis} = min (flywheel discharge characteristic, discharge control signal)

P_{ch} = min (flywheel charge characteristic, charge control signal)

Subsystem 4: Charging and Discharging Clocks

This subsystem counts the charge and discharge duration.

Subsystem 5: Power and Energy Calculation

This subsystem calculates instantaneous and accumulative charged and discharged power/energy from flywheel.

C) Model Validation

The model's power output characteristics (flywheel power output in kW versus time in seconds) of three different flywheels (120kW, 150kW and 160kW) are compared with the data from manufacturers, as shown in Fig. 4-15.
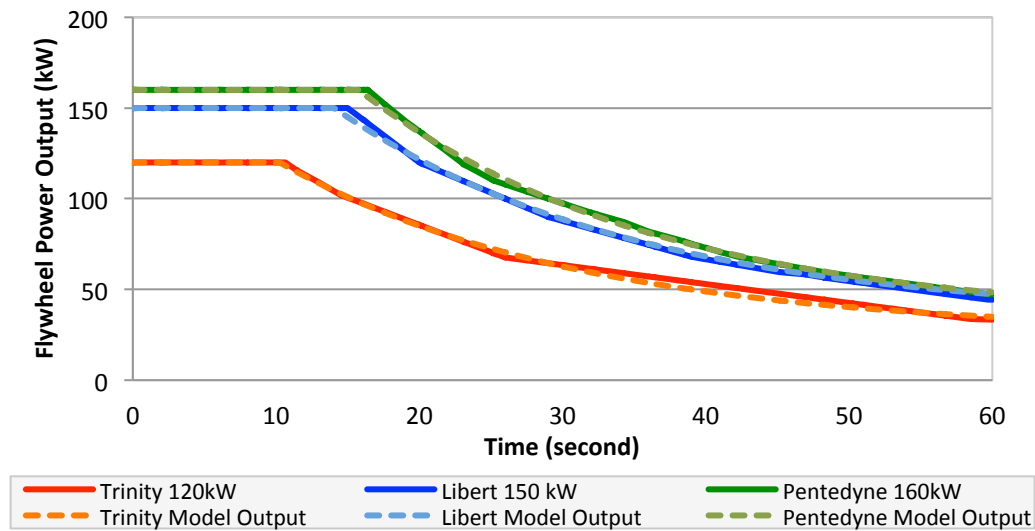
Fig. 4-15. Comparison of the model outputs with the data from manufacturers

Fig. 4-16 illustrates the operation of the developed flywheel model with different charging and discharging power cycles. It presents the flywheel power and energy levels for equal charging and discharging cycles.

Fig. 4-17 presents the flywheel power and energy levels when the charging cycle is shorter than the discharging cycle. As expected, when charging duration is less than the discharging duration, the energy available in Flywheel keeps on decreasing, and the flywheel cannot supply the required energy.
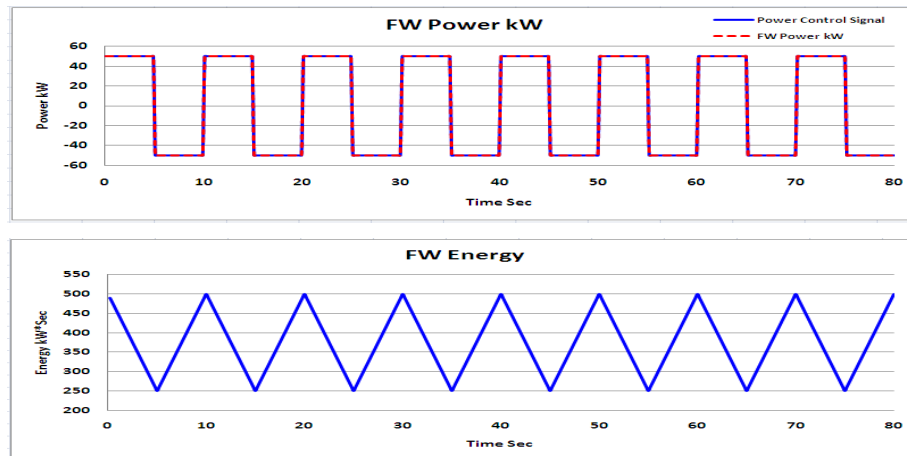
Fig. 4-16. Flywheel power and energy levels for equal charging and discharging cycles (model output)
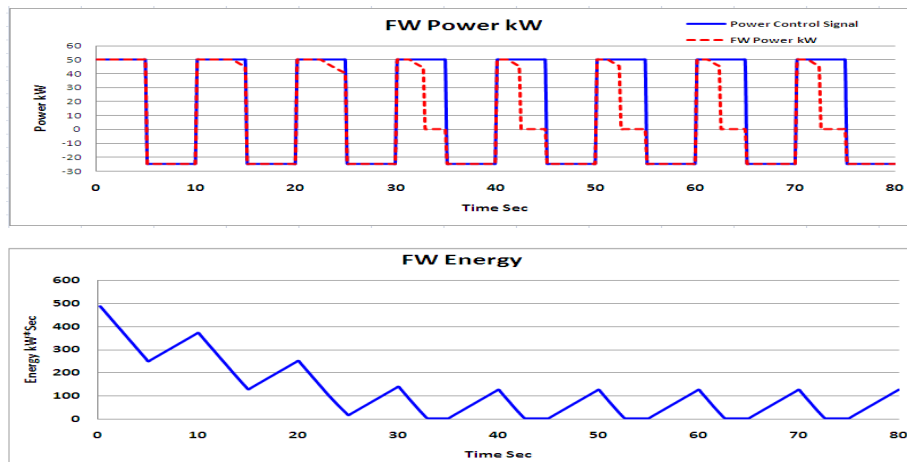
Fig. 4-17. Flywheel power and energy levels when the charging cycle is shorter than the discharging cycle (model output)

4.2 Load Models and Validation

This study focuses on developing generic load models for both residential (military housing) and commercial (office) buildings. For the purpose of this study, loads are classified into controllable and non-controllable loads.

- For residential customers: space cooling, space heating, water heating and clothes drying loads are considered controllable; while cooking, refrigeration, freezer, lighting and other plug loads are considered non-controllable.

- For commercial customers: space cooling and space heating loads constitute the largest share in a typical office building and can be controlled. Other loads used in office spaces, such as lighting, IT equipment and other plug loads, will not be controlled at this time.

This deliverable contains the methodology to develop load models, together with the simulation results and validation, organized by load type.

4.2.1 Space Cooling and Space Heating Load (HVAC)

A) HVAC Model Development

The space cooling and heating load models for both residential and commercial buildings are developed based on the basic operating principle. That is, the room temperature (T_i) is allowed to fluctuate around the thermostat set point (T_s) within a certain dead band ($\pm\Delta T$). The space cooling/heating unit is ON when the room temperature is above/below the threshold ($T_s\pm\Delta T$). The space cooling/heating unit is OFF when the room temperature is within the threshold ($T_s-\Delta T < T_i < T_s+\Delta T$).

Fig. 4-18 illustrates the block diagram of the HVAC load model.
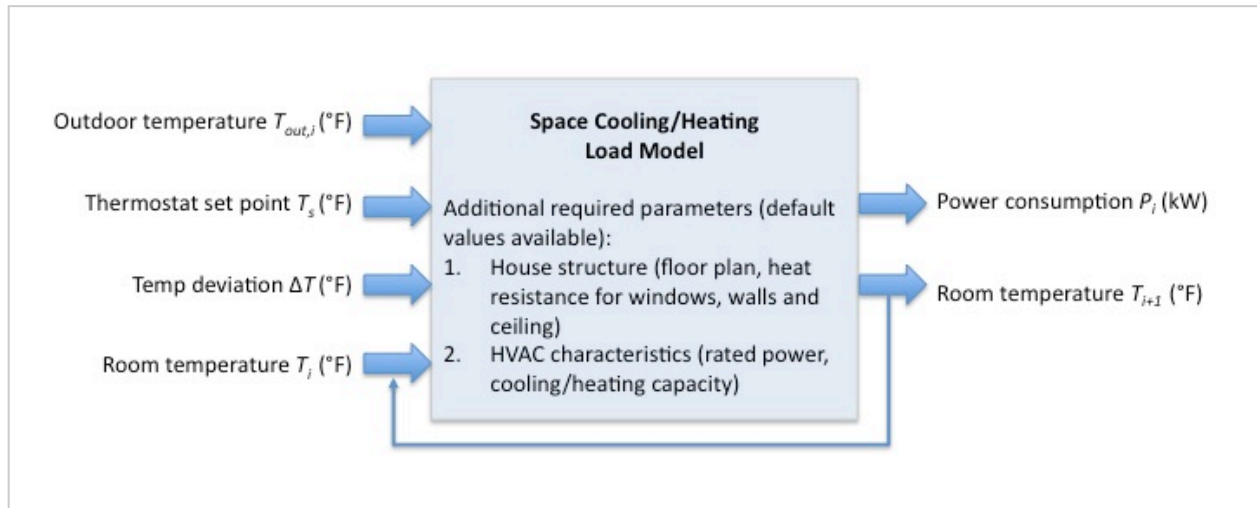
Fig. 4-18. HVAC load model block diagram

Inputs of the model are the time series outdoor temperature data (°F), a thermostat set point (°F), the allowable temperature deviation or dead band (°F), and the time series room temperature data (°F). The model outputs are the time series electric power consumption (kW) of the HVAC unit, and the room temperature (°F) at the next time step. The room temperature output is used as an input to the load model at the next time step.

Determination of power consumption P_i (kW): The power consumption of the HVAC unit at time step i can be expressed as:

$$P_i = P_{HVAC} \cdot w_i \qquad \text{(Eq. 29)}$$

Where,

P_i : Power consumption of the HVAC unit at time step i (kW)

P_{HVAC} : Rated power of the HVAC unit (kW)

w_i : ON/OFF status of the HVAC unit.

   - w_i is 1 when the HVAC unit is ON.

   - w_i is 0 when the HVAC unit is OFF.

The ON/OFF status of the HVAC load (w_i) depends on the room temperature, the thermostat set point and the temperature deviation dead band. In the winter, for example, when the room temperature is lower than a preset temperature ($Ts-\Delta T$), the HVAC system is ON ($w_i = 1$) and simply operates at its rated power (P_{HVAC}). Once the room temperature exceeds a certain threshold ($Ts+\Delta T$), the unit turns OFF ($w_i = 0$).

Determination of room temperature T_{i+1} (°F): Room temperature (°F) can be determined based on (a) the amount of heat gain/loss, which depends on the house structure and the outdoor temperature, and (b) the capacity of the HVAC unit. The room temperature can be expressed as:

$$T_{i+1} = T_i + \underbrace{\Delta t \cdot \frac{G_i}{\Delta c}}_{\substack{T\alpha \quad \text{Amount of} \\ \text{Heat Gain/Loss}}} + \underbrace{\Delta t \cdot \frac{C_{HVAC}}{\Delta c} \cdot \omega(i)}_{\substack{T\alpha \quad \text{Capacity of} \\ \text{HVAC unit}}} \qquad \text{(Eq. 30)}$$

Where,

T_{i+1} : Room temperature at time slot i+1 (°F)

T_i : Room temperature at time slot i (°F), assuming that $T_0 = T_s$

Δt : Length of time slot (hour)

G_i* : Heat gain rate of the house during time slot i (BTU/h)

   - G is positive when outdoor temp is higher than the indoor temp.

   - G is negative when outdoor temp is lower than the outdoor temp.

$\Delta c*$: Amount of energy needed to change the house temperature by 1 °F (BTU)

C_{HVAC} : Capacity of the HVAC unit (BTU/h)

- C$_{HVAC}$ is positive for the space heating load

- C$_{HVAC}$ is negative for the space cooling load

* G_i and Δc are explained in further details below.

Determination of heat gain rate (BTU/h):

The heat gain rate can be calculated as:

$$G_i = \left(\frac{A_{wall}}{R_{wall}} + \frac{A_{ceiling}}{R_{ceiling}} + \frac{A_{window}}{R_{window}} \right) \cdot \left(T_{out,i} - T_i \right) + \frac{A_{floor}}{R_{floor}} \cdot \left(T_i - T_{soil} \right) + SHGC \cdot A_{window\_south} \cdot H_{solar} \cdot \frac{3.412 Btu/Wh}{10.76 ft^2/m^2}$$

(Eq. 31)

Where,

$A_{wall}, A_{ceiling}, A_{window}, A_{floor}$	:	Area of the wall, ceiling, window, and ground floor of the house (ft2), respectively
$R_{wall}, R_{ceiling}, R_{window}, R_{floor}$	:	Heat resistance of the wall [49], ceiling, window, and ground floor of the house (°F·ft2·h/BTU), respectively
T_{soil}	:	Soil temperature (°F), which is usually very stable for a relatively long period like a month. The soil temperature can be found from Soil Climate Analysis Network (SCAN) [50].
$SHGC$	:	Solar heat gain coefficient of windows [51]
H_{solar}	:	Solar radiation heat power (Wh/m2)

Determination of the amount of energy needed to change the house temperature by 1°F:

To change the house temperature by 1°F, the amount of energy needed (Δc) can be calculated by:

$$\Delta c = C_{air} \cdot V_{house} \qquad \text{(Eq. 32)}$$

Where,

C_{air}	:	Specific heat capacity of air (BTU/ft3*ΔF)
V_{house}	:	Volume of the house (ft3)

C$_{air}$ can be determined using the following relationship:

$$C_{air} = 1.012 \frac{J}{g \cdot K} * 0.00095 \frac{BTU}{J} * 1.29 \frac{g}{L} * 28.32 \frac{L}{ft^3} * \frac{5}{9} \frac{\Delta K}{\Delta F} = 0.0195 \frac{BTU}{ft^3 \Delta F} \qquad \text{(Eq. 33)}$$

Note that:

- The specific heat capacity of air under typical room condition is 1.012 J/g·K.

- The density of air under normal condition is 1.29 g/L.

B) HVAC Model Validation

To validate the developed model, the HVAC model is run with the inputs (outdoor temperature, thermostat set point, dead band, house structure parameters, and HVAC unit size) from a real house in Charlottesville, VA. Using the same inputs, the model outputs (power consumption and indoor temperature) are compared with the actual measurements. This comparison is illustrated below for two 24-hour periods, one in the month of August for space cooling demand; and the other for the month of January for space heating demand.
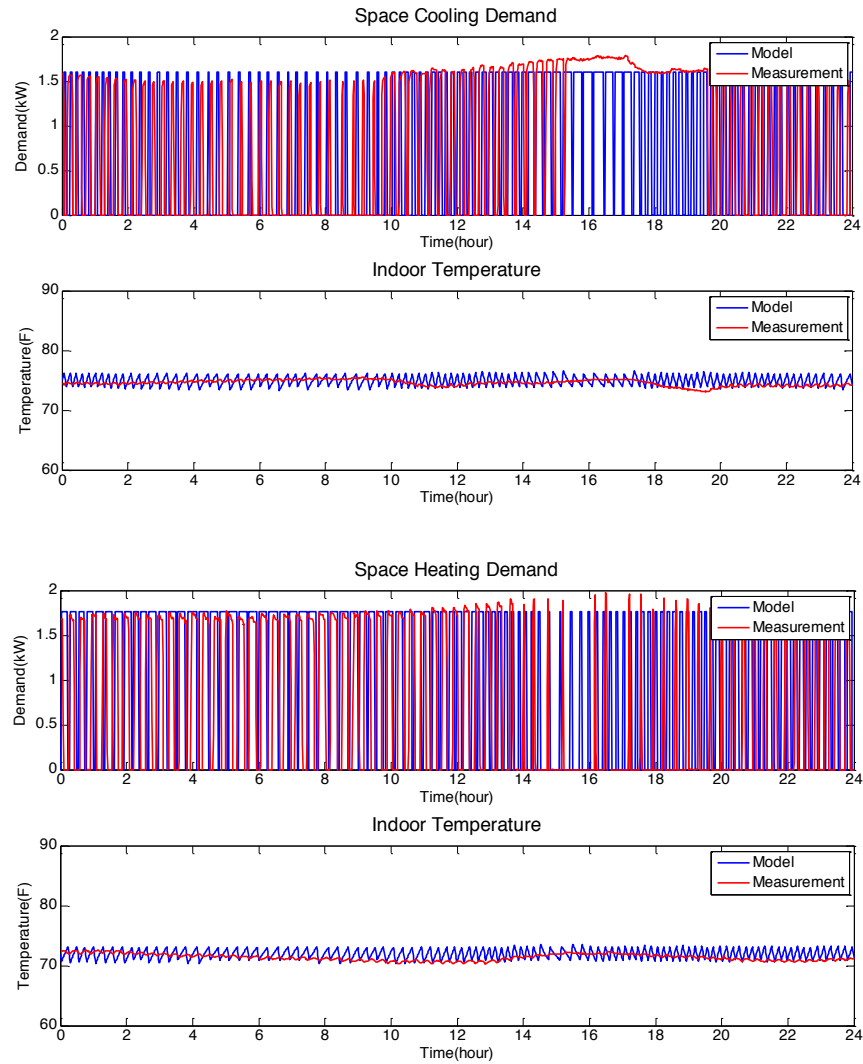
Fig. 4-19. HVAC model validation –comparison of load profile and indoor temperature

Fig. 4-19 indicates similarities between the actual power consumption and the model output. The discrepancy as shown may result from some assumptions made in house structure parameters, and possibly measurement errors from the real house.

36

4.2.2 Water Heating Loads

A) Water Heater Model Development

For a water heater with a tank for hot water storage, suppose the temperature set point of the hot water outlet is T_s, and the lower bound temperature tolerance is ΔT. When the mixed water temperature drops below the lower bound, i.e. $T_i < T_s - \Delta T$, the heating coils will start working, and consume electricity at its rated power until the outlet hot water temperature reaches the temperature set point, i.e. T_s. As long as the outlet water temperature is kept within the range of the dead band, i.e. $T_s - \Delta T < T_i < T_s$, the heating coils will keep their status.

Fig. 4-20 illustrates the block diagram of the developed water heater load model. Inputs of the model are hot water flow rate (gpm), inlet water temperature (°F), ambient temperature (°F), outlet hot water temperature set point (°F), temperature deviation (°F), and tank water temperature (°F). The model outputs are the time series electric power consumption (kW) of the water heater unit, and the tank water temperature (°F) at the next time step. The tank water temperature output is used as an input to the load model at the next time step.
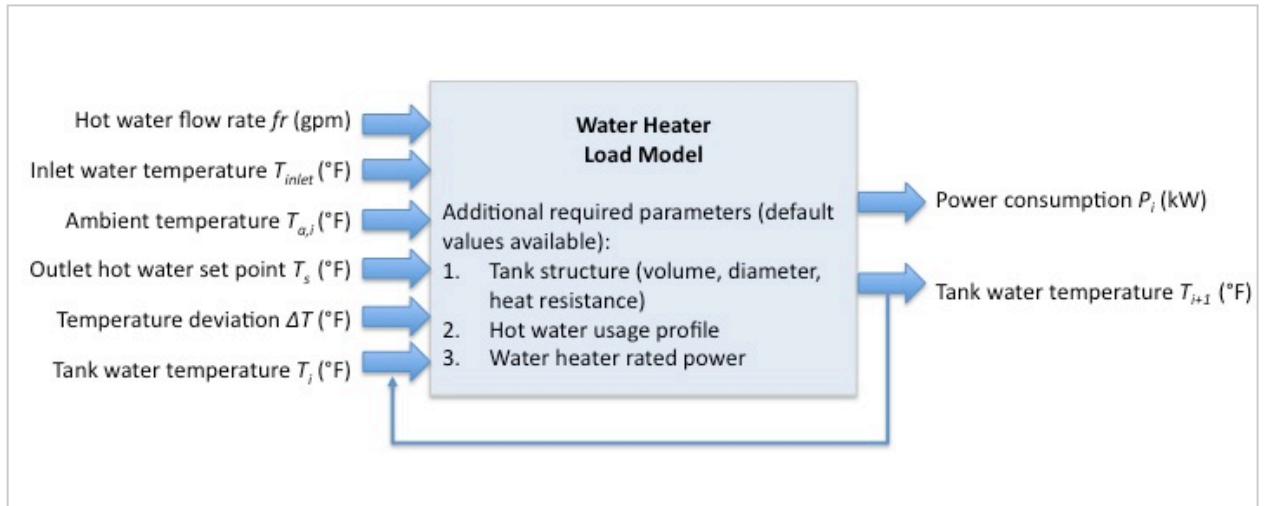
Fig. 4-20. Block diagram of the developed water heater load model

Determination of power consumption P_i (kW):

The water heater load model can be expressed as:

$$P_i = \eta \cdot P_{WH} \cdot w_i \qquad \text{(Eq. 34)}$$

Where,

P_i :   Power consumption of the water heating load at time step i (kW)

η :   Water heater efficiency

P_{WH} :   Rated power of the water heater (kW)

w_i : ON/OFF status of the water heater load.

- ω_i is 1 when the water heater is ON.

- ω_i is 0 when the water heater is OFF.

The ON/OFF status of the water heater load (w_i) depends on the tank water temperature, the outlet hot water temperature set point, the ambient temperature, the allowable temperature deviation dead band, the hot water flow rate, and the inlet water temperature. For example, when the tank water temperature is lower than a preset temperature, the water heater is ON ($w_i = 1$) and simply operates at its rated power. Once the tank water temperature exceeds a certain threshold, the water heater turns OFF ($w_i = 0$).

Determination of tank water temperature T_{i+1} (°F): The tank water temperature (°F) can be determined based on (a) the amount of heat loss, which depends on the tank structure and the ambient temperature, (b) the rated power of the water heater, (c) the inlet water temperature and flow rate (which equals the outlet hot water flow rate). The tank water temperature can be expressed as:

$$T_{i+1} = \frac{T_i \cdot \left(V_{\tan k} - fr_i \cdot \Delta t\right) + T_{inlet,i} \cdot fr_i \cdot \Delta t + \left(\dfrac{P_i \cdot 3412 BTU / kWh - L_{s,i}}{8.34 lb / gal}\right) \cdot \Delta t}{V_{\tan k}} \tag{Eq. 35}$$

Where,

T_{i+1} : Tank water temperature, i.e. outlet hot water temperature at time slot i+1 (°F)

T_i : Tank water temperature, i.e. outlet hot water temperature at time slot i (°F)

$T_{inlet,i}$ Inlet water temperature, assuming to be equal to the local soil temperature (°F)

V_{tank} : Water heater tank size (gallon)

fr_i : Hot water flow rate, i.e. inlet cold water flow rate in time slot I (gallon/hour)

Δt : Length of time slot (hour)

$L_{s,i}$: Heat loss rate of the tank during time slot i (BTU/hour)

* $L_{s,i}$ is explained in further details below. Note it requires 1BTU to heat 1 lb of water by 1F.

- Determination of heat loss rate (BTU/h):

The heat loss rate can be calculated as:

$$L_{s,i} = \frac{A_{\tan k} \cdot \left(T_i - T_a\right)}{R_{\tan k}} \tag{Eq. 36}$$

38

Where,

A_{tank} :   Water heater tank surface area (ft^2), which can be calculated as:

$$A_{\tan k} = \frac{1}{2}\pi \cdot d_{\tan k}^2 + \frac{4\, V_{\tan k} \cdot \left(0.134 ft^3 / gal\right)}{d_{\tan k}}$$

T_a :   Water heater tank ambient temperature (°F), which is assumed to be equal to room temperature set point Ts.

R_{tank} :   Heat resistance of the water heater tank (°F·ft2·h/BTU)

d_{tank} :   Diameter of the tank (ft)

Note that the definition of 1 Btu is the energy needed to heat 1 lb water up by 1F. Therefore for water heating, 1BTU = 1lb.°F.

B) Water Heater Model Validation

Fig. 21 shows the comparison of the water heater power consumption (kW) generated from the model (left) and the measured power consumption (right) recorded from a house by The Energy Detective (TED) device.
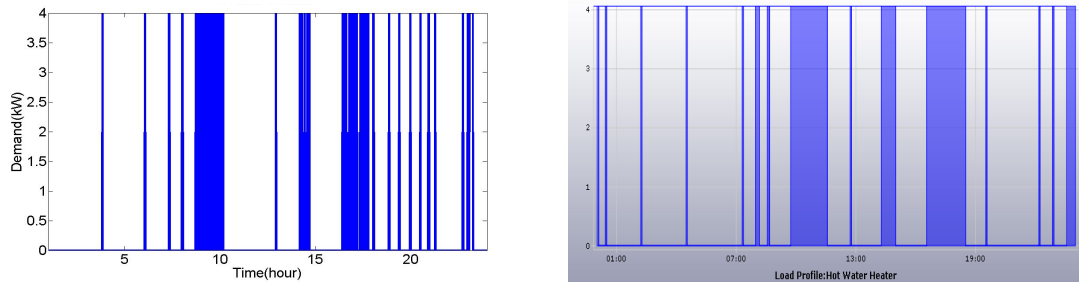
Fig. 4-21. Water heater model validation – load profile comparison

The comparison indicates some similarities between the two water heater load profiles. The discrepancy as shown may result from some assumptions made regarding the amount of water usage, and the water heater parameters.

4.2.3 Clothes Dryer Loads

A) Clothes Dryer Model Development

A typical clothes dryer comprises both the motor and the heating elements. The power requirement of the motor element is approximately several hundred watts, but that of the heating elements can be several kilowatts.

Fig. 4-22. Clothes dryer load model block diagram

The clothes dryer's power consumption can be expressed as:

$$P_i = P_h \cdot W_{h,i} \cdot W_{c,i} + P_m \cdot W_{m,i} \qquad \text{(Eq. 37)}$$

Where,

P_i : Power consumption of the clothes dryer at time slot i (kW)

P_h : Power consumption of the heating element (kW), which depends on the power set point level, e.g. low heat, medium heat or high heat

P_m : Power consumption of the motor element (kW)

$w_{h,i}$: Status of the heating element at time slot i
$w_{h,i} = 0$ when the heating element is OFF
$w_{h,i} = 1$ when the heating element is ON

$w_{c,i}$: Signal to control the status of the heating element at time slot i
$w_{c,i} = 0$ when the heating element is OFF
$w_{c,i} = 1$ when the heating element is ON

$w_{m,i}$: Status of the motor at time slot i
$w_{m,i} = 0$ when the heating element is OFF
$w_{m,i} = 1$ when the heating element is ON

40

In the developed clothes dryer model, it is assumed that the motor keeps running for 10 minutes to use up the remaining heat after the clothes is dried.

B) Clothes Dryer Model Validation

To validate the developed model, the clothes dryer model is run with the inputs (usage profiles and clothes dryer rated power) from a real house in Mclean, Virginia. Using the same inputs, the model output (power consumption) is compared with the actual clothes dryer power consumption measurements. This comparison is illustrated in Fig. 4-23, which shows the comparison of the clothes dryer power consumption (kW) generated from the model (red) and the measured power consumption (blue) recorded from a house by The Energy Detective (TED) device. The comparison indicates some similarities between the two water heater load profiles.
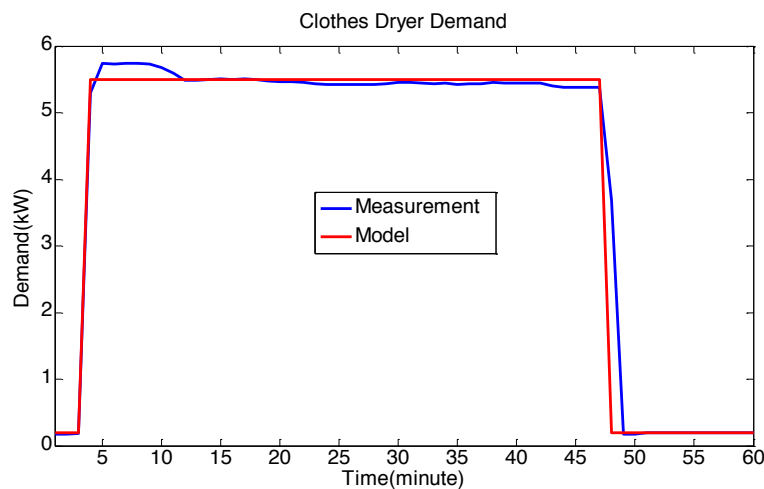
Fig. 4-23. Clothes dryer load comparison

4.2.4 Other Loads

Instead of developing the models of other loads that are not controllable, this study uses the historical data of non-controllable load profiles from the industry-accepted database, i.e. RELOAD database [52].

4.2.5 One-house Load Profile

To create household load profiles, this study develops controllable load models using a bottom-up approach as described earlier in Sections 4.2.1-4.2.3. Load profiles of the critical loads are derived from the RELOAD database, which is an industry accepted load profile database. This is discussed in Section 4.2.4.

An example of a residential house load profile (the output of the developed load models) is shown in Fig. 4-24, in comparison with the actual household electricity consumption of a house in central Virginia which has similar climatic conditions as in Ft. Bragg.
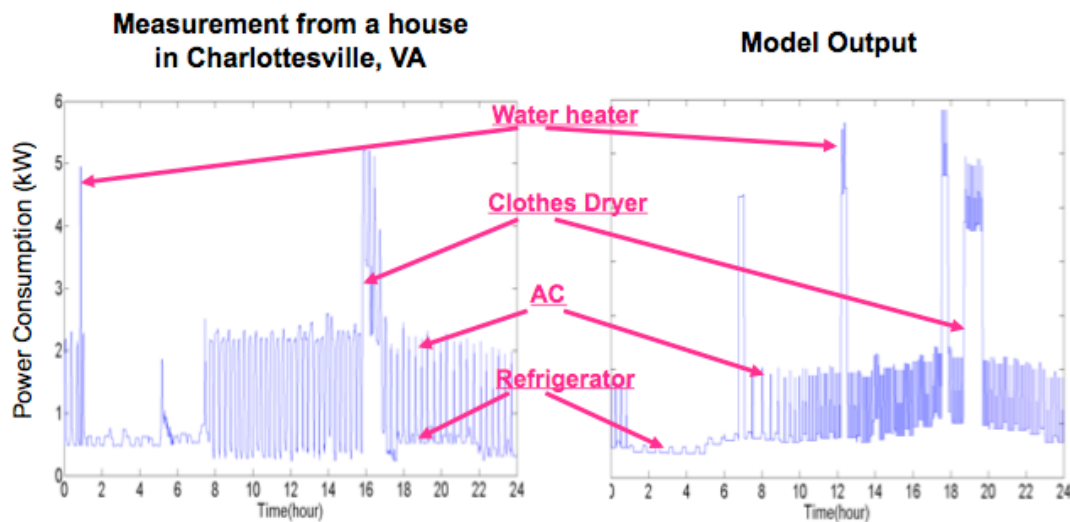
Fig. 4-24. Comparison of household load profiles from:
a house in central Virginia (left) and output from the developed load models (right)

The comparison indicates similarities between the actual power consumption and the model output. The discrepancy as shown may result from some assumptions made in house structure parameters, and possibly measurement errors from the real house. The one-house load profile as shown is diversified to generate a distribution circuit load profile in the next Section (4.2.6).

4.2.6 Aggregation of Load Profiles

To study the total demand in the whole distribution network, demand aggregation is needed to show the integrated result. To aggregate the demand, the most important thing is to find out how to model the difference between each building in the distribution network. This is to determine different input parameters for the models to represent different buildings. As the critical loads can be easily aggregated based on the numbers of each building type, the main work in demand aggregation is to diversify the controllable loads, namely HVAC, water heater and clothes dryer units.

A) Aggregation of HVAC Loads

The input parameters for space cooling/heating model can be divided into three categories: temperatures, building structures and HVAC characteristics.

The temperature category includes outdoor temperatures and indoor temperature set points. Outdoor temperatures can be acquired from National Climatic Data Center (NCDC) [53]. For indoor temperature set points, this study derives the indoor temperature set points for all residential houses in the distribution network as a uniform random function based on typical residential indoor temperature set points reported by ASHRAE [54]. The set points are between 74°F and 78°F in summer, and about 10 degree lower in winter. Based on the assumption above, the temperature set points can be derived using a random function as follows.

> *Ts_AC = round(random ('unif',74,78,[1,n])); % indoor temperature set point*

The building structure category includes the floor plan of the buildings, areas of walls, ceilings and windows as well as the R-values for each of them. Such typical data for residential houses and commercial buildings can be obtained from the American Housing Survey [55] and the Commercial Buildings Energy Consumption Survey [56], respectively. Based on the two sets of survey data, the building structure data for many homes and buildings are derived using uniform random functions, as follows.

> *R_window = round(random('unif',2,8,[1,n])); % heat resistance for windows*
> *R_wall = round(random('unif',16,24,[1,n])); % heat resistance for walls*
> *R_ceiling = 2.*R_wall; % heat resistance for ceilings*
> *A_floor = round(random('norm',1500,50,[1,n])); % house floor area in ft^2*
> *for m=1:n % number of stories*
> *if A_floor <= 900*
> *n_floor(m) = 1;*
> *else*
> *n_floor(m) = 2;*
> *end*
> *end*
> *h_house = 10.*n_floor; % house height in feet*
> *A_wall = .8*4.*nthroot(A_floor,3).*h_house; % wall area in ft^2*
> *A_window = .25.*A_wall; % window area in ft^2*
> *A_ceiling = A_floor./n_floor; % ceiling area in ft^2*

The HVAC characteristic category includes the cooling/heating capacities and power consumptions, which is usually known as HVAC sizing. Usually, the sizing is based on the building floor plans, activities, occupants and environment. In the same neighborhood, the environment factor can be assumed to be the same for all buildings. Thus, HVAC sizing can be calculated according to ASHRAE handbook of fundamentals [57].

After getting all three sets of random functions for these input parameters, the demand aggregation for HVAC is quantified by running the space cooling/heating model N+M times with different parameters. (N is the number of residential houses in the distribution network and M is the number of commercial buildings.)

B) Aggregation of Water Heater Loads

The input parameters for water heater model can be divided into three categories: temperatures, water heater characteristics and hot water usage.

The temperature category includes tank ambient temperatures, inlet water temperatures and hot water temperature set points. Tank ambient temperature is assumed to be the same as the room temperature, which can be acquired from the space cooling/heating model. Inlet water temperature is assumed to be the same as the soil temperature, which can be acquired from SCAN [58]. Hot water temperature set points is reasonably assumed to be between 110°F and 120°F [59]. The hot water temperature set points for all residential houses in the distribution network can be modeled using a uniform random function with 110°F and 120°F as the lower and upper limits. The dead band can be from ±5°F to ±10°F.

> *Ts_WH = round(random ('unif',110,120,[1,n])); % tank water temp set point*

The water heater characteristics include the R-values, tank sizes and rated powers. The R-value for a conventional water heater is between 12 and 25 [60]. Therefore the R-values for all the residential water heaters in the distribution network can be represented by a uniform random function with 12 and 25 as the lower and upper limits. As the hot water daily usage is between 30 and 60 gallons, it is reasonable to assume that the water heater tank sizes are between 40 gallon and 50 gallon. The rated power of the water heater is related to the size of the tank, usually between 4 to 5 kW. A uniform random function is used to represent the residential water heater characteristics in the distribution network.

> *V_tank = 5.*round(random('unif',8,10,[1,n])); % tank size in gallon.*
> *P_WH = V_tank./10; % water heater rated power in kW.*
> *R_tank = round(random('unif',12,19,[1,n])); % tank heat resistance*

Hot water usage can be categorized into four types for simplicity: kitchen, sink, laundry and shower/bath. According to [61], the four types have in general the daily water usage of 37.3%, 12%, 12.4% and 38.3% respectively. Based on the typical household hot water usage between 30 and 60 gallons per day [61], the water consumption duration in minute is the hot water demand in gallon divided by the flow rate in gallon per minute (gpm). Monte Carlo method is used to decide when the hot water is consumed based on data shown in [62]. The hot water usage profiles are then created by repeating this for four usage types and N residential houses.

> *% Kitchen 37.3%, Sink 12%, Laundry 12.4%, Shower and Bath 38.3%*
> *Type = [.373,.12,.124,.383];*
> *fr = [1.5,1.5,1.5,2.5]; % flow rate for each usage type*
> *V_total = round(random('unif',30,60,[1,n])); % daily hot water usage, in gallon*

C) Aggregation of Clothes Dryer Loads

Residential clothes dryers are large loads, consuming 4kW or more, and their running times vary according to people's life style. This study assumes that people use their clothes dryers at least once per week. The dryer start time profile is developed based on a probability distribution function that is similar to the average dryer power consumption profile obtained from the measurement of a home in Florida [63]. It is also assumed that the dryer start times vary from late morning to midnight, with the mean in the evening. Then, the demand aggregation of clothes dryers is acquired by combining the clothes dryer load model with the probabilistic start times to determine the aggregated dryer load profile for all N residential houses in a distribution network.

```
k = random('unif',0.8,1,[1,n]); % clothes drying level
P_CD = round(random('unif',4,5,[1,n])); % clothes dryer rated power
P_CD_h = k.*P_CD; % heating power
P_CD_Motor = 0.2; % in kW
pdf_CD = poisspdf(4:22,18); % clothes dryer using time
```

D) Aggregation of Critical Loads

As the critical loads come from average data, the aggregation of critical loads is to multiply the load profiles for one building by the number of each type of building.

E) Aggregation Results - Distribution Circuit Load Profiles

To create distribution circuit load profiles, the inputs to the load models are diversified based on the methodology described in Section 4.2.6. Fig. 4-25 shows the summer and winter load profiles of the distribution circuit of interest (761 residential customers) for a 24-hour period.
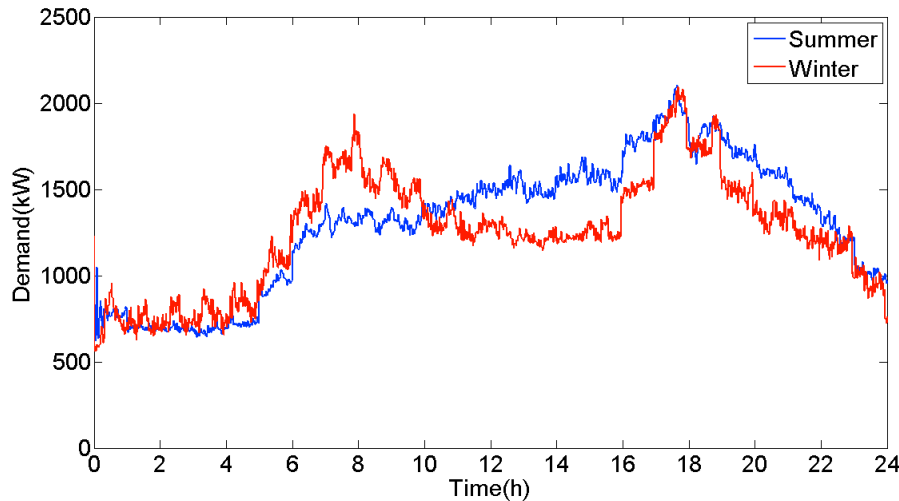
Fig. 4-25. 24-hour load profiles of a distribution circuit in summer/winter (simulation output)

45

Fig. 4-26 presents load profiles of appliance by type.
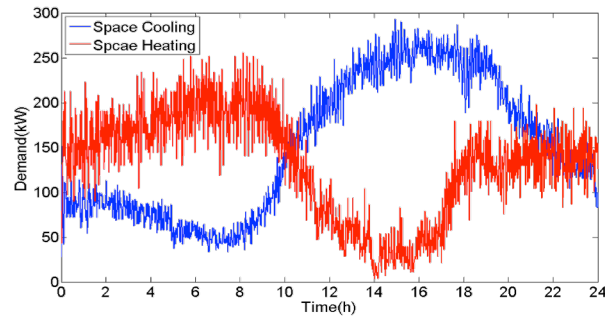
(a) HVAC load profiles in summer/winter
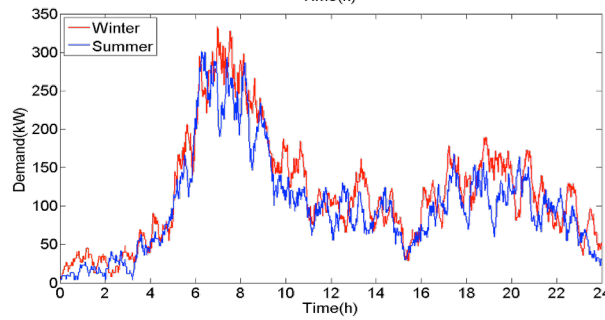
(b) Water heater load profiles in summer/winter
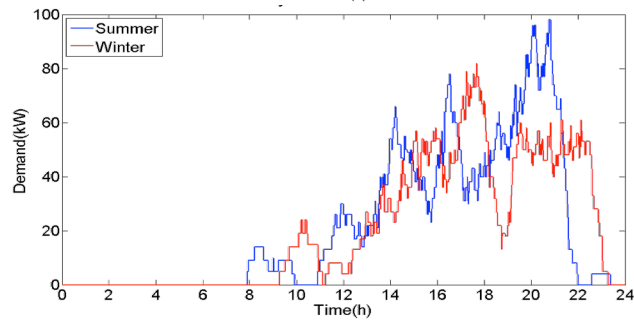
(c) Clothes dryer load profiles in summer/winter

Fig. 4-26. 24-hour load profiles by appliance (simulation output):
(a) HVAC; (b) water heater; (c) clothes dryer

4.3 Microgrid Management Strategies

This deliverable contains the microgrid management strategies to perform load and generation control during both the grid-connected and islanded modes.

During the grid-connected mode, many military bases, like Fort Bragg, are subject to real-time electricity pricing, which can vary every 15 minutes. During such high summer peak periods, the electricity price can go as high as 80 cents/kWh. Some military bases need to pay for demand charge ($/kW) if the demand for electricity for the whole base exceeds a certain value. Therefore there are significant potential saving opportunities through implementing load and generation controls in a microgrid environment to shave the peak demand. In these cases, the load and generation control algorithms can be initiated to:

- Keep the electricity demand/consumption low to avoid high peak prices.

During the islanded mode, an emphasis is put on controlling both loads and generation to secure critical loads and satisfying consumer's needs. In these cases, the load and generation control algorithms can be initiated to:

- Manage the microgrid's internal loads during a utility outage, given that there are one or more internal generation sources available in the microgrid.

4.3.1 Control Algorithms to Avoid High Peak Prices

This strategy involves both load and generation control, which can be described as follows:

> **Step 1: Renewable generation**
> - Electricity from renewable energy sources, e.g. PV, is utilized as much as possible.
>
> **Step 2: Distributed generator and storage control**
> - Diesel/gas engine generators and energy storage devices, if available on the base, can be used to shave the peak demand. The decision to run generators will depend on the number of hours a particular generator can run in a year for peak shaving purposes.
>
> **Step 3: Demand response**
> - Demand response can be performed to help reduce additional peak demand.

During a normal operating condition, there is no utility outage, and no load shedding should be performed. Renewable energy sources in the circuit should be utilized as the first priority, and as much as possible. Then, diesel/gas engine generators and energy storage devices, if available on the base, can be used to shave the peak demand. The decision to run generators will depend on the number of hours a particular generator can run in a year for peak shaving purposes. For example, at Ft. Bragg, this limit is 250 hours/year. In California, this limit is 40 hours/year due to

its stringent requirements. Therefore, it is necessary to carefully plan for generators' run times to maximize their peak shaving benefits. For storage, it is necessary to carefully plan for the storage unit's charge and discharge schedule to maximize storage use. Then, demand response can be performed to help reduce additional peak demand. For example, it is possible to increase HVAC temperature set points for office buildings during the peak periods. The methodology to perform demand response for both office buildings and residential houses (or military houses) is discussed in details in Section 4.3.3.

4.3.2 Control Algorithms to Manage the Demand during a Utility Outage

This strategy involves both load and generation control, which can be described as follows:

> **Step 1: Generation control**
> - Electricity from renewable energy sources, e.g. PV, is utilized as much as possible.
> - DER is called upon to serve the circuit's internal loads.
>
> **Step 2: Load Shedding and Demand response**
> - Demand limit is set by the availability of internal generation. Non-critical demand that exceeds the capacity of internal generation needs to be shed.
> - Demand response is performed as needed to limit the peak demand of critical loads not to exceed the capacity of available internal generation.

Once there is a utility outage, available internal generation or distributed energy resources (DERs) will be called upon. It is important when designing the microgrid that the locally available DERs must be sized to provide the real and reactive power requirements of critical loads. They must also be capable of providing frequency stability and operate within the voltage ranges as specified in ANSI C84.1. To balance load and generation, load shedding and demand response may become necessary if load requirements are greater than the generation available.

Loads on a military base can be classified by building function, for example:

- o Administration buildings
- o Barracks
- o Carwash facilities
- o Dining halls
- o Hospitals
- o Storage facilities
- o And others, e.g., maintenance facilities, training facilities, schools, classrooms, operation centers, water treatment plants, gyms, fire stations and EV charging stations.

Load prioritization by building function will allow for disconnecting or connecting the loads according to their priority, as needed. To start, one must rank order the loads from the most important load to the least important load, and list their kW size. For example, from the list of six building functions provided above, hospitals can be the highest priority load, followed by dining halls, barracks, admin buildings, carwash and storage facilities.

Depending on the capacity of available internal generation, the least important loads will need to be shed to allow matching between demand and supply within a microgrid. For a system with renewable energy sources, electricity from such sources, e.g. PV, should be utilized as much as possible. All other fossil fuel-based DERs should be operated according to their merit orders. Demand response can be performed as needed to limit the peak demand of critical loads not to exceed the capacity of available internal generation. The methodology to perform demand response for both office buildings and residential houses (or military houses) is discussed in details in Section 4.3.3.

4.3.3 Demand Response Strategy

Demand response can be performed in commercial (office) buildings or residential (military) houses. In office buildings, the most common demand response approach is to increase space cooling temperature set point. In military houses, with the advance in smart grid technologies and the introduction of smart appliances, it is possible to control household loads at the appliance level. This section presents an approach to perform demand response, taking into account load priority and consumer's preference. It is assumed that the infrastructure is readily available that allows the proposed demand response algorithm to take place.

In this study, for a residential home, HVAC loads, water heater loads, clothes dryer loads and electric vehicles (if any) are controllable, while all other loads are not to be controlled. The procedure to perform demand response taking into consideration consumer convenience and preference in the following manner:

- **Step 1. Consumers set their load priority.**
  The load priority is set based on consumer choices. For example, for house#1, HVAC may have the highest priority, water heater may lower priority and clothes dryer may have the lowest priority. Other houses may set their priority differently. If a house has an electric vehicle (EV), its priority must be set as well.

- **Step 2. Consumers set their convenience preference.**
  For example, operation clothes drying load must be completed within 2 hours; room temperature should not be higher than 81°F; and an electric vehicle, if applicable, must be completely charged during the night before 7am.

- **Step 3. The system performs automated demand response.**
  The automated demand response process is performed based on the preset load priority and convenience preferences. When the home control center sees the preferences are being violated, the corresponding loads' priorities will be temporarily raised to the highest.

An example of priority and preference settings is presented in Table 4-4.

Table 4-4. Example of Priority and Preference Settings in a Home

	Load			
	AC	Water Heater	Clothes Dryer	Electric Vehicle (EV)
Priority setting	2	1	4	3
Preference setting	<81°F	>= 100°F	Finish the job by midnight	Fully charged by 8pm

According to Table 4-4, this home sets the water heater load at the highest priority. This is followed by AC, electric vehicles and clothes dryer. This setting will vary from home to home based on the occupants' needs, and ambient conditions. In the example above, the preference settings are configured such that the room temperature does not to exceed 81°F, the hot water outlet temperature does not to drop below 100°F, the clothes dryer is required to finish its job by midnight, and the EV must be fully charged by 8pm.

The load control strategy implemented will vary by load type, as summarized in Table 4-5.

The control strategy for the HVACs is that, during a supply limit event, the HVAC units will be turned OFF. However, if the room temperatures go out of the comfort range pre-determined by a consumer, HVACs will be turned ON to keep the temperatures within the comfort zone.

The control strategy for the water heaters is that, during a supply limit event, the water heater units will be turned OFF. However, if the water temperatures go out of the comfort range pre-determined by a consumer, water heaters will be turned ON to keep the temperatures within the comfort zone.

The control strategy for clothes dryers is that, during a supply limit event, the motor elements of the cloth dryers will keep on operating while the heating elements of the clothes dryers will be turned OFF. However, the heating coils of a clothes dryer should not be kept OFF for more than a certain period of time. In such an event, the clothes dryer heating coil will be forced ON to complete its function according to the maximum duration specified by a consumer.

The control strategy for an electric vehicle (if applicable) is that, during a supply limit event, the electric vehicles will not be charged. The battery state of charge (SOC) is monitored to make sure the charging can be finished by a given time without requiring charge rate higher than the outlet rating. The central home controller will change the EV's priority to ensure that the EV can complete its charge by the time specified by an EV owner. EV is a special controllable load that can do better than other controllable loads that can only simply shut down or cycle. With EVs, the charging power can be reduced. This feature will not be a focus of this report at this time.

Table 4-5. The Proposed DR Strategy by Load Type

240V load	DR strategy
Air conditioning (AC)	**Load control strategy:** During the curtailment period, increase the temperature set point; The AC unit will automatically turn OFF once the room temperature falls below the new set point. The AC unit will turn ON once the room temperature exceeds the set point within the deadband. After the curtailment period, the default set point will be restored. **Preference consideration:** Changes in the temperature set point must still be within the preference setting limit;
Water heater	**Load control strategy:** During the curtailment period, turn the water heater OFF. After the curtailment period, the water heater will be turned back ON. **Preference consideration:** Force the unit ON when the hot water temperature falls below the preset comfort level.
Clothes dryer	**Load control strategy:** During the curtailment period, turn OFF the heating coil in the clothes dryer, while the tumbler motor keeps on running. After the curtailment period, turn the heating coil back ON. **Preference consideration:** Turn the heating coil back ON when the HMS detects that (a) the clothes drying job will not finish within the preset duration, or (b) the heating coil's off time reaches the maximum limit.
Electric vehicle (EV)	**Load control strategy:** During the curtailment period, stop charging the EV. After the curtailment period, allow the EV to charge. **Preference consideration:** Resume EV charging when the HMS control center foresees that the EV charging cannot be finished within the preset time.

The demand response algorithm is designed such that the home control center will perform demand response on the lowest priority loads as necessary to meet the designated demand limit. If the demand reduction from the lowest priority load is not sufficient, the home control center will perform demand response on the second lowest priority load on the list. The home control center will continue to perform demand response until the requested load curtailment amount is met. Therefore, the number and type of loads to be controlled will depend on the requested load curtailment amount (kW), load priority and preference settings.

To take into account the consumer's preference setting, the home control center will temporarily raise the priority of the load that violates the preset consumer's preference. For example, if the electric vehicle is being controlled (no charge to EV at the moment) and the home control center foresees that the EV charging will not be able to complete by 8pm, the home control center will temporarily raise the EV priority setting to 1. The EV will then resume its charging status.

4.4 Reliability Analysis using Distribution Engineering Workstation (DEW)

In this study, we analyze how the existing DGs at Ft. Bragg can help improve system reliability. We assume that the existing peak-shaving DGs on the circuit can be operated as either dedicated backup at individual buildings where DG is installed, or in parallel with the circuit to reduce peak load.

To evaluate the impact of both standard mode (parallel and emergency backup) and potential islanding mode (micro-grid/smart grid) DG operation on the Fort Bragg circuit, we have developed three different model versions of the circuit which were analyzed using EDD's DEW distribution system power flow and reliability analysis applications. The three model versions are as follows: (1) DG modeled as current sources operated in parallel at the secondary side of building transformer connections, (2) DG operated as voltage sources connected radially to the system on the primary side of building transformers, and (3) DG operated as a part of fixed islands defined by isolation switch locations with one DG in each island modeled as a voltage source and other DG in each island modeled as current sources.

This section presents in Section 4.4.1 – overview of the selected circuit developed in DEW; Section 4.4.2 – model assumptions; and 4.4.3 – three DG models as described above.

4.4.1 Overview of the Distribution Circuit developed in DEW

The selected distribution circuit at Ft. Bragg has the system voltage at 12.47kV. It consists of a combination of overhead and underground sections. The circuit contains a number of distribution transformer elements which are building load connection points, a voltage regulator installed at the start of circuit point, fuses and disconnect switches. At the time of this study, there are several back up generator sets with peak shaving capability serving this circuit.

The data obtained from Ft. Bragg are available in the MilSoft's WindMil format. These data are extracted and used to build a DEW model of the circuit. Fig. 4-27 provides legend information for the components that were included in the DEW model.
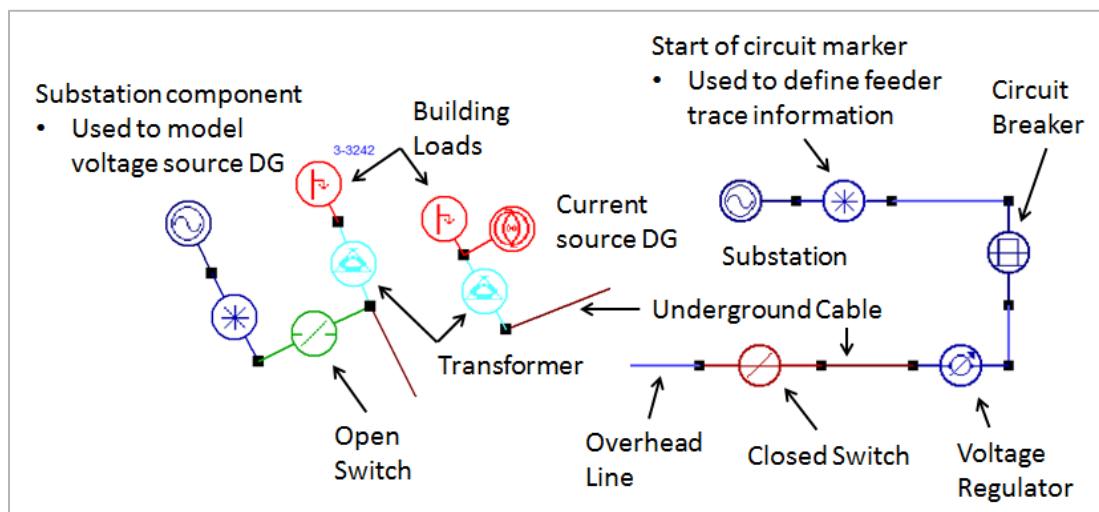
Fig. 4-27. Components used in models

4.4.2 Model Assumptions

The following assumptions are made when developing the Ft. Bragg distribution circuit in DEW.

1. Transformer loads: We modeled transformer loads by attaching load buses on the secondary side of each transformer. Loads were set at 28.6% of rated load at a 0.95 power factor at load bus components installed at the secondary side of each transformer. Each load point was set to have one customer.

2. DG Operation: DGs were set to operate at a power factor of 0.9. DG ratings were specified at a power factor of 0.8.

3. Transformer sizing: Transformer size was increased on four transformers where analysis showed that the combination of load and/or DG connection resulted in an overload or voltage constraint violation.

4. Disconnect Switches: We assumed that each one of disconnect switch sets was a single ganged three-phase disconnect switch, and built them as such.

5. Fuse Types: Fuse information in the WindMil extract files was limited. Fuses were defaulted to types that we had information for in its existing parts database. Where possible, fuse rating was set to match fuse rating information provided in the extract.

6. Cable sizing: All cables are assumed to be of 350 AL URD type.

4.4.3 DG Models as a Current Source, a Voltage Source and a part of a fixed Island Models

As mentioned above, we perform reliability analysis with three different DG model versions: (1) DG modeled as current sources operated in parallel at the secondary side of building transformer connections, (2) DG operated as voltage sources connected radially to the system on the primary side of building transformers, and (3) DG operated as a part of fixed islands defined by isolation switch locations with one DG in each island modeled as a voltage source and other DG in each island modeled as current sources.

Each DG model is further explained below.

a) DG operated as a current source model

For the DG current source model, we have added an alternate feed with a 1-amp capacity, to provide for limitations in the reliability analysis application which was designed for use with switched radial systems with multiple feeds. The DEW version of Ft. Bragg circuit with DGs modeled as current sources is illustrated in Fig. 4-28, showing DG numbers DG-0001 and DG-0002.
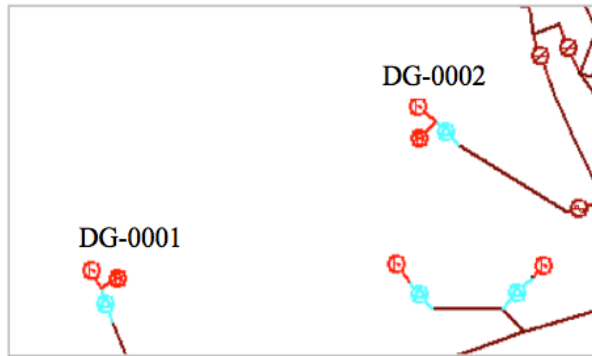
Fig. 4-28. DG-0001 and DG-0002 modeled as current sources
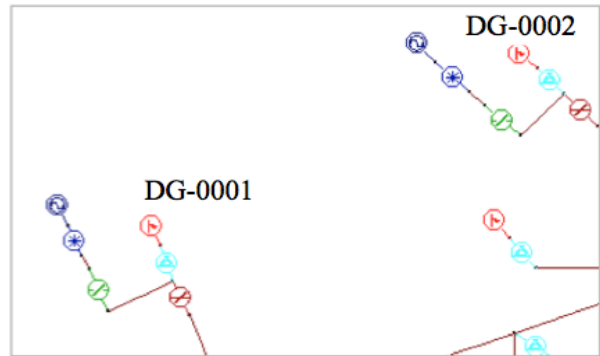
Fig. 4-29. DG-0001 and DG-0002 modeled as voltage sources

b) DG operated as a voltage source model

Fig. 4-29 shows a zoomed in section of the voltage source DG model, where each DG is connected to the system through a disconnect switch and then connected to the 12.47 kV primary voltage side of its respective distribution transformer. DG was modeled this way so that the reliability algorithm could configure each DG to remain off, run in dedicated mode feeding its respective building load, or feed a section of the system that has been isolated from the main feeder source. Voltage source DGs were connected to the primary side of transformers because the algorithm is currently set to only use primary side sources as alternate feeds.

c) DG operated as a part of fixed islands model

The DG operated as a part of fixed islands model is developed to evaluate effects on reliability if the circuit were operated in an islanded mode. To accomplish this, we broke the model up into segments bounded by isolation switches. In each circuit segment, there is one DG operated as a voltage source and the rest of the DGs are operated as current sources.

To simplify analysis run on the island mode model, all fuse cutout switches were removed to eliminate the effect the reliability algorithm would have on results.

Note that as each DG model (voltage source, current source or island mode models) are developed differently. While comparison of results between cases run from the same model version is valid, it is not reasonable to compare results among various model versions.

5.0 Results and Discussions

This section presents results and discussions, including the set of guidelines for microgrid deployment and estimation of benefits from microgrid deployment. The models developed as described in Section 4.0 are used to analyze benefits of implementing a microgrid in a real-world environment. Guidelines for a microgrid deployment are developed based on experience gained during the course of the project. This section comprises three key parts:

Part I   -   General Guidelines for Microgrid Deployment

Part II   -   Impact of DGs on System Reliability and Load Shape

Part III -   Analysis of Peak and Energy Saving Potentials with Energy Efficient Technologies and Demand Response

Part I – General Guidelines for Microgrid Deployment

The set of guidelines developed as a part of this report is based on experience gained during the course of this project, including extensive discussions with engineers from the Public Works Department at the base, and Sandhills Utility Services (the power distribution company that serves Ft. Bragg).

5.1 Microgrid Definition and Boundary Selection Criteria

Microgrid is defined as a power distribution network that consists of interconnected local distributed generation sources along with energy storage devices and controllable loads, and can operate in either a grid-connected or an islanded mode. Local generation sources may include conventional fossil fuel-based generators (e.g., diesel/gas engine generators) and renewable-based generators (e.g., such as solar panels, wind turbines and biomass). Energy storage technologies may include battery, compressed air and flywheel energy storage.

In general, a microgrid is a subsection or a subset of an electric power system. At a minimum, a microgrid comprises a single customer with local generation and loads. A part of a distribution feeder, or the whole distribution feeder, or the whole distribution substation can also be considered a microgrid. Examples of possible microgrid boundaries are illustrated in Fig. 5-1.
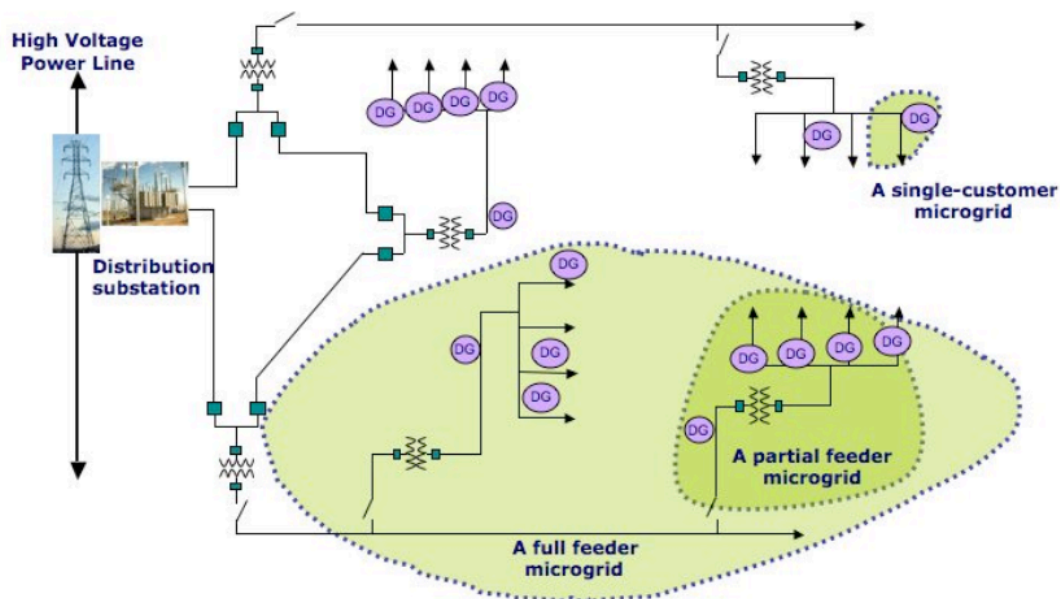
Fig. 5-1. Microgrids as a subsection of power systems

Many microgrids in existence today comprise a section of a distribution feeder and a set of distributed generation sources and loads. A microgrid should be able to allow islanding operation during an emergency situation by disconnecting itself from the main grid and operate autonomously.

A microgrid boundary must be selected on a case-by-case basis, and it depends greatly on the location of mission critical assets, the location of existing distributed generation and storage devices and the topology of local distribution feeders. Depending on the base's reliability and security requirements, this boundary may also vary by the amount of critical loads to be secured and the amount of local distributed energy resources available to serve internal loads within the selected microgrid boundary.

Table 5-1 summarizes a simple step for selecting a part of the power system that can be configured as a microgrid.

Table 5-1. Steps for microgrid boundary selection

Step for microgrid boundary selection	Recommendations for selecting microgrid boundary
1. Identify the location and size (kW) of mission critical assets	• The microgrid boundary should be selected to include the mission critical assets identified.
2. Identify the location and size (kW) of locally available distributed energy resources (DER)	• The microgrid boundary should be selected to include locally available DERs that can be used during emergencies to serve the critical loads. • If the existing DER units are not available or do not have enough capacity to serve the mission critical assets, analysis should be performed whether to expand the microgrid boundary to include other DERs available at the base, or to install a new DER unit(s) at or near the selected critical loads.
3. Identify a section of a feeder that can be isolated	• The microgrid boundary should be selected to include mission critical assets and DERs as previously identified, and include a section of a (or the whole) distribution feeder that can be easily isolated from the utility grid in an event of an upstream outage. Installation of additional switches for proper islanding operation may be required.

5.2 Recommended Microgrid Design Criteria with respect to its Robustness, Resilience and Security Requirements

The design of a microgrid with respect to the number of alternate power feeds, switches for automatic restoration and size and type of distributed generators to be installed varies according to the base's robustness, resilience and security requirements.

- *'Robustness'* is referred to the property of a system that enables the system to continue its operation under perturbations or conditions of uncertainty.
- *'Resilience'* is referred to the ability of a system to recover itself quickly from a failure or a disturbance.
- *'Security'* is referred to the ability of a system to remain intact even after outages or equipment failures.

Table 5-2 summarizes selected microgrid design criteria that can increase the system robustness, resilience and security according to the technical and operational criteria specified.

Table 5-2. Recommended design criteria to increase system robustness, resilience and security

Robustness, resilience and security requirements	Recommended design criteria
To increase system robustness	• Install an alternate power feed(s) to allow the selected loads to be fed from two or more utility sources.
To increase system resilience	• Install intelligent switches, together with their necessary communication technologies, to allow for automatic restoration from other power source(s).
To increase power system security	• Install DERs to allow the selected critical assets to be served from local back-up sources in case of the main grid failure. DERs can include both renewable energy sources in combination with energy storage devices. • The type and size of DER units to be installed will depend on the size of the mission critical assets to be secured and the base's specific requirements. This is discussed in Section 5.3. • Install load shedding devices to allow selected non-critical loads to be shed when the available supply is not enough to serve the entire microgrid load in an emergency situation. • Install a microgrid master controller and necessary communication technologies to coordinate coordination of different microgrid components.

5.3 Recommended Microgrid Design Criteria for selecting Type and Size of DERs

Distributed Energy Resources (DERs), which include both distributed generation (DG) and energy storage technologies, can be used to secure critical loads during utility outages. DER candidates for a microgrid in a military base may include solar photovoltaics, internal combustion (IC) engine generators, microturbines, fuel cells, and energy storage technologies, which can be either battery or flywheels. Characteristics of candidate DERs are summarized in Table 5-3 in terms of their size, cost, efficiency, and footprint.

Table 5-3. DER candidates for a microgrid

Technology	Distributed Energy Resources (DERs)					
	Distributed Generation (DG)				Energy Storage Devices	
	Solar PV	IC engine	Micro-turbine	Fuel cells	Battery	Flywheel
Fuel	Sun	Natural gas, diesel, or dual fuels	Natural gas	Hydrogen	Can be charged by DG or grid	Can be charged by DG or grid
Size	1W-350W (modular)	10kW – few MW	30kW – 350kW	1kW – 200kW	Multiple of 25kW-1hr	Modular, for example: 120kW-10sec, 150kW-15secs, 250kW-15secs
Cost	$5,000/ kW	<$300/ kW	<$1000/ kW [64]	<$4000/ kW	<$4000/ kWh	$0.867-$3.17/ kW-sec [65]
Efficiency (%)	5-17%	15-40%	14-28%	36-60%	85%	98%
Footprint (sqft/kW)	63-220	0.1-0.8 [66]	0.27-0.34 [67]	0.9-2.4 [68]	0.4-0.5 [69]	0.02-0.03 [70]

There are also many other emerging storage technologies, which include for example Sodium Sulfur (NaS) battery, Vanadium Redox Battery, Ultracapacitors and Superconducting Magnetic Energy Storage. These technologies are emerging and therefore they are not included in the comparison in Table 5-3.

Distributed generation (DG) technologies:

IC engines running on either natural gas or diesel or dual fuels are the most common types of distributed generation technologies being used today as back-up or peak-shaving generators in many military bases. This is because of (a) its low capital cost per kW output, in the range of $300/kW output; (b) its wide selection of unit sizes, ranging from 10kW to a few MWs; (c) its technological maturity and (d) easy availability of such fuels.

Solar photovoltaics (PV) is also a mature technology that has gained tremendous attention in many military bases due to its ability to displace carbon dioxide emissions from traditional fossil fuel generators. The capital cost of a PV system, including inverters and balance of plants, is approximately $5,000/kWp.

Microturbines and fuel cells have entered the market in the past several years. Their capital costs per kW output are still high (several thousand dollars per kW) as compared to IC engines.

Energy storage technologies

The most common types being used today are battery and flywheel energy storage devices. They are used in two different applications. While batteries are suitable for a long-term (i.e. minutes-hours) emergency back up, flywheels are used to serve sensitive loads during a short-term (i.e. seconds-minutes) transition from a utility grid to a back-up generator. At the time of this study, the capital cost of battery energy storage is estimated at $4000/kWh, and the capital cost of flywheel energy storage is estimated at $0.867-$3.17/kW-sec, depending on flywheel material used.

Selecting suitable type and size of DERs for a microgrid to increase security of a local power system will depend on the type of mission critical facilities to be served and the base's specific requirements (i.e. emission reduction target or percentage share of renewable generation). Table 5-4 summarizes recommended design criteria for selecting the type and size of DERs based on the type of mission-critical facilities and their requirements.

Interconnecting DERs in a microgrid environment should comply with IEEE 1547 standard for Interconnecting Distributed Resources with the Electric Power Systems [71].

Table 5-4. Recommended design criteria for selecting type and size of DERs based on the type of mission-critical facilities

Type of critical loads	Recommended design criteria for size and type of DERs

(a) Mission-critical facilities that require continuous operation	• It is recommended that fossil fuel-based generators be used in conjunction with energy storage devices to serve mission-critical facilities that require continuous operation.
	    o Fossil fuel-based generators may include internal combustion engines running on diesel, natural gas or both fuels, microturbines or fuel cells.
	    o Energy storage devices may include battery energy storage or flywheel energy storage.
	Usually, it takes less than 30 seconds for the generator to start up and synchronize with the grid to serve critical loads. During the generator start up, energy storage devices can be used to secure critical loads to allow a smooth transition from the grid-connected to islanded-mode operation.
	• For fossil fuel-based generators, the size of DER units should be at least the same size as the critical assets (kW). The type of generators to be deployed will depend on fuel availability onsite and budgetary constraints. The duration that the critical assets can be served by the generators will depend on the amount of fuel (or storage tank) available onsite.
	• For energy storage devices, the kW size should be selected to cover the size of the critical loads (kW) to be served during the transition. The energy (kWh) of storage will depend on the base's requirement of how long to secure the critical assets, e.g. 30 seconds during the transition, or 1 hour, 2 hours, 3 hours for longer backup needs.
	    o Flywheel is suitable for serving critical loads for a short duration (e.g. < 30 seconds).
	    o Battery is suitable for serving critical loads for a longer duration (e.g. 1 hour or more).

(b) Mission-critical facilities that can be interrupted momentarily	• It is recommended that fossil fuel-based generators be used to serve the loads that can be interrupted momentarily. • The size of DER units should be at least the size of the critical assets (kW). The duration that the critical assets can be served by the generators will depend on the amount of fuel (or storage tank) available onsite.

Note: In order to operate back-up generators in an islanded mode, black-start capability may need to be provided.

5.4 Recommended Microgrid Design Criteria for Load Prioritization

In most microgrids, the chosen DER capacity is just sufficient to serve critical loads (kW). In this case, some non-important loads must be shed or disconnected as necessary. Loads can be prioritized and ranked-ordered according to their functions. Table 5-5 summarizes steps for load prioritization within a microgrid. Installation of additional switches may be required to allow disconnecting or connecting the loads according to their priority.

Table 5-5. Steps for load prioritization within a microgrid

Step for load prioritization	Expected results

1. Perform load inventory (i.e. building functions and kW size) within the microgrid boundary of interest	• Loads can be classified by building function, for example:
	    o Administration buildings
	    o Barracks
	    o Carwash facilities
	    o Dining halls
	    o Hospitals
	    o Storage facilities
	    o And others, e.g., maintenance facilities, training facilities, schools, classrooms, operation centers, water treatment plants, gyms, fire stations and EV charging stations.

2. Prioritize loads by building function	• Rank order from the most important load to the least important load, and list their kW size. For example, from the list of six building functions above, hospitals can be the highest priority load, followed by dining halls, barracks, admin buildings, carwash and storage facilities. • Load prioritization by building function will allow for disconnecting or connecting the loads according to their priority, as needed.

In addition to load prioritization by their function, it is also possible to classify and prioritize loads by type, e.g. lighting loads, HVAC loads and plug loads. Reconfiguration and rewiring of electrical distribution circuits at the building level (i.e. circuit breakers) is necessary to allow disconnecting or connecting the loads by load type.

5.5 Recommended Microgrid Operation Strategies

Microgrid operation is divided into two modes: grid-connected and islanded mode operations. Table 5-6 summarizes recommended microgrid operation strategies in both grid-connected and islanded modes, as well as during the transitions between the two modes.

Table 5-6. Recommended microgrid operation strategies*

Microgrid operation	Microgrid operation strategies

Grid-connected mode	• There is no utility outage, and no load shedding should be performed. All DERs should operate in accordance with IEEE 1547 standard [71].
	• For a system with renewable energy sources, electricity from such sources, e.g. PV, should be utilized as much as possible.
	• For a system with distributed generators and/or battery energy storage, these DERs can be used to shave the peak demand to avoid high electricity prices during peak hours.
	   o In most cases, there is a limit on the number of hours a diesel generator can run in a given year for peak-shaving purposes. For example, at Ft. Bragg, this limit is 250 hours/year. In California, this limit is 40 hours/year due to its stringent requirements. Therefore, it is necessary to carefully plan for generators' run times to maximize their peak shaving benefits.
	   o For storage, it is necessary to carefully plan for the storage unit's charge and discharge schedule to maximize storage use.
	• Demand response -- for example, increasing HVAC temperature set points -- can be performed to help reduce additional peak demand.

Transition to the islanded mode	• Transitions to the islanded mode can be a scheduled event, e.g. initiated by a customer to isolate from the grid during bad weather conditions, or an unscheduled event, e.g. initiated by loss of area voltage or frequency.
	• In an unscheduled event, the key is to sense abnormal conditions from the grid. This can be accomplished by:
	   o Voltage and frequency sensing
	   o Current sensing (magnitude and direction)
	   o Power flow sensing (magnitude and direction)
	   o Others, e.g. phase shift or rate of change of any parameters
	• Additional equipment may be added to supplement the functionality of DERs. For example, it may be necessary to dampen any transients produced in the island to prevent a protective relay from tripping-off DERs.

* Table 5-6 continues on next page.

Table 5-6 (Continued)

Microgrid operation	Microgrid operation strategies

Islanded mode	• Prior to islanding operation, each DER shall meet the requirements of IEEE 1547 standard [71].
	• System studies should be performed to support the islanded operation. It may be necessary to conduct load-flow and stability studies to identify any potential risks.
	• Locally available DERs must be designed to provide the real and reactive power requirements of critical loads.
	• They must also provide frequency stability and operate within the voltage ranges as specified in ANSI C84.1 [72].
	• Voltage regulation equipment may need to be adjusted to meet the need of the microgrid in the islanded operation.
	• Internal DERs should be able to provide adequate reserve margin for the microgrid, considering the load factor, peak load, load shape, reliability requirement and availability of DERs.
	• To balance load and generation:
	   ○ Consideration should be given to achieving generation and load balance for each phase.
	   ○ Load shedding and demand response may become necessary if load requirements are greater than the generation available.
	   ○ It may be required to change DER output to match the demand.
	• Protective device coordination should be maintained in both grid-connected and islanded operations.
	• For a system with renewable energy sources, electricity from such sources, e.g. PV, should be utilized as much as possible.
	• All other fossil fuel-based DERs should be operated according to their merit orders.

Reconnection/ resynchronization mode	• Voltage of the main grid must be within the range as specified by ANSI C84.1-1995, Table 1, before reconnection of the two systems, and frequency range of 59.3 Hz to 60.5 Hz. • The island reconnection device may delay reconnection for up to five minutes after the system voltage and frequency are restored. • DERs must be able to adjust the island voltage and frequency to synchronize with the utility grid.

5.6 Recommended System Studies and Necessary Standards

To evaluate whether the designed microgrid (including the boundary, DER size/type and load prioritization and shedding schemes selected) can be operated in an islanded mode, it is necessary to conduct a range of system studies. These system studies may include: load-flow, short-circuit and protection coordination, as well as transient stability studies.

In these cases, the following information will need to be gathered from site surveys:

- Inventory of load (e.g. size, function and location)
- Inventory of internal generation (e.g. location, size, type, characteristics, fuel source, and back start capability)
- Inventory of distribution circuit components (e.g. distribution line length and parameters, capacitor banks, voltage regulation equipment, protection devices and schemes and transformers)
- Acceptable operating condition (e.g. frequency, voltage, phase imbalance and harmonic range)
- Protection equipment and settings

The following list of standards is indispensable for the design of a microgrid and should be taken as references when possible.

- ANSI/NEMA C84.1-2006, American National Standard for Electric Power Systems and Equipment—Voltage Ratings (60 Hertz).
- ANSI/NEMA MG 1-2006, Motors and Generators.
- IEEE Std 399™-1997, IEEE Recommended Practice for Industrial and Commercial Power Systems Analysis (IEEE Brown Book™).
- IEEE Std 446™, IEEE Recommended Practice for Emergency and Standby Power Systems for Industrial and Commercial Applications (IEEE Orange Book™).
- IEEE Std 519™, IEEE Recommended Practices and Requirements for Harmonic Control in Electrical Power Systems.
- IEEE Std 1100™, IEEE Recommended Practice for Powering and Grounding Electronic Equipment (IEEE Emerald Book™).
- IEEE Std 1547™-2003 (Reaff 2008), IEEE Standard for Interconnecting Distributed Resources with Electric Power Systems.
- IEEE Std 1547.2™, IEEE Application Guide for IEEE Std 1547™ Interconnecting Distributed Resources with Electric Power Systems.
- IEEE Std 1547.3™-2007, IEEE Guide for Monitoring, Information Exchange, and Control of Distributed Resources Interconnected with Electric Power Systems.
- IEEE Std 1547.4™-2011, IEEE Guide for Design, Operation and Integration of Distributed Resources Island Systems with Electric Power Systems.

5.7 Potential Risks – Microgrid Deployment and Operation

Microgrid deployment will involve partial upgrade and expansion of both existing electrical and IT networks at the base. After carefully designing the microgrid, including selection of a microgrid boundary, type and size of DER and load shedding schemes to be used, the installation phase may involve certain risks – which may include unknowns associated with upgrading the existing electrical and IT networks in the subject circuit, and extra permit applications and approvals that may be necessary. This can result in delays in microgrid deployment or incur additional expenses.

There are also risks associated with the operation of a microgrid. One of the high-impact risks accounts for the safety of electrical equipment due to possible frequency/voltage mismatch when paralleling several DERs. This situation is likely to happen in an islanded operation. To mitigate the risk, the microgrid master controller should be programmed to operate multiple generation sources and loads in the sequence that can avoid any potential problems. Also each switch chosen for installation should be capable of performing a synchronization check before connecting any two systems.

It is also possible that there is a failure in operation of microgrid components, including the microgrid master controller. This will have a high-level impact on microgrid operation. To mitigate the risk, operational readiness testing of individual equipment and the whole system should be performed to ensure that the microgrid can deliver the expected performance.

Size of DERs should be carefully designed during the planning phase of the microgrid deployment to ensure that critical loads can be served during emergencies. Regular testing and maintenance should be conducted to minimize the risk of any unreliable DER operation.

Load configuration in a three-phase system should also be carefully studied. Adjustment will need to be made before implementing an islanded microgrid to prevent any possible load imbalance.

Delays in communications between the microgrid master controller and each microgrid component may have a significant impact on real-time microgrid operation. It is recommended that high-speed and secure communication channel (i.e. optical fiber) be selected to provide communications among microgrid components and devices. This will avoid any potential network delays caused by wireless or other unreliable means of communications.

The most important risk is pertaining to cyber security. A microgrid is vulnerable to cyber risks if attackers can gain at least a partial control to manage a microgrid. A local network can be brought down accidentally, and the impact level is extreme. To mitigate the risk, it is recommended to follow DoD's extensive information security and information assurance requirements at the planning phase of the microgrid. Additional cyber-related requirements may impact the selection of the technology by requiring compliance with the installation, DoD or federal regulations.

Table 5-7 summarizes general risks due to microgrid operation, together with the associated risk management strategies.

Table 5-7. Potential risks and their mitigation strategies

Risk Identification	Risk quantification		Risk management strategies
	Impact level	Prob. level	
Risks during the installation			
1. The risk of upgrading the existing electrical and IT networks in the subject circuit, which is unknown and may cause some delays and additional expenses.	Med	High	Thorough engineering analysis should be performed during the microgrid design phase and discussions should be initiated with engineers at a local electric utility to minimize any potential delays and additional expenses.
2. Permit applications and approvals, which can take longer than expected	Med	High	The microgrid installation team should work with a local utility and an energy manager at a microgrid deployment site; and apply for any necessary permits and electrical or interconnection agreements early.
Risks during operation			
3. Possible damage to electrical equipment due to frequency/ voltage mismatch when paralleling several DERs in an islanded operation	High	Depend on the risk mitigation strategy implemented.	The microgrid master controller should be programmed to operate multiple generation sources and loads in the sequence that can avoid any potential problems. Also each switch chosen for installation should be capable of performing a synchronization check before connecting any two systems.
4. Failure in operation of microgrid components	High		Operational readiness testing should be performed for the proposed system to ensure that the proposed microgrid can deliver the expected performance.
5. Inadequate and unreliable internal generation	High		Size of DERs should be carefully designed during the planning phase of the microgrid deployment; regular testing and maintenance should be conducted to minimize the risk of unreliable operation.
6. Load imbalance	High		Load configurations must be studied and planned before implementing islanding operation
7. Communication between the master controller and each microgrid component that may impact operation of the microgrid	High		High-speed and secure communication channel (optical fiber) should selected to provide communications among microgrid components and devices.
8. Cyber security	High		Follow DoD's extensive information security and information assurance requirements

5.8 Guideline to Estimate Microgrid Benefits

5.8.1 Overview of Reliability Benefits

Key benefits of deploying a microgrid on military bases are the improvement in system robustness, resiliency and security during an emergency situation. This is accomplished by installation of an alternate power feed(s), intelligent switches, as well as distributed generation (DG), storage and load shedding devices.

For DGs that are capable of performing peak shaving, these can be operated as either dedicated backup at individual buildings where they are installed, or in parallel with the circuit to reduce peak load. The primary means by which the DG can be used to improve circuit level reliability when operated in these two modes is to use it to relieve overload and low voltage problems that impact the use of alternate feeds. If overload and under voltage is not a problem, it is likely that the DG installed on this circuit will have little effect, if any, on reliability. Additional ways that DGs can be used to improve circuit level reliability is to use it as a part of an islanding/microgrid type scheme that includes coordinated DG control and load shedding, as part of a smart grid scheme that uses automated switching together with fault location, isolation and recovery, or as part of a scheme that uses some combination of both.

To evaluate the impact of both standard mode (emergency backup and parallel) and a potential islanded-mode (microgrid/smart grid) DG operation on the Fort Bragg circuit, we built three different models of the circuit which were analyzed using EDD's DEW distribution system power flow and reliability analysis applications. The three model versions were as follows: (1) DG modeled as a current source operated in parallel at the secondary side of building transformer connections, (2) DG operated as a voltage source connected radially to the system on the primary side of building transformers, and (3) DG operated as part of fixed islands defined by isolation switch locations with one DG in each island modeled as a voltage source and other DG in each island modeled as a current source. These models are described in Section 4.4.

Our study shows that:

- DGs operated in parallel for peak shaving at Ft. Bragg will have little or no effect on reliability unless the circuit is heavily loaded, i.e. at least three times the current loading level at the base. The same is true for DG operated in an emergency backup mode, providing a dedicated feed to a specific building. This follows expected results for distribution systems operated with large margins of reserve capacity. See Sections 5.8, 5.9 and 5.10.

- Potential exists for improving circuit reliability by installing some combination of smart grid automated fault location, isolation and recovery control scheme either by itself, or in combination with the addition of microgrid type control that coordinates DG operation and load shedding. Reliability improvement will depend on the type of control schemes used and the locations of DGs in reference to the critical loads. See Sections 5.11.

5.8.2 Overview of Peak Shaving and Energy Reduction Benefits

Since emergency situations do not occur often, i.e. less than a few times a year, additional benefits from deploying a microgrid can be derived from peak reduction and energy saving potentials in a day-to-day operation. During a normal operating condition, a microgrid can be operated to allow peak shaving and electricity consumption reduction by running generators, deploying energy efficient technologies, HVAC control and demand response.

Running DERs during the peak load hours is one way to shave the peak demand. DERs may include a generator, PV and storage. In most cases, there are limits on the number of hours a fossil-fuel generator can run during a one-year period. Deploying energy efficient technologies, such as by replacing existing linear fluorescent lamps (T12) with more energy efficient lighting technologies, including T8 and LED lamps, can help reduce the peak demand. Additional savings can be achieved by increasing the HVAC thermostat set points and coordinating the operation of other controllable loads accordingly.

By utilizing the models developed in Sections 4.2 and 4.3, it is possible to estimate potential benefits of a microgrid during day-to-day operations. Our study shows that:

- Replacement of the existing T12 light fixtures by the more energy efficient T8 light fixtures can reduce peak demand and energy consumption approximately 20%. Similarly, replacement of existing T12 light fixtures by the more energy efficient LED light fixtures could reduce peak demand and energy consumption approximately 45%. See Section 5.14 for details.

- Performing demand response by adjusting thermostat set point can result in 2-3% electrical energy saving per degree F increase in temperature set point. See Section 5.15.

- Demand response can be used to shave peak demand during the high peak price periods. See Section 5.16.

5.8.3 Other Microgrid Benefits

Other microgrid benefits may include:

- The ability to integrate renewable energy technologies, and therefore resulting in carbon footprint reduction;
- The ability to utilize advanced energy management for optimal DER dispatch, and therefore increasing operating efficiency for the local area; and
- The ability to automate microgrid operation, which is expected to reduce the complexity of operator involvement during the transition from the grid connected to the islanded mode.

5.8.4 Estimation of Microgrid Benefits

Overall, the benefits of implementing microgrid can be classified into: operational, quantitative and qualitative benefits. Key benefits of a microgrid are pertaining to the improvement in robustness, resilience and security of the selected local area, which cannot be measured in monetary terms. A microgrid can also result in a reduction in electrical energy usage and an increase in renewable energy capacity. This in turn contributes to a reduction in electricity bill and carbon dioxide emission. In addition, a microgrid can also provide electricity users a feeling of reliability improvement, and provide system operators a more streamlined (automated) process for microgrid operation.

The table below summarizes key microgrid benefits, as well as the metric to evaluate the benefits and the data requirements. The information in this table is intended to serve as a guideline to quantify microgrid benefits, but it is not an exclusive list

Table 5-8. Microgrid benefits: operational, quantitative and qualitative*

Microgrid benefits	Metric	Data Requirements
Operational benefits		
(1) Increase in robustness of a local area	% of the time that the local area is transferred from the main source to an alternate feed successfully	Number of times that the local area is successfully transferred from its main feed to an alternate feed, as compared to the number of time the transfer is unsuccessful.
(2) Increase in resiliency of a local area	Outage restoration time	Outage data and restoration time before/after microgrid deployment. The restoration time includes the duration when transferring to an alternate feed, and the duration when islanding the microgrid, until the critical loads are served.
(3) Increase in security of a local area	% of time that the critical load is served during an islanded operation	Duration that the critical loads can be served in an islanded mode, as compared to the total duration in an islanded mode.

* Table 5-8 continues on next page.

Table 5-8 (Continued)

Microgrid benefits	Metric	Data Requirements
Quantitative benefits		
(4) Reduction in electrical energy usage	Annual electricity savings from microgrid deployment (kWh/yr)	Meter readings of loads and electricity generated by microgrid components
(5) Increase in renewable energy capacity and generation	Renewable energy installed and generated on installation (kW, kWh)	Installed capacity of renewable energy sources (kW) and total energy generation from renewable source (kWh)
(6) Reduction in CO_2 emission	Reduction in CO_2 emission (lbs of CO_2 per year)	Meter readings of loads and electricity generated by microgrid components; and CO2 emission rate (lbs/kWh) at the installation site
(7) Reduction in electricity bill	Annual savings in electricity cost ($/yr)	Meter readings of loads and electricity generated by microgrid components, hourly electricity price ($/kWh) Savings from demand response may not be directly measured. Estimation of benefits can be made using mathematical models presented in this report.
Qualitative benefits		
(8) User perception of reliability improvement	Survey, feedback	Survey and feedback from individuals (users) with respect to the operation of microgrid
(9) Operator perception of automated process	Survey, feedback	Survey and feedback from individuals (operators) with respect to the operation of microgrid

Part II - Impact of DGs on System Reliability and Load Shape

In this study, we analyze how the existing DGs at Ft. Bragg can help improve system reliability. The methodology to perform the analysis, case study description and model assumptions are presented in Section 4 – Methodology and Methods. This section presents results and discussions of the study.

5.9 Base Case Analysis – No DGs

a) Base case – Constraint violation and loading analysis

To establish a basis for our analysis, we have evaluated constraint violations by component for various load levels with a base case model that has no DG installed using Distribution Engineering Workstation (DEW). The load scaling factor of 1.0 represents the base case loading level, which is assumed to be at a level equal to 28.6% of distribution transformer rating. The 28.6% transformer loading level corresponds to the peak load of the selected circuit. Table 5-9 summarizes various load scaling factors (from 1.0x to 3.5x), their corresponding transformer loading levels, total loads (kW, kVAR, kVA, pf) and constraint violation results.

Table 5-9. Reliability analysis base system loading (no DG installed)

Load Scale Factor	% Transformer Load	KW	KVAR	KVA	pf	Constraint Violations
1	28.60%	4273	1490	4525	0.94	No Overloads, No Voltage Violations
1.25	35.80%	6415	2310	6818	0.94	No Overloads, No Voltage Violations
1.5	42.90%	8514	3164	9083	0.94	No Overloads, No Voltage Violations
1.75	50.10%	10597	4059	11348	0.93	No Overloads, No Voltage Violations
2	57.20%	12741	5021	13695	0.93	No Overloads, No Voltage Violations
2.5	71.50%	10596	3781	11250	0.94	3 of 237 Overloaded lines and cables (Avg Overld = 2.5%), No voltage violations
3	85.80%	12741	5021	13695	0.93	69 of 237 Overloaded lines and cables (Avg Overld = 10.1%), No voltage
3.5	100.10%	14799	6009	15973	0.93	80 of 237 Overloaded lines and cables (Avg Overld = 26.2%), No voltage

From review of the results shown Table 5-9, it appears that the system does not experience any overloads until it reaches loading equivalent to 71% of transformer ratings, which in the DEW analysis corresponds with a load factor setting of 2.5. This indicates that significant overloading will not be experienced until the system reaches a loading level equivalent to 86%, which is equivalent to three times the peak load for the given Ft. Bragg circuit. Our analysis also indicates that the system does not experience any low voltage problems up through a loading level equivalent to 100% of transformer rated load.

b) Base case – Impact of loading levels on Reliability and Voltage (No DG)

We have performed reliability analysis for the base system (no DG/PV installed) for load scaling factors of 1.0x, 1.50x, and 2.0x. This is because we believe it is unlikely that the load will double in the next five to ten years. The system reliability results are based on the System Average Interruption Duration Index (SAIDI) and the Customer Average Interruption Duration Index (CAIDI), which are defined as:

$$SAIDI = \frac{\text{sum of all customer interuption durations}}{\text{total number of customers served}}$$

$$CAIDI = \frac{\text{sum of all customer interuption durations}}{\text{total number of customer interuptions}}$$

Table 5-10 summarizes system reliability indices (SAIDI and CAIDI values) and voltage levels for the base case (no DG) at various locations on the distribution circuit. The numbers B-xxxx represent building numbers. Note that SAIDI is the system index, therefore only one SAIDI value is presented for each load scaling factor case.

Table 5-10. Impact of system loading on reliability and voltage for the base case scenario

Xfmr#/ building#	Load scale factor = 1.0			Load scale factor = 1.50			Load scale factor = 2.0		
	SAIDI	CAIDI	Volts	SAIDI	CAIDI	Volts	SAIDI	CAIDI	Volts
Xfmr 1 B-0001		0.848	123.5		0.848	123.7		0.848	123.1
Xfmr 2 B-0002		1.851	123.0		1.851	123.0		1.851	122.3
Xfmr 3 B-0003		1.711	123.5		1.711	123.7		1.711	123.1
Xfmr 4 B-0004		1.508	123.7		1.508	124.1		1.508	123.6
Xfmr 5 B-0005		1.335	123.4		1.335	123.6		1.335	123.0
Xfmr 6 B-0006		1.454	123.9		1.454	124.3		1.454	124.0
Xfmr 7 B-0007		1.454	123.0		1.454	123.0		1.454	122.3
Xfmr 8 B-0008		0.801	123.8		0.801	124.2		0.801	123.9
Xfmr 9 B-0009		0.809	123.5		0.809	123.8		0.809	123.3
Xfmr 10 B-0010		0.801	123.9		0.801	124.3		0.801	123.9
Xfmr 11 B-0011		0.801	123.4		0.801	123.6		0.801	123.0
Xfmr 12 B-0012		0.801	122.9		0.801	122.9		0.801	122.1
Overall System	4.0833	4.0716		4.0833	4.0716		4.0833	4.0716	

As discussed earlier, at load scaling factors of 2.0x and below the system does not appear to experience any overloading or under-voltage problems. As a result, it is not expected that DG will have any impact on reliability if the system is operated within this range of loading. As shown in Table 5-10, changes in loading between load scaling factor 1.0x (28.6% transformer rating) to 2.0x (57.2% transformer rating) did not result in any change in SAIDI and CAIDI.

Note that for the analysis shown in Table 5-10, as well as all other analyses presented in this section, the base customer voltage at the start of circuit voltage regulator was set to 124.5V with a bandwidth setting of 1.0V. During the analysis, the regulator was set to operate automatically. From the voltage result review, it appears that changes in voltage at transformer secondary connection points for different load scaling factor cases are a result of changes in loading and normal operation changes in voltage regulator set points.

5.10 Impact of DGs on System Reliability and Voltage – DG as a Current Source

For this case, all DGs were modeled as current sources operating in parallel with the system. Analysis was run at load scale factors of 1.0x, 1.5x, 2.0x, 3.0x and 3.5x. The system reliability indices (SAIDI and CAIDI) are provided in Table 5-11.

DG configuration combinations analyzed are shown below:

- 1 DG (at building B-0012) - This is the largest 900kW DG located at the end of the line.
- 3 DGs (at buildings B-0012, B-0003 and B-0001) – These are three DGs located at the end of the three lines. Their sizes are 900kW, 350kW and 400kW, respectively.
- 3 DGs (at buildings B-0006, B-0005 and B-0004) – These are three DGs located at the largest building in the middle of the circuit.
- 6 DGs (combined the DG from the previous two cases)
- 12 DGs – All 12 DGs connected.

Table 5-11. Summary results for current source model analysis

Case Summary	Load Scale Factor = 1.0		Load Scale Factor = 1.5		Load Scale Factor = 2.0		Load Scale Factor = 3.0		Load Scale Factor = 3.5	
	Sys SAIDI	Sys CAIDI	Sys SAIDI	Sys CAIDI	Sys SAIDI	Sys CAIDI	Sys SAIDI	Sys CAIDI	Sys SAIDI	Sys CAIDI
Base	4.4832	4.1795	4.4832	4.1795	4.4832	4.1795	5.0845	4.6341	5.7942	5.2995
DG at B-0012	4.4833	4.1797	4.4833	4.1797	4.4833	4.1797	4.8652	4.3269	5.2007	4.7978
3 DGs Case 1	4.4837	4.1799	4.4837	4.1799	4.4837	4.1799	4.8656	4.3272	5.085	4.6344
3 DGs Case 2	4.4851	4.1813	4.4851	4.1813	4.4851	4.1813	4.867	4.3285	5.0864	4.6358
6 DGs	4.4856	4.1816	4.4856	4.1816	4.4856	4.1816	4.4856	4.1816	4.8675	4.3289
12 DGs	4.4861	4.1823	4.4861	4.1823	4.4861	4.1823	4.4861	4.1823	4.4861	4.1823

Review of these results shows that:

- DG operation in parallel with the circuit to reduce peak load does not impact reliability for load factors from 1.0x through 2.0x. This is because between the load scaling factors of 1 and 2, there is no overload or low voltage problem in the circuit. If overload and under voltage is not a problem, it is intuitive that the DG installed on this circuit will have little effect if any on reliability.
- Improvement in system reliability is noticeable with DGs at the load scaling factors of greater than 3.0x.
- Our simulation results also indicate that, for DGs operated in parallel with the system, varying DG locations does not appear to effect the system level SAIDI and CAIDI

values, and does not affect CAIDI for the load points at or near where the DG is located. Varying fuel availability at a particular DG site will also does not affect reliability.

5.11 Impact of DGs on System Reliability and Voltage – DG as a Voltage Source

For this case, all DGs were modeled as voltage sources that can be switched on in an emergency as a dedicated source for the building location it is installed at. As a part of the simulation, DG isolation switches were installed at each DG location and were sized to match rated power output for each individual DG. By design, the DEW reliability algorithm used to analyze the circuit only allows one voltage source to feed any part of the system at any time. As the reliability algorithm reconfigures the system in response to failures set on the system, any DG that exceeds power output limits set for its respective isolation switch would be disconnected from feeding the system. The algorithm was also free to remove load from the system by switching DG to provide dedicated supply to the load at its respective location.

The same general DG configuration and loading used with the current source model was also used with the voltage source model. It should be noted that because of the additional switches added to the model to provide for DG reconfiguration by the reliability algorithm, SAIDI and CAIDI results for the voltage source and current source models are not directly comparable. Summary results for voltage source model analysis are shown in Table 5-12.

Table 5-12. Summary results for voltage source model analysis

Case Summary	Load Scale Factor = 1.0		Load Scale Factor = 1.5		Load Scale Factor = 2.0		Load Scale Factor = 3.0		Load Scale Factor = 3.5	
	Sys SAIDI	Sys CAIDI	Sys SAIDI	Sys CAIDI	Sys SAIDI	Sys CAIDI	Sys SAIDI	Sys CAIDI	Sys SAIDI	Sys CAIDI
Base	3.3305	3.1978	3.3305	3.1978	3.3305	3.1978	4.0084	3.5985	4.8084	4.4053
DG at B-0012	3.2907	3.0578	3.1462	2.9163	3.2907	3.0578	3.9685	3.4585	4.624	4.1237
3 DGs Case 1	3.2931	2.9611	3.1485	2.8243	3.2931	2.9611	3.8264	3.2118	4.7709	4.129
3 DGs Case 2	3.7025	3.4039	3.7025	3.4039	3.7025	3.4039	4.3804	3.7915	6.92	6.3213
6 DGs	3.7058	3.2495	3.1613	2.7053	3.7058	3.2495	3.8391	3.0747	6.9233	6.0302
12 DGs	3.1667	2.4829	3.1667	2.4829	3.1667	2.4829	3.8445	2.8206	5.5027	4.2833

Results show that voltage source islanded and dedicated emergency mode operation of DG has some positive effects on system SAIDI and CAIDI.

5.12 Impact of DGs on System Reliability and Voltage – DG in an Islanded Mode

To attempt to better simulate islanded model operation, we divided the system up into segments, and set one DG in each segment (for segments that have DG) to operate as a voltage source, and setup the remaining DG in each segment to operate in parallel as current sources.

As noted earlier in the report, to simplify the analysis all fuse cutout switches were removed from the model to eliminate the effect that operation of these switches by the reconfiguration algorithm would have on reliability results. As a consequence of this change, reliability results between this model and current source and voltage source models are not directly comparable.

A number of cases were analyzed that involved adding a 500 kW DG at three different locations, and add these 500 kW DGs in various combinations. In addition, different DG combinations were also analyzed together with adding two additional isolation switches at two different locations. Switch 1 was added to reduce the number of loads directly affected by faulting line sections in the main feed. Switch 2 was added to make it possible for the reliability algorithm to split how DG is used to feed the top and center sections of the system.

Table 5-13. DG island mode analysis summary of results

Case Summary	Load Scale Factor = 1.0		Load Scale Factor = 1.5		Load Scale Factor = 2.0		Load Scale Factor = 3.0		Load Scale Factor = 3.5	
	Sys SAIDI	Sys CAIDI	Sys SAIDI	Sys CAIDI	Sys SAIDI	Sys CAIDI	Sys SAIDI	Sys CAIDI	Sys SAIDI	Sys CAIDI
Base	11.7415	5.2474	11.7415	5.2474	11.7415	5.2474	11.7415	5.2474	11.7415	5.2474
Case 1 Add 500 kW at TR-1	11.7143	5.2385	11.7143	5.2385	11.7143	5.2385	11.7143	5.2385	11.7142	5.2385
Case 2 Add 500 kW at TR-2	11.7128	5.2372	11.7128	5.2372	11.7128	5.2372	11.7128	5.2372	11.7128	5.2372
Case 3 Add 500 kW at TR-3	11.7128	5.2372	11.7128	5.2372	11.7128	5.2372	11.7128	5.2372	11.7128	5.2372
Case 4 (Case 1 & 2)	11.7175	5.2397	11.7175	5.2397	11.7175	5.2397	11.7175	5.2397	11.7175	5.2397
Case 5 (Case 2 & 3)	11.716	5.2383	11.716	5.2383	11.716	5.2383	11.716	5.2383	11.716	5.2383
Case 6 (Case 1, 2 & 3)	11.7207	5.2408	11.7207	5.2408	11.7207	5.2408	11.7207	5.2408	11.7207	5.2408
Case 7 (Base & Sw 1)	11.7096	5.249	11.7096	5.249	11.7096	5.249	11.7096	5.249	11.7096	5.249
Case 8 (Base & Sw 2)	10.9989	5.5263	10.9989	5.5263	10.9989	5.5263	10.9989	5.5263	10.9989	5.5263
Case 9 (Base, Sw 1 & 2)	10.9989	5.5214	10.9989	5.5214	10.9989	5.5214	10.9989	5.5214	10.9989	5.5214
Case 10 (Case 1 & Sw 1)	11.7143	5.2514	11.7143	5.2514	11.7143	5.2514	11.7143	5.2514	11.7143	5.2514
Case 11 (Case 2 & Sw 2)	11.0021	5.5276	11.0021	5.5276	11.0021	5.5276	11.0021	5.5276	11.0021	5.5276
Case 12 (Case 3 & Sw 2)	11.0021	5.5276	11.0021	5.5276	11.0021	5.5276	11.0021	5.5276	11.0021	5.5276
Case 13 (Case 4 & Sw 2)	11.0053	5.529	11.0053	5.529	11.0053	5.529	11.0053	5.529	11.0053	5.529
Case 14 (Case 1 & Sw 2)	11.0036	5.5289	11.0036	5.5289	11.0036	5.5289	11.0036	5.5289	11.0036	5.5289
Case 15 (Case 4 & Sw 1 & 2)	11.0068	5.5252	11.0068	5.5252	11.0068	5.5252	11.0068	5.5252	11.0068	5.5252
Case 16 (Case 6 & Sw 1 & 2)	11.01	5.5266	11.01	5.5266	11.01	5.5266	11.01	5.5266	11.01	5.5266

Results indicate that adding DG without adding additional isolation switches does not have a significant effect on reliability (Case 1 through Case 6). The addition of switch 2 in Case 8 shows the biggest effect on reliability out of all cases. The addition of DG and switches together also shows improvement in reliability.

5.13 Impact of Solar PV on System Reliability and Voltage

Potential reliability effects of adding 250 kW PV at building B-0012 and 200 kW PV at building B-0011 are evaluated by adding DG rated at 250 kW and 200 kW at the respective sites. The following installation scenarios are evaluated:

- Scenario 1: 250kW solar PV added to the base case at building B-0012
- Scenario 2: 200kW solar PV added to the base case at building B-0011
- Scenario 3: 250kW and 200kW solar PV added to the base case at building B-0012 and building B-0011, respectively.

CAIDI, SAIDI and voltage results for all three scenarios are shown in Tables 5-14, 5-15 and 5-16, respectively. A review of these tables shows that installation of PV for the cases analyzed does not appreciably affect reliability or voltage for normal loading. As a result, variation of PV throughout the day should also not have any effect on reliability and voltage.

Table 5-14. Scenario 1: 250kW solar PV Installed at Building B-0012

Xfmr#/ building#	Load scale factor = 1.0			Load scale factor = 1.50			Load scale factor = 2.0		
	SAIDI	CAIDI	Volts	SAIDI	CAIDI	Volts	SAIDI	CAIDI	Volts
Xfmr 1 B-0001		0.848	123.5		0.848	123.7		0.848	123.2
Xfmr 2 B-0002		1.851	123.1		1.851	123.1		1.851	122.3
Xfmr 3 B-0003		1.711	123.5		1.711	123.7		1.711	123.2
Xfmr 4 B-0004		1.508	123.7		1.508	124.1		1.508	123.7
Xfmr 5 B-0005		1.335	123.4		1.335	123.6		1.335	123
Xfmr 6 B-0006		1.454	123.9		1.454	124.4		1.454	124.1
Xfmr 7 B-0007		1.454	123.1		1.454	123.0		1.454	122.3
Xfmr 8 B-0008		0.802	123.9		0.802	124.3		0.802	123.9
Xfmr 9 B-0009		0.809	123.6		0.809	123.9		0.809	123.4
Xfmr 10 B-0010		0.802	123.9		0.802	124.3		0.802	124
Xfmr 11 B-0011		0.802	123.4		0.802	123.6		0.802	123.1
Xfmr 12 B-0012		0.801	124.7		0.801	124.7		0.801	123.9
Overall System	4.0834	4.0717		4.0834	4.0717		4.0834	4.0717	

Table 5-15. Scenario 2: 200kW PV Installed at Building B-0011

Xfmr#/ building#	Load scale factor = 1.0			Load scale factor = 1.50			Load scale factor = 2.0		
	SAIDI	CAIDI	Volts	SAIDI	CAIDI	Volts	SAIDI	CAIDI	Volts
Xfmr 1 B-0001		0.848	123.5		0.848	123.7		0.848	123.2
Xfmr 2 B-0002		1.851	123.1		1.851	123.1		1.851	122.3
Xfmr 3 B-0003		1.711	123.5		1.711	123.7		1.711	123.2
Xfmr 4 B-0004		1.508	123.7		1.508	124.1		1.508	123.7
Xfmr 5 B-0005		1.335	123.4		1.335	123.6		1.335	123.0
Xfmr 6 B-0006		1.454	123.9		1.454	124.4		1.454	124.1
Xfmr 7 B-0007		1.454	123.0		1.454	123.0		1.454	122.3
Xfmr 8 B-0008		0.802	123.9		0.802	124.3		0.802	123.9
Xfmr 9 B-0009		0.809	123.6		0.809	123.9		0.809	123.4
Xfmr 10 B-0010		0.802	123.9		0.802	124.3		0.802	124.0
Xfmr 11 B-0011		0.801	125.0		0.801	125.2		0.801	124.7
Xfmr 12 B-0012		0.802	123.0		0.802	122.9		0.802	122.1
Overall System	4.0834	4.0717		4.0834	4.0717		4.0834	4.0717	

Table 5-16. Scenario 3: 250kW and 200KW solar PV Installed at Buildings B-0012 and B-0011, respectively

Xfmr#/ building#	Load scale factor = 1.0			Load scale factor = 1.50			Load scale factor = 2.0		
	SAIDI	CAIDI	Volts	SAIDI	CAIDI	Volts	SAIDI	CAIDI	Volts
Xfmr 1 B-0001		0.848	123.5		0.848	123.8		0.848	123.2
Xfmr 2 B-0002		1.851	123.1		1.851	123.1		1.851	122.4
Xfmr 3 B-0003		1.711	123.5		1.711	123.8		1.711	123.2
Xfmr 4 B-0004		1.508	123.8		1.508	124.1		1.508	123.7
Xfmr 5 B-0005		1.335	123.5		1.335	123.6		1.335	123.1
Xfmr 6 B-0006		1.454	124.0		1.454	124.4		1.454	124.1
Xfmr 7 B-0007		1.454	123.1		1.454	123.1		1.454	122.3
Xfmr 8 B-0008		0.802	123.9		0.802	124.3		0.802	124.0
Xfmr 9 B-0009		0.809	123.6		0.809	123.9		0.809	123.4
Xfmr 10 B-0010		0.802	123.9		0.802	124.4		0.802	124.0
Xfmr 11 B-0011		0.801	125.1		0.801	125.3		0.801	124.7
Xfmr 12 B-0012		0.802	124.7		0.802	124.7		0.802	123.9
Overall System	4.0835	4.0178		4.0835	4.0178		4.0835	4.0178	

5.14 Solar PV and their Impact on the System Load Shape

This section looks at solar photovoltaics (PV) and their impact on load shape change. The use of solar PV on a military base has a great potential in reducing carbon footprint. In this study it is assumed that two sets of PV panels of 200kW and 250kW (with a total of 450kW in size) are installed on rooftops of two buildings within the circuit. Sizes of the PV panels are determined based on available roof areas for PV installation.

Fig. 5-2 shows the circuit's system load profiles for five consecutive weekdays (starting from August 24, 2010 to August 29, 2010) with and without the 450kW PV output. It can be seen that the PV output can somewhat reduce the system peak demand as peak sunshine hours typically coincide with the peak demand hours between 2 and 4pm.
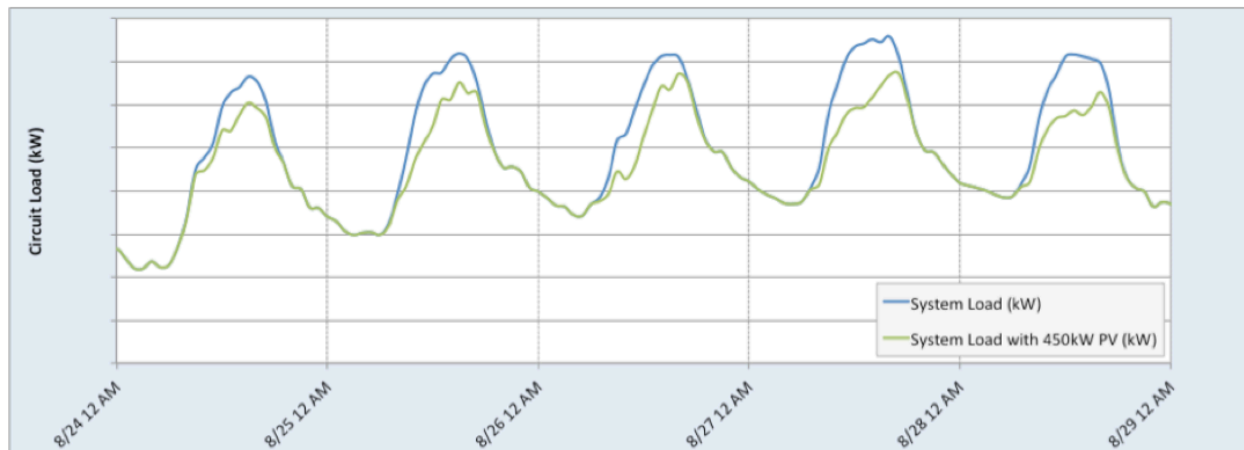

Fig. 5-2. Load profiles with and without 450kW PV units

Depending on whether the day is clear or cloudy and the size of PV units installed, the amount of energy and peak reduction potentials can vary. For the study with 450kW PV units and actual weather data at Ft Bragg, NC, the total energy reduction for a day ranges from 902 kWh to 2,325 kWh and the peak reduction ranges from 117 kW to 291 kW. This information is summarized in Table 5-17 for the month of August 2010.

Table 5-17. Peak and energy reduction potentials for 450kW PV

	Energy/peak reduction potentials for 450kW PV
Energy reduction potential (kWh)	902 kWh to 2,325 kWh/day
Peak reduction potential (kW)	117kW to 291 kW

Part III - Analyzing Peak and Energy Saving Potentials with Energy Efficient Technology and Demand Response

In this study, we analyze potential benefits of deploying a microgrid on day-to-day operations in both commercial buildings and residential houses. These benefits include peak shaving and energy reduction potentials, which can be achieved by deploying energy efficient technologies, HVAC control and demand response. Utilizing the models developed (as presented in Section 4.0 – Methodology and Methods), this section presents results and discussions of the study.

5.15 Peak and Energy Saving Potential with Energy Efficient Lighting Technology (Commercial Buildings)

According to our survey of an office building at Ft. Bragg, 65 sets of linear 2x40W T12 fluorescent (F40T12) light fixtures are used in this building. The characteristics of T12 lamps, as well as the replacement (T8 and LED) lamps are shown in Table 5-18, in terms of their power input, lumen output and mercury content.

Table 5-18. Performance comparison of linear fluorescent lamps (T12 and T8) and LEDs

	T12* (2x4ft F40T12 linear fluorescent lamp)	T8** (2x4ft F32T8 linear fluorescent lamp)	LED*** (2x4ft replacement LED lamp)
Total power input (W)	80	64	44
Output (initial lumen)	3,200	2,800	N/A
Output (design mean lumens)	2,880	2,660	1,650
Mercury content (milligram)	4.4	1.7	0
Life (hours)	20,000	36,000	40,000

* Based on Philips F40T12 Cool White Plus
** Based on Philips F32T8 Cool White Plus
*** Based on Philips EnduraLED T8 Tube GA 22W 48" G13

Minute-by-minute electric power consumption of the lighting circuit in this building, which comprises 65 sets of linear 2x40W T12 fluorescent (F40T12) light fixtures, was recorded over a one-week period. This is as shown in Fig. 5-3 (solid black line). The power consumption measurement indicates the peak electrical consumption of approximately 5.2kW. This is consistent with the total lighting capacity of 80W/set*65 sets.

Fig. 5-3 also shows the electric power consumption of the lighting circuit when the T12 linear fluorescent lamps are replaced with the T8 linear fluorescent lamps (simulation) and LED lamps (simulation), whose characteristics are summarized in Table 5-18. The potential peak power and energy savings are summarized in Table 5-19.
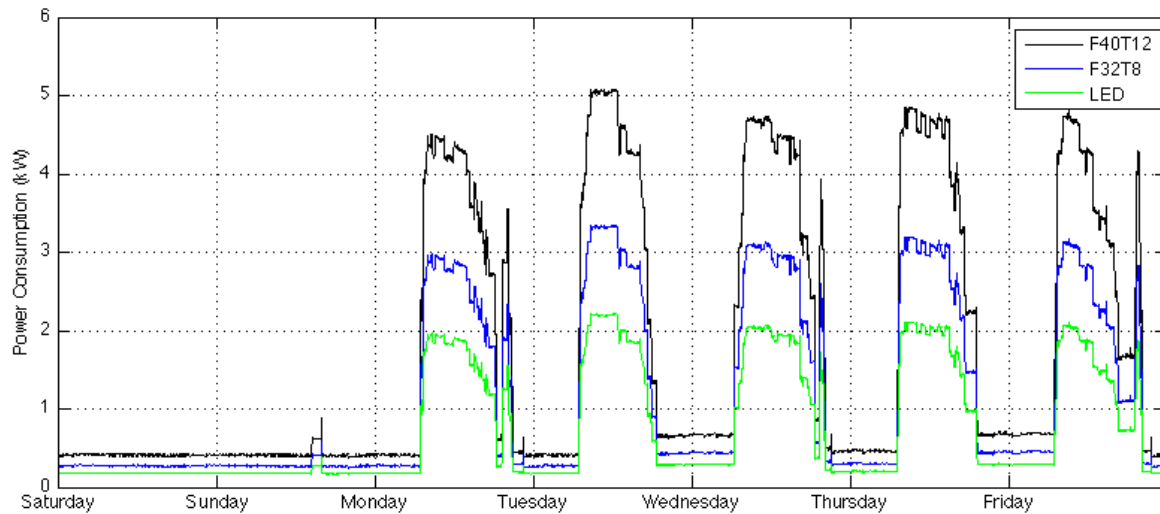
Fig. 5-3. Minute-by-minute power consumption of fluorescent lamps (T8 and T12) with LED replacements for a period of one week

Table 5-19. Power and energy saving potentials achievable by replacing T12 with T8 and LEDs

	Lighting technologies			Saving	
	T12	T8	LED	T12->T8	T12->LED
Total power input (kW)	65*80 = 5.2kW	65*64 = 4.16kW	65*44 = 2.86kW	20%	45%
Weekly energy consumption (kWh)	293	234	161		
Annual energy consumption (kWh)	15,214	12,171	8,368		

Results indicate that approximately 20% energy and peak savings can be expected when replacing T12 with T8; and 45% energy and peak savings can be expected when replacing T12 with LEDs.

5.16 Energy Saving Potential by adjusting HVAC Temperature Set Point (Commercial Buildings)

The HVAC load model as presented in Section 4.2 is used to analyze energy saving potentials that can be achieved by adjusting HVAC temperature set points. Energy saving potentials that can be achieved will depend on building size and envelope, ambient temperatures, and temperature set points.

In this study, we have gathered building-level data from Ft. Bragg to understand characteristics of a set of buildings located in a particular distribution circuit. We have collected the data for 24 office buildings, including their building sizes (square footage), their functions and number of floors. Some assumptions are made regarding the buildings' insulation levels (R-Value) for windows, walls and ceilings. The R-Values used are randomly selected for these 24 buildings, the range of which is according to the recommended levels of insulation by EnergyStar [73]. The parameters used as inputs to our simulation models are summarized below:

- Number of buildings: 24
- Building sizes: from 4,200 sq ft to 81,000 sq ft
- Number of stories: 2 and 3
- R_{window}:   random between 0.4 and 5
- R_{wall}:   random between 25 and 35
- R_{celing}:   random between 38 and 60

The aim of this work is to determine estimated % energy saving of space cooling units when the default temperature set point is raised by 1-8 deg F during a day for various average daytime ambient temperatures. It is expected that the simulation results as presented here can help provide a better understanding of the level of electrical energy that can be saved with the increase in the temperature set point. Real insulation data (R-Value) from Ft. Bragg, if available, can be used as inputs to the developed model. This will allow a more realistic estimation of energy saving potentials with respect to the increase in temperature set point on the Ft. Bragg campus.

Fig. 5-4 shows ambient temperature profiles of four selected days that have average daytime ambient temperatures of 80 deg F, 85 deg F, 90 deg F and 95 deg F.
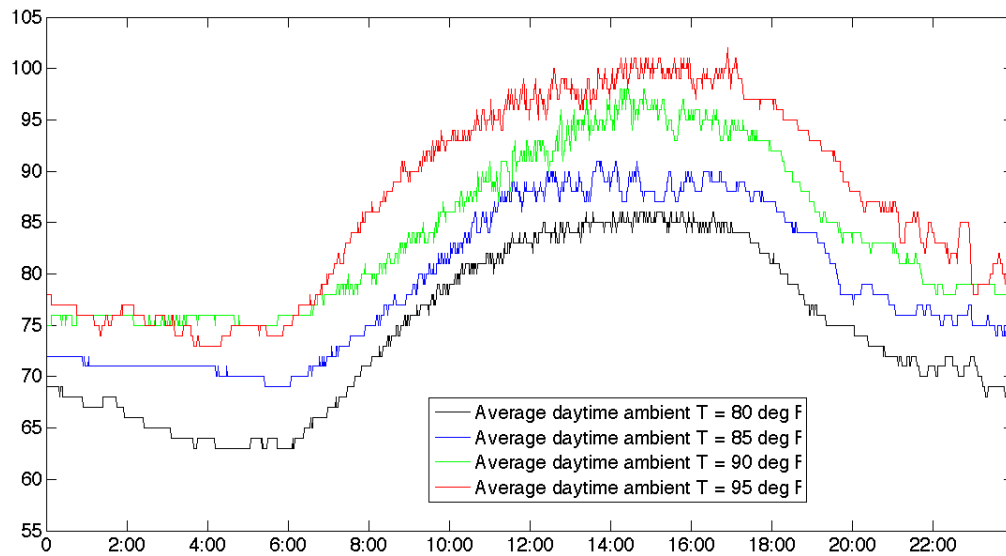
Fig. 5-4. Ambient Temperature (Y-axis) vs Time (X-axis) for four selected days

Table 5-20 summarizes the estimated % energy saving of space cooling units when the default temperature set point is raised by 1-8 deg F during a day at various average daytime ambient temperatures.

Table 5-20. Electricity saving potentials at various set points

% Energy saving from a default setting at various average daytime ambient temperatures	Day 1 80 deg F		Day 2 85 deg F		Day 3 90 deg F		Day 4 95 deg F	
	% saving /deg F	% total saving	% saving /deg F	% total saving	% saving /deg F	% total saving	% saving /deg F	% total saving
Set point = 72 deg F* (default)	-	-	-	-	-	-	-	-
Set point = 73 deg F (+ 1 deg F)	2.2%	2.2%	2.7%	2.7%	2.7%	2.7%	2.2%	2.2%
Set point = 74 deg F (+ 2 deg F)	2.0%	4.2%	2.5%	5.1%	2.7%	5.4%	2.6%	4.8%
Set point = 75 deg F (+ 3 deg F)	2.1%	6.2%	2.5%	7.5%	2.9%	8.1%	2.6%	7.3%
Set point = 76 deg F (+ 4 deg F)	2.3%	8.3%	2.3%	9.7%	2.6%	10.5%	2.2%	9.3%
Set point = 77 deg F (+ 5 deg F)	2.0%	10.1%	2.3%	11.7%	2.5%	12.8%	2.3%	11.4%
Set point = 78 deg F (+ 6 deg F)	2.0%	12.0%	2.1%	13.6%	2.5%	15.0%	2.4%	13.5%
Set point = 79 deg F (+ 7 deg F)	2.2%	13.9%	2.0%	15.3%	2.3%	17.0%	2.2%	15.4%
Set point = 80 deg F (+ 8 deg F)	2.3%	15.9%	2.2%	17.2%	2.3%	18.9%	2.1%	17.2%

Research findings indicate that:

- Electricity saving potentials are in the range of 2-3% for every one degree F increase in the temperature set point.

- Higher electricity saving can be achieved with higher increase in temperature set point.

- Approximately 15-19% electricity saving is achievable by raising the temperature to 80 deg F from the default setting of 72 deg F.

- In general, higher electricity saving can be expected for a day with higher average daytime ambient temperatures than a day with lower average daytime ambient temperature.

  >> For example, on Day 1 when the average daytime ambient temperature is 80 deg F, the electricity saving is estimated at 15.9% when the temperature is set at 80 deg F. These savings are higher in Day 2 and Day 3 when the average daytime ambient temperatures are at 85 deg F (17.2%) and 90 deg F (18.9%), respectively. This is because in Day 1, the AC operation can only be reduced during the day; the AC is turned off at night as the nighttime ambient temperature is much cooler than the set point. See Fig. 5-5.

  >> On the other hand, on Day 2 and Day 3, the AC operation can be reduced during the nighttime as well. See Fig. 5-6 and Fig. 5-7. Note that during the nighttime, although ambient temperatures are lower than the set point, AC still needs to operate intermittently to compensate for the residual heat gain from daytime hours.
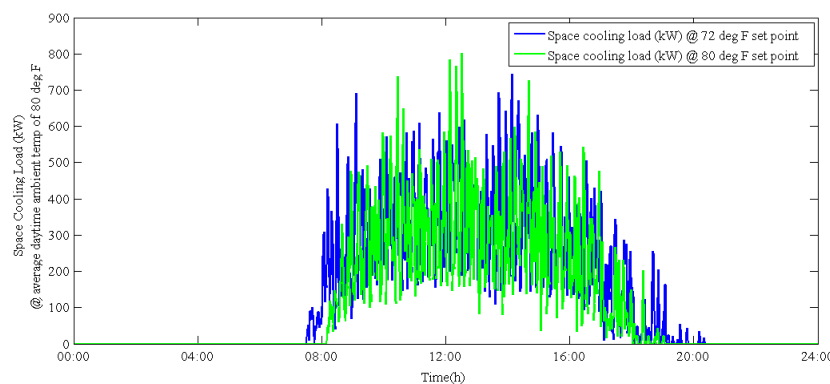

Fig. 5-5. Space cooling load (kW) in Day 1 with average ambient temperature of 80 deg F.
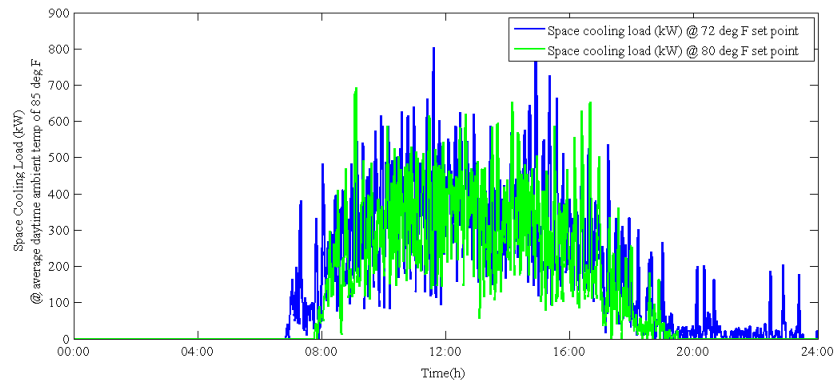
Fig. 5-6. Space cooling load (kW) in Day 2 with average ambient temperature of 85 deg F.
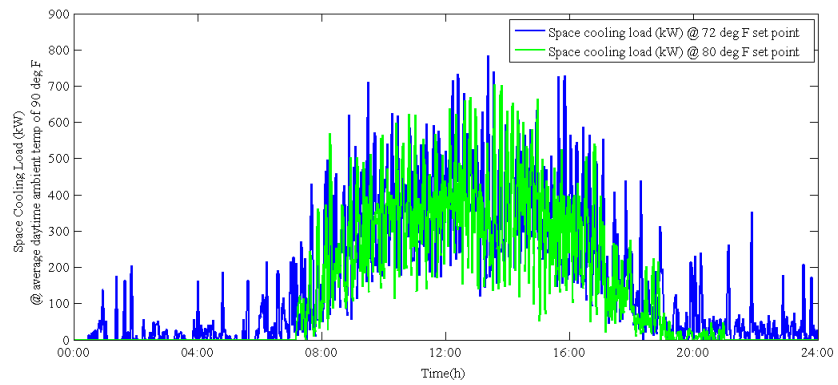

Fig. 5-7. Space cooling load (kW) in Day 3 with average ambient temperature of 90 deg F.
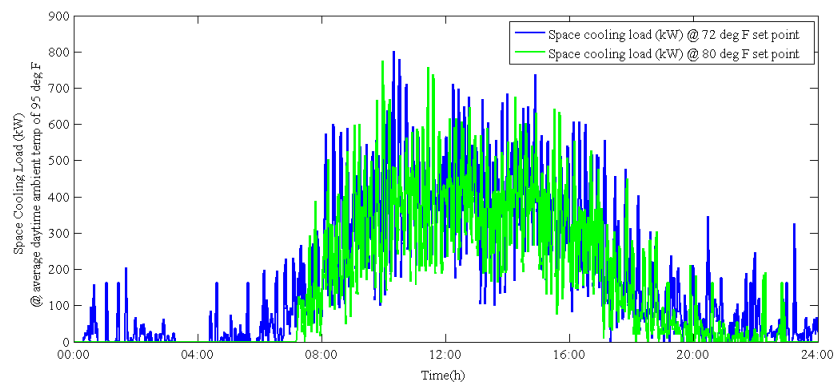

Fig. 5-8. Space cooling load (kW) in Day 4 with average ambient temperature of 95 deg F.

- On Day 4, the total electricity saving when the temperature set point increases to 80 deg F (17.2%) appears to be lower than that (18.9%) on Day 3. This is because, although the nighttime temperatures during Days 3 and 4 are almost comparable (See Fig. 5-4), the AC in Day 4 has to operate more to compensate for higher daytime temperatures. See Fig. 5-7 and Fig. 5-8.

- One would expect to see higher electricity saving per degree F as the temperature set point is higher. This is true if the solar heat gain and heat gain from people are not taken into account. In this study, simulation results indicate that the solar heat gain constitutes a large share of the total heat gain in buildings. This is why the % saving per degree F appears to be consistent at 2-3% when the temperature set points increase from 72 deg F to 80 deg F.

As the findings as described here are consistent with the information available in the literature (see below):

- California Energy Commission indicates a saving of 1% to 3% per degree for each degree the thermostat is set above 72 deg F [74].
- A study to improve energy efficient cooling at a data center indicates that 1% to 3% savings of cooling energy per degree F can be expected [75].
- Focus on Energy indicates, in a cooling mode, each degree the thermostat is set above 75 degrees Fahrenheit can cut cooling costs by about 3 percent [76].

5.17 Peak Shaving Potential with Demand Response (Military Housing)

In Sections 5.15 and 5.16, peak and energy reduction potentials in commercial buildings are analyzed focusing particularly on lighting and HVAC loads. In this section, we focus on peak shaving potentials when demand response is implemented at a household level to control end-use appliances (i.e. space heating/cooling, clothes drying, water heating and electric vehicle loads) given a preset load priority and comfort level setting.

To demonstrate potentials of using the demand response strategy (presented in Section 4.3) to shave the peak demand, we focus on a distribution circuit that serves a group of homes and small commercial buildings. Using information available from an electric distribution company, we have developed a simulation model of a hypothetical distribution circuit in Matlab[1]. The modeled distribution circuit has a distribution voltage of 12.47kV, serving 761 residential customers and 9 small commercial customers. Commercial customers include 2 schools, 1 office building, 2 churches, 2 parks, 1 aquatic center and 1 seven-eleven. This is a typical residential distribution circuit that resembles a distribution circuit setting (that serves military housing) in many military campuses in terms of the distribution voltage level and variety of customers served. The peak load of this circuit is approximately 2MW in summer between 4pm to 6pm. See Fig. 5-9.

The aim of this work is to present simulation results that can help provide a better understanding of what can be accomplished at a household level to reduce the peak electrical demand during high electricity price periods. Real data from Ft. Bragg on military housing sizes, housing insulation values and inventory of end-use appliances, if available, can be used as inputs to the developed model. This will allow a more realistic estimation of peak shaving potentials when demand response is performed in a distribution circuit that serves military houses on the Ft. Bragg campus.

Demand Response Results – a Distribution Circuit Level:

Results as presented in this section aim at illustrating the impact of the demand response strategy on end-use loads to avoid high peak prices. For the purpose of this study, an electricity distribution feeder is chosen which has publicly available information. It is assumed that the electric power consumption limit for this feeder is 1.9 MW and any overload will result in a high demand charge ($/kW). In this case, the proposed demand response strategy is used to keep the electric power consumption within the limit of 1.9MW.

Fig. 5-9 illustrates the impact of demand response when the target supply limit is 1.9 MW, showing the circuit load profile before and after demand response is implemented. The simulation results indicate that the proposed demand response strategy can manage the electric power demand to remain below the pre-set limit of 1.9MW between 4pm to 6pm.

---

[1] Note that due to sensitivity of Ft. Bragg data, we have chosen to use publicly available information so that the models can be validated for various conditions prevailing in different parts of the country.
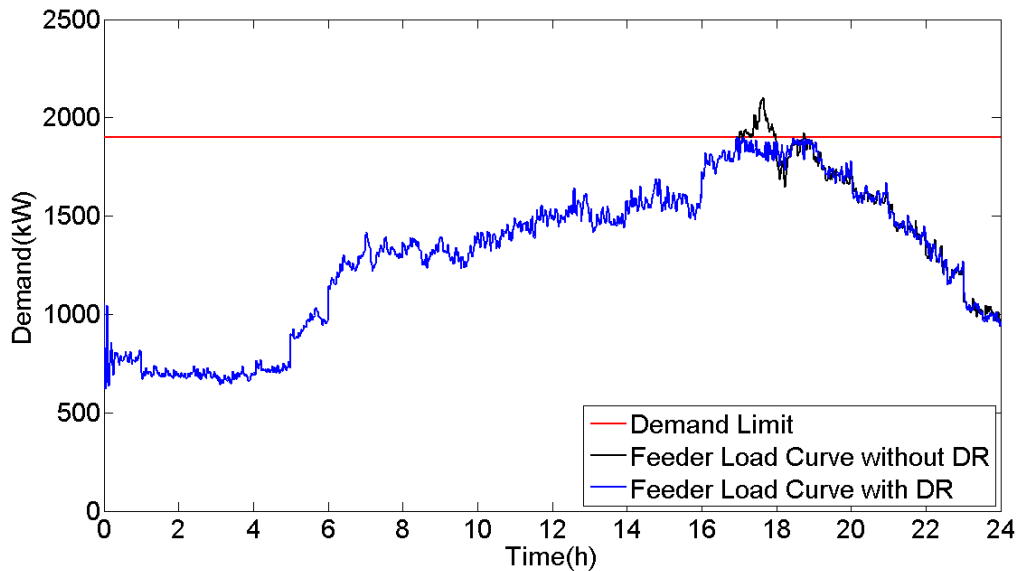
Fig. 5-9. Distribution circuit load profile with and without demand response

To obtain the demand response results, the following assumptions are made:

- Controllable loads in residential houses are space cooling/space heating units, water heaters, clothes dryers and electric vehicles (if any).
- There is only one controllable load in commercial buildings, which are space cooling/space heating units.
- Commercial buildings' space cooling/space heating loads have higher priority than household loads during office hours (8am-5pm). During this time, AC units are not turned OFF but are controlled to allow room temperatures to be within the preset comfort level.
- Household loads (space cooling/heating, water heating, clothes drying and EV loads) have higher priority than commercial buildings' controllable loads outside office hours (5pm-8am). Office buildings' AC units will be turned OFF if demand response is necessary during these hours.
- Household load priority for each of the 761 homes is randomly set. While some houses may give their highest priority to space cooling/heating load, the others may set their water heating load to have the highest priority.
- Space cooling/heating units allow 1-2 deg F variation in room temperatures from the set point. Water heating units allow 5-10 deg F variation in water temperature from the set point.

The demand reduction amount is allocated to both commercial buildings and residential customers within the circuit. The only controllable load in commercial buildings is air conditioning. In this case, the peak hours are between 2pm and 4pm and commercial buildings' space cooling loads have higher priority than household loads. Therefore, during this time, the air conditioning units in commercial buildings will be turned OFF as long as the room temperatures are within 1-2 deg F deviation from the set point, and turned ON if the room temperature exceeds the preset comfort level.

Fig. 5-10 illustrates the aggregated load profiles of commercial buildings before and after demand responses. It can be seen that demand response has an impact between 4pm to 6pm.
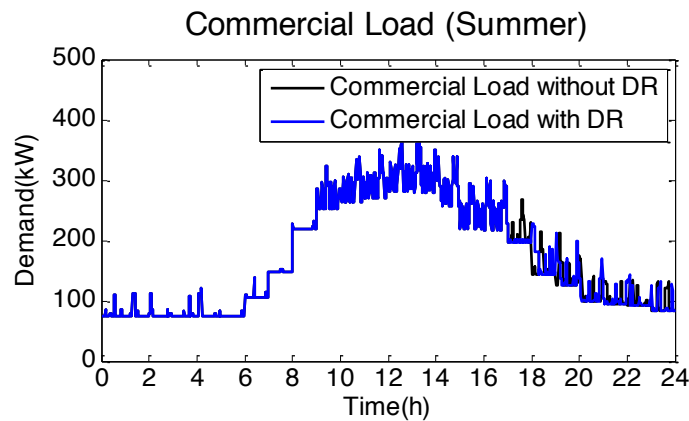

Fig. 5-10. Commercial building's load profiles with and without demand response under the supply limit of 1.9 MW

Fig. 5-11 to Fig. 5-13 show further details of the demand response results imposed for residential homes for each group of appliance, including air conditioning load, water heating load and clothes drying load, respectively.
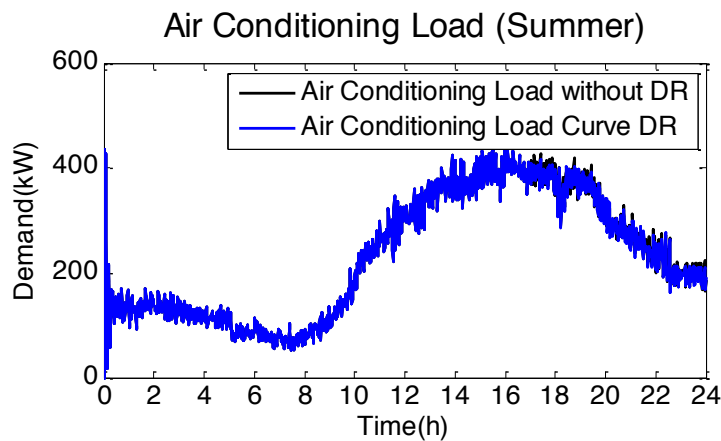

Fig. 5-11. AC load profiles with and without demand response under the supply limit of 1.9 MW
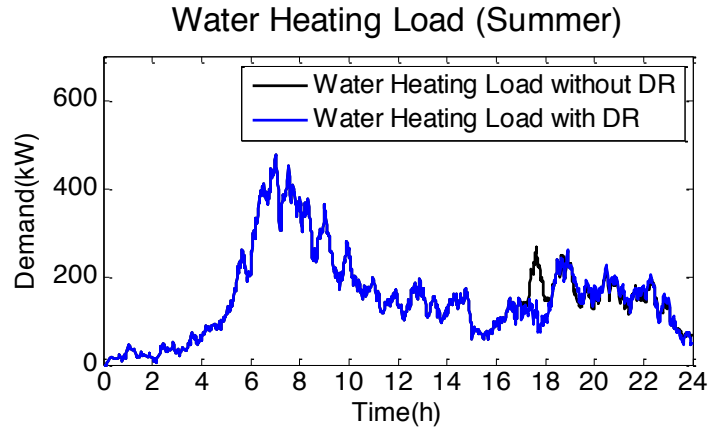
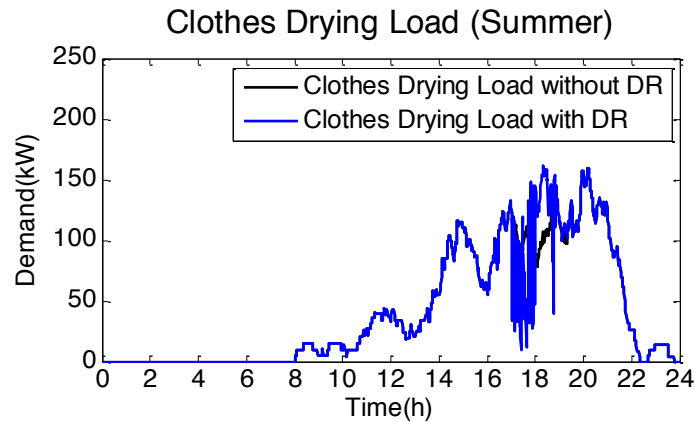Fig. 5-12. Water heating load profiles with and without demand response under the supply limit of 1.9 MW

Fig. 5-13. Clothes drying load profiles with and without demand response under the supply limit of 1.9 MW

Overall, it can be seen that the supply limit of 1.9 MW does not impact the air conditioning load much for both residential and commercial customers, while other loads show obvious demand reduction and shift. This is because of the tight dead-band set to allow only 1-2 deg F variation in room temperature from the set point. The water heating load is slightly affected during the peak hours (between 4pm and 6pm) but the hot water temperature outputs are guaranteed to be within 5-10 deg F from the set point according to the comfort level setting. It also appears that the clothes drying load is mostly affected, and there is an obvious load compensation between 6pm and 8pm after the 4-6pm peak hours.

Demand Response Results – a Household Level

Fig. 5-14 presents demand response at a household level, illustrating the impact of demand response on scheduling different appliances in a house.

House#1: For this particular house (1500 sq ft), the priority and the rated power for each household appliance are summarized in the table below.

Table 5-21. Load priorities and convenience preference setting of a sample house #1

	Space Cooling	Water Heating	Clothes Drying	EV Charging
Rated Power	2 *kW*	4 *kW*	4.2 *kW*	3.3 *kW*
Comfort Setting	76 *°F*±1 *°F*	112 *°F*±5 *°F*	-	-

The red line in the picture (bottom graph) indicates the demand limit assigned to this house. When the red line remains at 25kW, it means there is no demand limit during that time period and no load control is needed. For this house, the demand limit is imposed to this house starting at around 4:15pm, and continues to around 8pm. The reason that the demand response period is imposed beyond the peak hours is due to the compensation of the loads that are shifted during the peak hours.
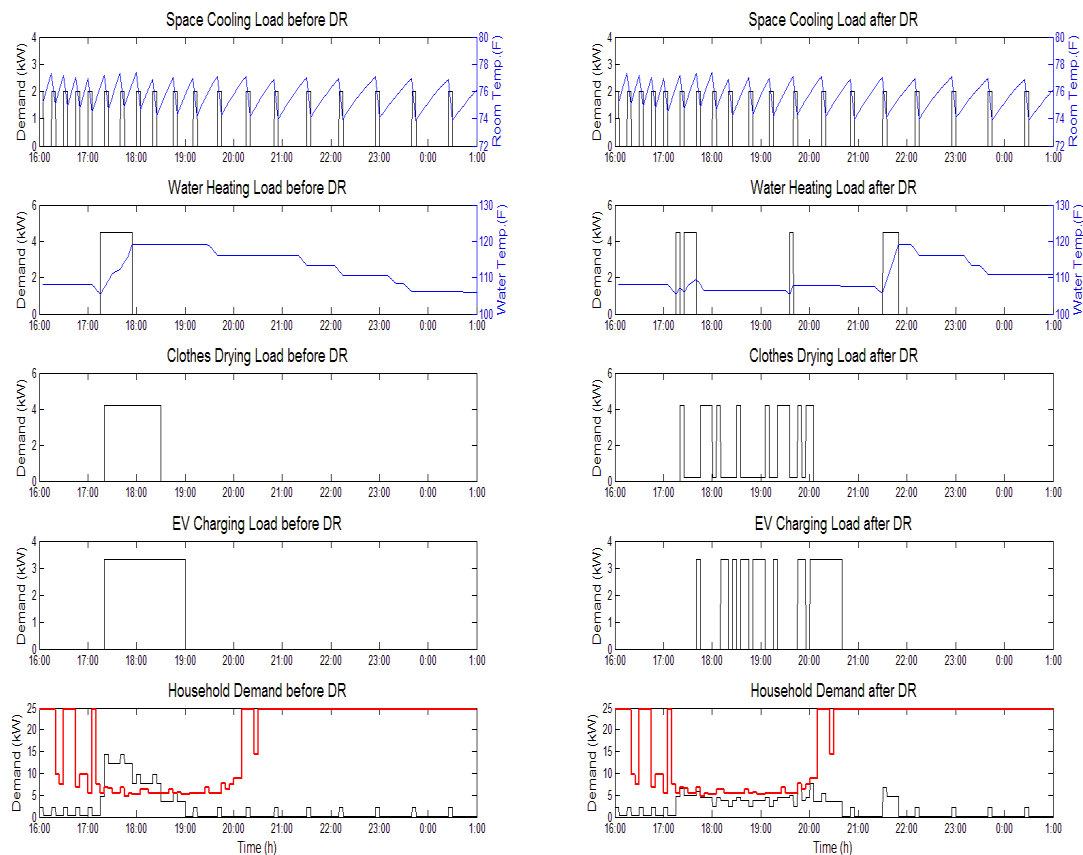

Fig. 5-14. Household load profiles (sample house #1) before and after demand response

It can be seen from the figure that demand response for this house starts at 17:20. This is when the clothes dryer and the EV start at the same time while the water heater is on. To keep the household demand under the assigned limit, the EV charging is stopped to allow the operation of the water heater and the clothes dryer since they are of higher priority. Then, between 17:40 and 20:05, the clothes dryer and the EV are cycling with each other to keep the total household demand under the limits (varying between 5.4kW and 6.9kW). The air conditioner (AC) is not affected since it has the highest priority.

House#2: The information below presents an example of another house (1,800 sq ft) with different house sizes, equipment rated power and comfort setting. Table 5-22 summarizes the priority and rated power for each household appliance in this house.

Table 5-22. Load priorities and convenience preference setting of a sample house #2

	Space Cooling	Water Heating	Clothes-drying	EV Charging
Rated Power	2 *kW*	4.5 *kW*	4 *kW*	3.3 *kW*
Comfort Setting	75 *°F*±1 *°F*	120 *°F*±5 *°F*	-	-

Fig. 5-15 shows the overall results of the household load profile before and after the demand response.
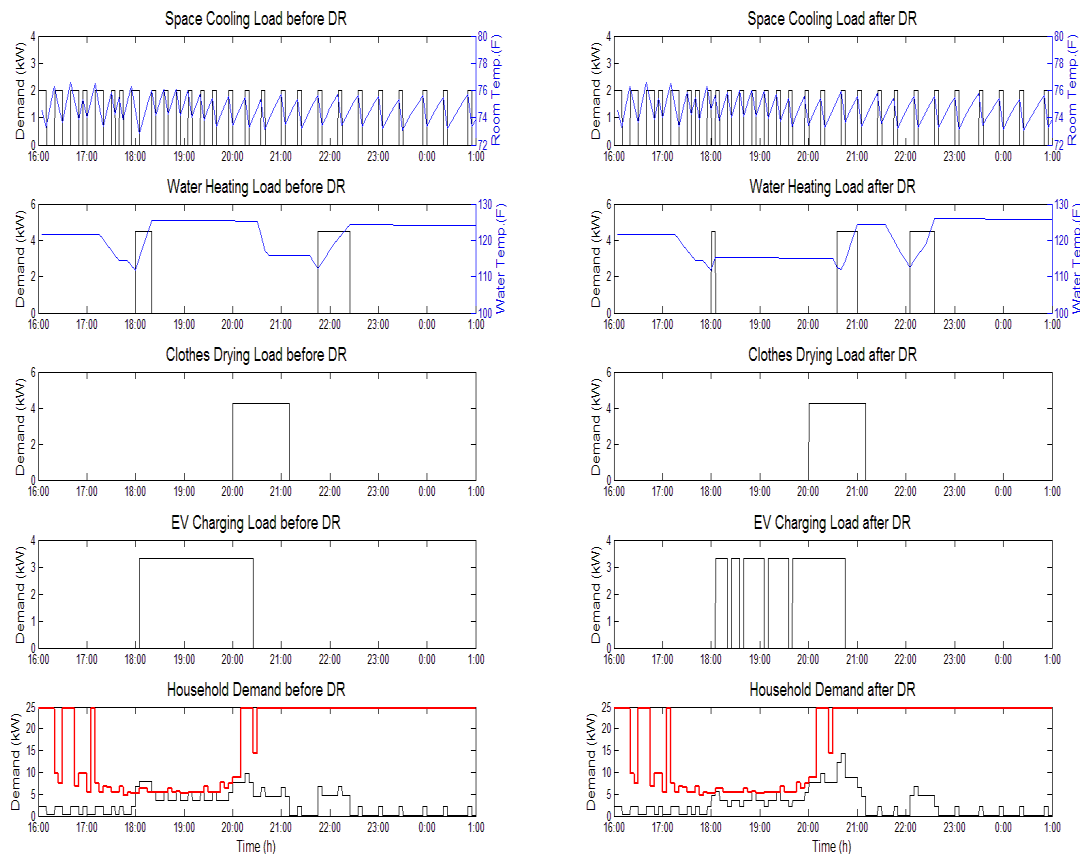
Fig. 5-15. Household load profiles (sample house #2) before and after demand response

99

It can be seen that the DR starts at 18:00, when the water heater and the AC are running at the same time. To keep the household demand under the limit, the AC is turned off to keep the water heater running even though the AC has a higher priority. This is because the water heater has to be on to keep the hot water temperature within the comfort range. At 18:05, the EV is plugged in. The water heater is turned off due to its low priority. From 18:05 to 19:40, the EV charging is interrupted from time to time to keep AC running due to the priority settings. After 19:40, the demand limit is no longer having impact on the appliances.

6.0 Conclusions and Implication for Future Research/Implementation

The key outcome of this project is a set of design criteria and general guidelines that can be used as a reference for deploying a microgrid in a campus-type facility, and establishing their cost-benefit impacts. There are seven design criteria and guidelines as reported in Sections 5.1-5.8, dealing with various phases of microgrid deployment, e.g. planning, design, operation, risk and benefit assessment.

Guideline 1 – A microgrid definition and its boundary selection criteria;

Guideline 2 – Recommended microgrid design criteria to achieve three microgrid properties - robustness, resilience and security;

Guideline 3 – Recommended microgrid design criteria for selecting type and size of distributed energy resources (DERs) for microgrid deployment;

Guideline 4 – Recommended microgrid design criteria for load classification and prioritization;

Guideline 5 – Recommended microgrid operation strategies;

Guideline 6 – Recommended system studies and necessary standards;

Guideline 7 – Potential risks on microgrid deployment and operation; and

Guideline 8 – Guideline to estimate microgrid benefits.

The simulation tool/methodology -- that comprises various DER and load models as well as demand response algorithms -- is the other significant outcome of this work. The project team uses the developed simulation models to estimate potential benefits of deploying a microgrid. Real-world data are utilized as available to us and some assumptions were made as necessary.

The first and foremost benefit of deploying a microgrid is its ability to improve system robustness, resilience and security. Reliability analysis has been conducted with a case study of Ft. Bragg. Our study shows that:

- Distributed generators (DGs) operated in parallel for peak shaving will have little or no effect on reliability unless the circuit is heavily loaded, i.e. at least three times the current loading level at the base. The same is true for DG operated in an emergency backup mode, providing a dedicated feed to a specific building. This follows expected results for distribution systems operated with large margins of reserve capacity.

- Potential exists for improving circuit reliability by installing some combination of smart grid automated fault location, isolation and recovery control scheme either by itself, or in combination with the addition of microgrid type control that coordinates DG operation and load shedding. Reliability improvement will depend on the type of control schemes used and the locations of DGs in reference to the critical loads.

Secondary benefits from deploying a microgrid can be derived from peak reduction and energy saving potentials in day-to-day operations. During a normal operating condition, a microgrid can be operated to allow peak shaving and electricity consumption reduction by running generators, deploying energy efficient technologies, HVAC control and demand response. Estimation of potential benefits due to introduction of energy efficient lighting technologies and load control (demand response) in a microgrid environment has been studied. Our findings indicate that:

- Replacement of the existing T12 light fixtures by the more energy efficient T8 light fixtures can reduce peak demand and energy consumption by approximately 20%. Similarly, replacement of existing T12 light fixtures by the more energy efficient LED light fixtures could reduce the same by approximately 45%.

- Performing demand response by adjusting thermostat set point for commercial buildings can result in 2-3% electrical energy saving per degree F increase in temperature set point.

- Demand response can be used at a household level to shave peak demand during the high peak price periods.

In summary, the set of guidelines as presented in this report is expected to provide DoD with general recommendations when deploying a microgrid -- including how to select microgrid boundary; how to design a microgrid to achieve its robustness, resilience and security requirements; how to select DER size and type; how to classify and prioritize microgrid loads; how to operate a microgrid in a grid-connected operation, an islanded mode, and during transitions; what potential risks exist in microgrid deployment and their mitigation strategies; and lastly, how to estimate microgrid benefits. Additionally, the simulation tool/methodology and simulation results as presented in this report are expected to provide an insight into the estimation of microgrid benefits, including reliability improvement, as well as peak shaving and energy reduction potentials due to management of both supply-side and demand-side resources. With this set of guidelines and the experience of evaluating the benefits of a microgrid in one facility (e.g., Ft. Bragg), DoD will be able to plan, analyze and evaluate the operational benefits and risks of deploying such microgrids on many of their bases.

7.0 Literature Cited

[1] Agrawal, P., "Overview of DOE microgrid activities", Symposium on Microgrid, Montreal, June 23, 2006 [Online]. Available: http://der.lbl.gov/2006microgrids_files/USA/Presentation_7_Part1_Poonumagrawal.pdf. Retrieved: October 2011.

[2] Concortium for Electric Reliability Technology Solutions (CERTS), "Integration of Distributed Energy Resources: The CERTS microgrid concept", October 2003 [Online]. Available: http://certs.lbl.gov/pdf//50829.pdf. Retrieved: October 2011.

[3] Department of Energy, Research and Development Page [Online]. Available: http://energy.gov/oe/mission/research-and-development-rd. Retrieved: October 2011.

[4] Consortium for Electricity Reliability Technology Solutions (CERTS) [Online]. Available: http://certs.lbl.gov/certs-derkey-mgtb.html. Retrieved: October 2011.

[5] Sandia National Laboratories, Energy Surety Microgrid [Online]. Available: http://energy.sandia.gov/?page_id=819. Retrieved: October 2011.

[6] Sandia National Laboratories, SPIDERS [Online]. Available: http://energy.sandia.gov/?page_id=2781. Retrieved: October 2011.

[7] FedBizOpps.gov, Phase One SPIDER Joint Concept Technology Demonstration [Online]. Available: https://www.fbo.gov/index?s=opportunity&mode=form&id=b7e846f8b73bf094c4f3281a32ffe16d&tab=core&_cview=1. Retrieved: October 2011.

[8] E. Lorenzo, "Solar electricity engineering of photovoltaic systems", Spain, ISBN: 8486505550.

[9] A. Mellit, M. Benghanem and S. A. Kalogirou, "Modeling and simulation of a stand-alone photovoltaic system using an adaptive artificial neural network: proposition for a new sizing procedure", Renewable Energy, Vol. 32, Iss. 2, February 2007.

[10] M. park, D. Lee and I. Yu, "PSCAD/EMTDC modeling and simulation of solar-powered hydrogen production system", Renewable Energy, Vol. 31, Iss. 14, November 2006.

[11] E. Radziemska, "The effect of temperature on the power drop in crystalline silicon solar cells", Renewable Energy, Vol. 28, Iss. 1, January 2003.

[12] J. N. Ross, T. Markvart and W. He, "Modeling battery charge regulation for a stand-alone photovoltaic system", Solar Energy,Vol. 69, Iss. 3, 2000.

[13] M. A. de blas, J.L. Torres, E. Prieto and A. Garcia, "Selecting a suitable model for characterizing photovoltaic devices", Renewable Energy, Vol 25, Iss. 3, March 2002.

[14] J.C.H. Phang, D.S.H. Chan and J.R. Phillips, Accurate analytical method for the extraction of solar cell model parameters. Electron. Lett. 20 10 (1984), pp. 406–408.

[15] D.S.H. Chan, J.R. Phillips and J.C.H. Phang, A comparative study of extraction methods for solar cell model parameters. Solid-St. Electron. 29 3 (1986), pp. 329–337.

[16] Sandia Advisory Model (SAM) [Online]. Available: https://www.nrel.gov/analysis/sam/. Retrieved: October 2011.

[17] Measured data from Florida Solar Energy Center (FSEC) [Online]. Available: http://securedb.fsec.ucf.edu/pv/pv_description?fsys_id=90004. Retrieved: October 2011.

[18] D.L. King, W.E. Boyson, J.A. Kratochvill, "Photovoltaic Array Performance Model", SANDIA REPORT, SAND2004-3535, Unlimited Release, Printed December 2004

[19] David L. King, Jay A. Kratochvil, and William E. Boyson, "MEASURING SOLAR SPECTRAL AND ANGLE-OF-INCIDENCE EFFECTS ON PHOTOVOLTAIC MODULES AND SOLAR IRRADIATION SENSORS", 26th IEEE Photovoltaic Specialists Conference, September 29-October 3, 1997, Anaheim, California.

[20] T. Petru and T. Thiringer, "Modeling of wind turbines for power system studies," *Power Systems, IEEE Transactions on* , vol.17, no.4, pp. 1132-1139, Nov 2002.

[21] B. Malinga, J. E. Sneckenberger and A. Feliachi, "Modeling and control of a wind turbine as a distributed resource," *System Theory, 2003. Proceedings of the 35th Southeastern Symposium on* , vol., no., pp. 108-112, 16-18 March 2003.

[22] Y. Lei, A. Mullane, G. Lightbody, R. Yacamini, "Modeling of the wind turbine with a doubly fed induction generator for grid integration studies," *Energy Conversion, IEEE Transaction on* , vol.21, no.1, pp. 257-264, March 2006.

[23] M. Yin, G. Li, Z. Ming and C. Zhao, "Modeling of the Wind Turbine with a Permanent Magnet Synchronous Generator for Integration," *Power Engineering Society General Meeting, 2007. IEEE* , vol., no., pp.1-6, 24-28 June 2007.

[24] Surya Santoso and Ha Thu Le, Fundamental time–domain wind turbine models for wind power studies, Renewable Energy 32 (2007) 2436-2452.

[25] L. N. Hannett and A. Khan, "Combustion Turbine Dynamic Model Validation from Tests", IEEE Trans. On Power Systems, Vol. 8, No. 1, Feb 1993.

[26] S. R. Guda, C. Wang and M. H. Nehrir, "Modeling of Microturbine Power Generation Systems", Electric Power Components and Systems, 34: 1027-1041, 2006.

[27] D. N. Gaonkar and R. N. Patel, "Modeling and Simulation of Microturbine Based Distributed Generation System", IEEE 2006.

[28] M. A. Rendon, M. A. R. Nascimento and P. P. C. Mendes, "Load Current Control Model for a Gas Microturbine in Isolated Operation", In Proc. IEEE Power Systems Conference and Exposition, 2006, pp. 1139-1149.

[29] A. Al-Hinai and A. Feliachi, "Dynamic model of a microturbine used as a distributed generator", In Proceedings of the Thirty-Fourth Southeastern Symposium on System Theory, 2002, Page(s): 209 – 213.

[30] W. I. Rowen, "Simplified Mathematical Representations of Heavy-Duty Gas turbines", Journal of Engineering for Power, Oct 1983, Vol. 105.

[31] Balikci, A.; Zabar, Z.; Czarkowski, D.; Levi, E.; Birenbaum, L.; Flywheel motor/generator set as an energy source for coil launchers, Magnetics, IEEE Transactions on, Volume 37, Issue 1, Part 1, Jan. 2001 Page(s):280 – 283.

[32] Babuska, V.; Beatty, S.M.; deBlonk, B.J.; Fausz, J.L.; A review of technology developments in flywheel attitude control and energy transmission systems, Aerospace Conference, 2004. Proceedings. 2004 IEEE, Volume 4, 13-13 March 2004 Page(s):2784 - 2800 Vol.4.

[33] Jiancheng Zhang; Zhiye Chen; Lijun Cai; Yuhua Zhao; Flywheel energy storage system design for distribution network, Power Engineering Society Winter Meeting, 2000. IEEE, Volume 4, 23-27 Jan. 2000 Page(s):2619 - 2623 vol.4.

[34] Meng, Y.M.; Li, T.C.; Wang, L.; Simulation of controlling methods to flywheel energy storage on charge section, Electric Utility Deregulation and Restructuring and Power Technologies, 2008. DRPT 2008. Third International Conference on, 6-9 April 2008 Page(s):2598 – 2602.

[35] Jinbo Wu; Jinyu Wen; Haishun Sun; A new energy storage system based on flywheel, Power & Energy Society General Meeting, 2009. PES '09. IEEE, 26-30 July 2009 Page(s):1 – 6.

[36] Yoo, S.Y.; Lee, H.C.; Noh, M.D.; Optimal design of micro flywheel energy storage system, Control, Automation and Systems, 2008. ICCAS 2008. International Conference on, 14-17 Oct. 2008 Page(s):492 – 496

[37] Björn Bolund, Hans Bernhoff, Mats Leijon, Flywheel energy and power storage systems, Renewable and Sustainable Energy Reviews, Volume 11, Issue 2, February 2007, Pages 235-258.

[38] Understanding Flywheel Energy Storage: Does High Speed Really Imply a Better Design?, white papers no 112, Active power Inc 2008.

[39] Material Property Hand book, Titanium alloy, R.Boyer, ASME ,1994.

[40] E. R. Furlong and W. Wiltsch, Performance and Operational Characteristics of an Advanced Power System, GE library.

[41] Leung, T.T.; Concept of a modified flywheel for mega-joule storage and pulse conditioning, Magnetics, IEEE Transactions on, Volume 27, Issue 1, Jan 1991 Page(s):403 – 408.

[42] Samineni, S.; Johnson, B.K.; Hess, H.L.; Law, J.D.;Industry, Modeling and analysis of a flywheel energy storage system for voltage sag correction, Applications, IEEE Transactions on, Volume 42, Issue 1, Jan.-Feb. 2006 Page(s):42 – 52.

[43] Vir Schaper, Oliver Sawodny, Tobias MaIll and Vii Blessing, Modeling and torque estimation of an automotive Dual Mass Flywheel, 2009 American Control Conference, St. Louis, MO, USA, June, 2009.

[44] Meng, Y.M.; Li, T.C.; Wang, L.; Simulation of controlling methods to flywheel energy storage on charge section, Electric Utility Deregulation and Restructuring and Power Technologies, 2008. DRPT 2008. Third International Conference on, 6-9 April 2008 Page(s): 2598 – 2602.

[45] Long Zhou; ZhiPing Qi; Modeling and simulation of flywheel energy storage system with IPMSM for voltage sags in distributed power network, Mechatronics and Automation, 2009. ICMA 2009. International Conference on, 9-12 Aug. 2009 Page(s): 5046 – 5051.

[46] Kascak, P.; Jansen, R.; Kenny, B.; Dever, T.; Demonstration of attitude control and bus regulation with flywheels, Industry Applications Conference, 2004. 39th IAS Annual Meeting. Conference Record of the 2004 IEEE, Volume 3, 3-7 Oct. 2004 Page(s):2018 - 2029 vol.3.

[47] Balikci, A.; Zabar, Z.; Czarkowski, D.; Levi, E.; Birenbaum, L.; Flywheel motor/generator set as an energy source for coil launchers, Magnetics, IEEE Transactions on, Volume 37, Issue 1, Part 1, Jan. 2001 Page(s):280 – 283.

[48] Long V. Truong, Frederick J Wolff, and Narayan V. Dravid, Simulation of energy sharing among flywheels in parallel configuration, IEEE 37th lntersociety Energy Conversion Engineering Conference (IECEC), 2002.

[49] Insulation Fact Sheet. Online [Available]:
http://www.ornl.gov/sci/roofs+walls/insulation/ins_05.html. Retrieved: October 2011.

[50] Soil Climate Analysis Network (SCAN) [Online]. Available: http://www.wcc.nrcs.usda.gov/scan/.
Retrieved: October 2011.

[51] Solar Heat Gain FAQ [Online]. Available: http://www.energycodes.gov/support/shgc_faq.stm.
Retrieved: October 2011.

[52] RELOAD Database Documentation and Evaluation and Use in NEMS [Online]. Available:
http://www.onlocationinc.com/LoadShapesReload 2001.pdf. Retrieved: October 2011.

[53] National Climatic Data Center [Online]. Available: ftp://ftp.ncdc.noaa.gov/pub/data/asos-onemin/.
Retrieved: October 2011.

[54] American Society of Heating, Refrigerating and Air-Conditioning Engineers, Inc. 2008 ASHRAE
handbook: heating, ventilating, and air-conditioning systems and equipment. Atlanta, Ga. :
ASHRAE, c2008.

[55] American Housing Survey National Tables: 2009. Online [Available]:
http://www.census.gov/hhes/www/housing/ahs/ahs09/ahs09.html. Retrieved: October 2011.

[56] Commercial Buildings Energy Consumption Survey. Table C14. Electricity Consumption and
Expenditure Intensities for Non-Mall Buildings. 2003 [Online]. Available:
http://www.eia.doe.gov/emeu/cbecs/cbecs2003/detailed_tables_2003/2003set10/2003pdf/c14.pdf.
Retrieved: October 2011.

[57] American Society of Heating, Refrigerating and Air-Conditioning Engineers. Knovel (Firm). 2009
ASHRAE Handbook: Fundamentals. Atlanta, GA. : ASHRAE, c2009.

[58] Soil Climate Analysis Network (SCAN) [Online]. Available: http://www.wcc.nrcs.usda.gov/scan/.
Retrieved: October 2011.

[59] Energy Savers Tips [Online]. Available:
http://www1.eere.energy.gov/consumer/tips/water_heating.html. Retrieved: October 2011.

[60] Conventional Storage Water Heaters. Energy Efficiency and Renewable Energy Website [Online].
Available: http://www.energysavers.gov/your_home/water_heating/index.cfm/mytopic=12980.
Retrieved: October 2011.

[61] NAHB Research Center, Inc. Prepared for NREL. Domestic Hot Water System Modeling for the
Design of Energy Efficient Systems. 2002. Online [Available]:
http://www.allianceforwaterefficiency.org/WorkArea/linkit.aspx?LinkIdentifier=id&ItemID=2256.
Retrieved: October 2011.

[62] Hourly Water Heating Calculations. MAY 15, 2002. PG&E 2005 Title 24 Building Energy
Efficiency Standards Update [Online]. Available:
http://www.energy.ca.gov/title24/2005standards/archive/documents/2002-05-30_workshop/2002-
05-17_WTR_HEAT_CALCS.PDF. Retrieved: October 2011.

[63] Danny S. Parker, John R. Sherwin, Jeffrey K. Sonne, Stephen F. Barkaszi, David B. Floyd, Charles
R. Withers. Florida Solar Energy Center (FSEC). Measured Energy Savings of a Comprehensive
Retrofit in an Existing Florida Residence. FSEC-CR-978-97 [Online]. Available :
http://www2.fsec.ucf.edu/en/publications/html/FSEC-CR-978-97/index.htm. Retrieved: October
2011.

[64] Energy Nexus Group, "Technology Characterization: Microturbines", March 2002 [Online]. Available: http://www.epa.gov/chp/documents/microturbines.pdf. Retrieved: October 2011.

[65] ActivePower, Understand Flywheel Energy Storage: Does High-Speed Really Imply a Better Design [Online]. Available: http://www.activepower.com/fileadmin/documents/white_papers/WP112_FlywheelEnergyStorage.pdf. Retrieved: October 2011.

[66] Based on a 10kW model (http://www.costco.com/images/content/misc/pdf/11671393spec.pdf) and a 2000 kW model (http://cumminspower.com/www/common/templatehtml/technicaldocument/SpecSheets/Diesel/na/s-1514.pdf). Retrieved: October 2011.

[67] Capstone microturbine Product Specification [Online]. Available: www.capstone.ru/pdf/ProductSpecification.pdf. Retrieved: October 2011.

[68] Based on a 1kW PEM FC from Relion [Online]. Available: www.relion-inc.com/products-t1000.asp and a 200kW PAFC fuel cell from UTC. Retrieved: October 2011.

[69] S&C, Community Energy Storage [Online]. Available: http://www.sandc.com/products/energy-storage/ces.asp. Retrieved: October 2011.

[70] Vycon Energy, Flywheel Energy Storage Brochure [Online]. Available: http://www.vyconenergy.com/pq/VyconVDCBrochure_Sept_11.pdf. Retrieved: October 2011.

[71] IEEE 1547 Standard for Interconnecting Distributed Resource with Electric Power Systems [Online]. Available: http://grouper.ieee.org/groups/scc21/1547/1547_index.html. Retrieved: October 2011.

[72] ANSI C84.1 American National Standard for Electric Power Systems and Equipment – Voltage Ratings (60 Hertz) [Online]. Available: http://www.nema.org/stds/complimentary-docs/upload/ANSI%20C84-1.pdf. Retrieved: October 2011.

[73] Energy Star, Recommended Levels of Insulation [Online]. Available: http://www.energystar.gov/index.cfm?c=home_sealing.hm_improvement_insulation_table. Retrieved: October 2011.

[74] California Energy Commission. Consumer energy center: Summertime energy-saving tips [Online]. Available: http://www.consumerenergycenter.org/tips/summer.html. Retrieved: October 2011.

[75] Julius Neudorfer, Energy Efficient Cooling [Online]. Available: http://viewer.media.bitpipe.com/979246117_954/1272654908_660/Handbook_SearchDataCenter_Cooling_FINAL.pdf. Retrieved: October 2011.

[76] Focus on Energy. Residential Fact Sheet [On-line]. Available: http://www.focusonenergy.com/files/document_management_system/residential_programs/managingthermostatcomfortenergysavings_factsheet.pdf. Retrieved: October 2011.